University of Florence

School of Engineering - Department of industrial engineering of Florence "DIEF"

Thesis submitted in fulfillment of the requirements for the award of the degree of:

Doctor of Philosophy in

Energy Engineering and Innovative Industrial Technologies

Ph.D. School of Industrial Engineering – XXX Cycle (2015-2017)

Settore disciplinare ING-IND/09

Innovative techniques for the Condition Monitoring of an Internal Combustion Engine using Turbocharger Speed

Tutor

Prof. *Giovanni Ferrara*

Candidate

Dr. M*ichele Becciani*

Ph.D. Course Coordinator

Prof. *Maurizio De Lucia*

Florence, Italy, November 2017

Declaration

I hereby declare that this submission is my own work and, to the best of my knowledge and belief, it contains no material previously published or written by another person, nor material which to a substantial extent has been accepted for the award of any other degree or diploma at University of Florence or any other educational institution, except where due references are provided in the thesis itself.

Any contribution made to the research by others I have been working with is explicitly acknowledged in the thesis.

Michele Becciani

November 2017

Ringraziamenti

Per primo ringrazio il Prof. Giovanni Ferrara per la possibilità concessami di intraprendere e seguire il percorso del dottorato di ricerca di alta formazione scientifica e professionale e di crescita personale.

Grazie a tutti i colleghi del gruppo di ricerca REASE, Alessandro, Alfonso, Andrea F., Andrea T., Francesco, Fabio, Giovanni G., Giovanni V., Giulia, Isacco, Lorenzo, Luca e Simone per aver reso questi tre anni di dottorato piacevoli e costruttivi e per aver condiviso tante risate e un po' di preoccupazioni, in questo una menzione speciale non può non andare ai coniugi V.

Un ringraziamento particolare a Giovanni Vichi e Luca Romani per il contributo sostanziale alla realizzazione di questo lavoro di Tesi, e per aver condiviso e superato assieme le difficoltà incontrate durante tutta l'attività.

A Claudia va la dedica più grande per aver condiviso e superato con me molte difficoltà e che mi ha supportato in ogni momento di questo percorso formativo.

Infine, ultimi ma non per importanza, ringrazio i miei genitori, che con il loro sostegno e i loro insegnamenti hanno reso possibile la realizzazione di quello che ritengo un grande successo personale.

Abstract

A numerical and experimental analysis of the turbocharger speed in a four-stroke turbo-diesel engine is presented in this work. The first part of the research is focused on the possibility to monitor the performance of the engine injectors that are characterized by a time deterioration, which is the effect of deposits of particulates in the nozzles. With this aim three different methodologies were developed, exploiting the numerical model, based on time and frequency content of the turbocharger speed. The first methodology is based on the evaluation of the area between the turbocharger speed and the line connecting the extreme values of the influencing windows related to the cylinder object of the analysis. The second methodology is based on the acceleration of the turbocharger, the peak value of the acceleration in each contribution window is evaluated and compared with the expected one to quantify the amount of fuel injected in each cylinder. Finally, the methodology based on the frequency content of the turbocharger speed is presented, for this case two main parameters are considered: the module of the fourth order, that allows to measure the fuel quantity injected in all cylinders, and the first order phase to detect if there is a problem in the injection in one cylinder and to detect which cylinder is involved.

A specific experimental campaign was carried out to verify the reliability of these three methodologies, this experimental campaign was conducted with the engine provided by Yanmar Japan and exploited for the calibration of the numerical model. For the purpose of detecting injection issues, two different set of injectors were tested, one, set new, with a homogeneous performance among cylinders and one, used and

deteriorated, with a different performance for each cylinder. From the analysis of the results related of the methodologies developed a very good reliability of each method was detected. In addition, the possibility of detect misfiring events was positively tested.

Finally, a technique to distinguish among different typical faults of diesel engines was presented. This strategy relies on different engine parameters such as the temperature and the pressure of the exhaust manifold. Exploiting the information coming from these sensors and the turbocharger speed it is possible to detect the fault that is responsible for a change in the engine condition among selected possibilities: EGR variation, Injection variation, in terms of timing and injected fuel mass, and turbine backpressure. The fault detection strategy was developed and tested both numerically and experimentally confirming its ability to monitor the condition of the engine.

Contents

List of figures

List of tables

List of symbols and acronyms

b	Dynamic damping	[N s/m]
D	Piston diameter	[m]
i	Imaginary part	-
l	Rod length	[m]
m	Mass	[kg]
$\dot{m}$	Mass flow	[kg/s]
M	Mass	[kg]
p	Pressure	[Pa]
s	Displacement	[m]
S	Surface	[m^2]
t	Time	[s]
T	Temperature	[K]
Z	Acoustic impedance	[kg/(m^2 s)]

Greek symbols

Δp	Pressure drop	[Pa]
ρ	Gas density	[kg/m^3]
ω	Pulsation frequency	[rad/s]
Ω	Area	[m^2]

Subscripts

1	Upstream
2	Downstream
cyl	Cylinder
exp	Experimental

Acronyms

BC	Boundary Condition
BDC	Bottom Dead Centre
CA	Crank Angle
ECN	End of Combustion Noise
FFT	Fast Fourier Transform
ICE	Internal Combustion Engine
MBF	Mass Fraction Burned
SOI	Start of Injection
SCN	Start of Combustion Noise
TCAF	Turbocharger Acceleration Factor
TCSF	Turbocharger Speed Factor
TTL	Transistor-Transistor Logic
WG	Waste Gate

Introduction

Internal combustion engines, thanks to their reliability and efficiency, are used throughout the world in multiple roles such as transport, power generation and industrial application. Due to their wide diffusion, in order to ensure a high level of performance and to comply with every day more severe limitations in terms of fuel consumption and pollution emissions, a continuous supervision of the engine operating conditions is needed. In this context, the monitoring of the engine thermodynamic cycle is the most suitable approach during both the development stage and the real operating conditions.

Direct analyses of the in-cylinder pressure are commonly performed on the test bench in order to optimize the engine thermodynamic cycle while paying particular attention to the combustion process. Indeed, the in-cylinder pressure is one of the most important parameters for the combustion evaluation, but its direct measurement using a pressure sensor is often intrusive and expensive.

Up to now, many studies on non-direct measurements evaluating the quality of the engine thermodynamic cycle have been performed with the purpose of employing non-intrusive and low-cost sensors.

The growing use of turbochargers (TC), in all modern compression ignited and spark ignited internal combustion engines, combined with its direct connection with the thermal and fluid-dynamic conditions at the inlet and outlet of the engine suggests the use of the average and instantaneous TC speed as a feedback of the engine operating conditions.

In this thesis, a numerical and experimental analysis of the turbocharger speed in a four-stroke turbo-diesel engine is presented. A 1D numerical model of the engine was

calibrated with experimental data furnished by Yanmar, the industrial partner of the research. The model allows the TC characteristics to be considered both the fluid dynamic aspects (by using compressor and turbine working maps) and the mechanical characteristics by introducing the TC inertia.

The first part of the research is focused on the possibility to monitor the performance of the engine injectors that are characterized by a time deterioration, effect of deposits of particulates in the nozzles. With this aim three different methodologies were developed, exploiting the numerical model, based on time and frequency content of the TC speed.

A specific experimental campaign was then carried out to verify the reliability of these three methodologies. For this purpose, two different set of injectors were tested, one set new with a homogeneous performance among cylinders and a used and deteriorated one with a different performance for each cylinder. In addition, the possibility of detecting misfiring events was positively tested.

Finally, a preliminary fault detection strategy that involves issues related to injection, EGR and exhaust treatment system is developed exploiting numerical and experimental data. Since the necessity to distinguish among different faults other sensors such as pressure and temperature sensors in the exhaust manifold and lambda sensor, in addition to the TC speed one, are exploited for the developed strategy

In the first chapter of the thesis an overview of the existing and potential monitoring technique is presented then, the second chapter shows the experimental activity and the numerical calibration phase of the model with its results. In the third chapter the methodologies developed during the numerical activity are explained in detail while the fourth chapter presents the experimental campaign with the setup and the results of the validation process of the methodologies. The last chapter presents all the results related to the fault detection strategy.

1 Internal Combustion Engine Monitoring Techniques

Condition monitoring of internal combustion engines consists of the analysis of information from the engine and the subsequent data elaboration to perform fault detection and/or diagnosis activities using different strategies whether the engine is on a test bench or in a vehicle. During the development of an ICE, test bench operations are exploited to investigate the engine status by performance analysis, oil circuit analysis, visual inspection, durability, vibration and acoustic analysis. During the use on-field of the ICE, the objective of the engine monitoring is to predict engine failure to prevent serious mechanical failure, losing performance and increasing emissions, this would be useful for the user to reduce maintenance costs and to correctly plane the maintenance actions with an increased reliability.

Many techniques have been developed during the long lifetime of ICEs, the most important ones are reported below:

- Direct in-cylinder pressure measurement
- Vibration analysis
- Acoustic emission
- Crankshaft engine speed

In the next paragraph, each of the cited methods for the condition monitoring of the ICE will be briefly explained.

1.1 Direct in-cylinder pressure method

The cylinder pressure is the most important parameter of the ICE, in fact, most aspects and parameters of the engine are in different ways linked to the combustion process that represents the main element of engine operation. By measuring and monitoring the cylinder pressure the check of the combustion process can be performed which is crucial for the control of the emissions and fuel consumption. Further, in the case of a multi-cylinder engine, the state of each cylinder can be monitored.

The in-cylinder pressure is the most direct parameter associated with the combustion process and for this reason, represent a key tool in engine research development, so in the case of test bench operation, the use of direct in-cylinder pressure measurement represents a standard. By measuring the in-cylinder pressure, it is possible to obtain lots of fundamental information, such as indicated and friction mean effective pressures (IMEP, FMEP), maximum pressure and its angular position and other thermodynamic proprieties. The first system used to measure the in-cylinder pressure involved the use of a mechanical sensor system that plotted the pressure-volume curve on a sheet of paper (from which the name "indicated" of IMEP), invented by James Watt and John Southern in 1796, this was the first device intended to measure the varying pressures within a steam engine's cylinder as it was working.

Figure 1. Replica of the original steam indicator invented in the early 18th Century by James Watt of Scotland.

Nowadays measurement systems consist of a piezoelectric sensor with a high-frequency response.

Hountalas *et al.* [1] carried out a detailed experimental investigation on a single cylinder diesel engine. They used the in-cylinder pressure as a parameter to develop a methodology to determine the actual cause for a reduced cylinder compression pressure. The most relevant results are the possibility to find out cylinder ring wear, without dismantling the cylinder head assembly, and detecting the actual cause of reduced pressure.

Cylinder and injection pressures, experimentally measured, were used by Watzenig *et al*. [2] as input parameters in a detailed engine model of a large two-stroke diesel engine (marine application) to evaluate engine condition. The authors were able to detect a series of causes that negatively affect the engine performance.

Despite being essential in the research field, the direct measurement of the in-cylinder pressure could be very expensive because a high-performance pressure transducer has to be used and the harsh environment in the cylinder causes the transducer to have a limited lifetime. Furthermore, this kind of measurement involves an intrusive approach to the engine head. However, there are examples of integration of a piezoelectric cylinder pressure sensor into diesel engines that have been used in the engine control unit (ECU) of the systems, for the regulation and control of fuel injection timing, exhaust gas recirculation (EGR) rate and turbocharger operation [3].

The industrial partner of this research uses the direct measurement of the in-cylinder pressure in their large marine dual-fuel engine in order to take under control problem such as misfiring. Still, the possibility to substitute this kind of sensor with a more economical solution it is object of research and investigation.

1.2 Acoustic emission method

The generation of noise in ICEs comes from aerodynamic and mechanical sources. The source of noise caused by air perturbation can be defined as an aerodynamic source, i.e. turbulence within the exhaust and intake system. Noise generated through contacts,

impacts and shocks between surfaces are the mechanical source: impacts between cylinders and pistons, shafts and supports, etc.

ICE noise emissions are composed by many different sources such as mechanical and aerodynamic noise and combustion process. As a result, in the acoustic emissions, a lot of information from the engine are contained. The difficulty on the isolation of each contribution to this emission represents one of the biggest issue related to engine condition monitoring based on acoustic emission.

Acoustic emission methods have been successfully used in non-intrusive testing applications. In 1998 Gill *et al*. [4] conducted one of the earliest investigations regarding acoustic emission for engine condition monitoring. In this research, the authors demonstrated the possibility to detect misfire and reduced injector discharge pressure by using acoustic emission signals.

A recent study, carried out by Barelli *et al.* [5], proposes to use, as a diagnosis methodology for engine working conditions, acoustic pressure and vibration measured on the engine head. This study was carried out by an experimental campaign on an ICE of a cogeneration plant. It shows that a strict relationship between the phenomena inside the cylinder and both the vibration and acoustic signals on the cylinder head is present, depending on the engine conditions (load and regime). To find out the reference values for fault detection, acoustic and vibration indexes were introduced to evaluate the working regime and load of the engine. The conclusion shows that if the intensity of the signal is not congruent with the reference signal it is possible to state that there is a combustion irregularity in the cylinder object of the measurement with a possible consequent anomalous value of the associated IMEP. Further, the study shows that vibration and acoustic pressure levels could be employed without distinction.

Jiang *et al.* [6] studied an effective monitoring approach to diesel engine combustion based on acoustic one-port source theory and exhaust acoustic measurements. Their experimental results, carried out with a two-load acoustic method, shows that the acoustic measurement could be used for fault detection. The source pressure alone is considered as the signal for condition monitoring because it proves more sensitive than the exhaust source impedance. They found that, by using the local deviation of the

Waveform, two common faults could be accurately detected, localized and differentiated, in particular: these faults were the reduced injection pressure and the increased valve clearance.

Research conducted by Lowe [7] demonstrate the possibility to use acoustic emission to recognize four different operating conditions: faulty operation of diesel fuel injector nozzles, different kind of dual-fuel based on the rate of ethanol substitution, poor valve-train dynamics and abnormal valve motion and piston slap.

In 2016, Nicolò Cavina et al [8] proposed a method to extract fundamental information about combustion process (such as Knock and misfire), turbo speed and air path fault by actuate analysis of acoustic emissions of a 4 cylinder 1.4L GDI TC engine, measured by a simple microphone located on the intake side of the engine, under the intake manifold.

By using specific algorithms and by means of Fast Fourier Transformation (FFT) of acoustic emissions, they could identify:

• Knock: sound emission associated with knock events is emitted from pressure waves that are generated inside the combustion chamber. Thus, knock detection is performed through the analysis of the frequency band close to combustion natural modes.

• Misfire: Under the normal operating condition, the sound signal is characterized by different frequency components where the main frequency is the firing one. In case of a misfire, the sound emitted presents differences in the frequency content of the sound signal.

Chiatti et al [9] carried out a research activity on a naturally aspirated, two cylinders diesel engine. They analyzed, by using only sound radiation signal as input, the emission noise to characterize both the noise and the in-cylinder pressure behavior. It was highlighted the existence of a correlation between the combustion parameters (CI, MBF50, MBF100), injection Process (SOI) and indices for noise radiation such as SCN (start of combustion noise) and ECN (end of combustion noise). Based on these findings, a closed-loop algorithm can be integrated into the ECU, in which the real-time processing of acoustic data is performed and the combustion properties could be evaluated.

Bondarenko et al [10] carried out a research focused on the detection of knocking phenomena through the acoustic emission analysis. It was demonstrated that a knock condition can be detected using the acoustic emission recorded by a microphone. Knock fundamental frequencies and features were extracted analyzing the frequency content and then, by applying the transformed singular value decomposition (TSVD) method, it was possible to classify appearance and severity of knock.

The use of acoustic signals is currently limited by the masking effect given by the background noise, even for the faults detection mentioned, pre-processing operations seem mandatory to obtain a reliable signal of interest [11].

1.3 Vibration Method

The vibration method is often adopted for the detection and control of engine knock in spark ignition engines. Diesel engines present four different sources of vibrations: combustion, piston slap, fuel injection valve operation and the inertial forces that move the engine block in its supports. *Antoni et al.* [12] pointed out that the majority of these sources of vibration are linked with events that occur in a small crank-angle window around piston top-dead-center. The consequent overlapping vibration signatures represent, in the analysis of engine vibration signals, one of the most important problems.

A large amount of research focuses on the issue related to the source separation and on the development and application of source separation techniques. An important investigation in this direction was conducted by Badawi *et al.* [13] using a single cylinder diesel engine. Referring to a simulation that replicates the acquisition with a single channel accelerometer, they separated the following sources of vibration: exhaust valve closing, inlet valve closing, fuel injection, combustion, piston slap, exhaust valve open and inlet valve open. The separation was performed using segmentation independent component analysis and vibration. In this research, the gas dynamics contribution to engine vibration was also underlined.

An overview of the issues present for the vibration based methods is explained by Antoni *et al.* [14]. They found two main reasons:

- Most the pressure trace energy is contained in low frequencies (< 500 Hz) where generally vibration signals contain minimal energy because of engine block rigidity.
- Vibration signals are corrupted by non-negligible additive noise due to piston slap and inertial forces.

However, the authors discovered that the issues mentioned could be overcome by using their cylinder pressure reconstruction method.

Sharma *et al* [15] carried out an investigation on an IC four-cylinder petrol engine based on the misfire detection. Misfire situations were simulated by cutting the electric supply to individual spark plugs. The main vibration signal features, measured by accelerometers, were computed by an FFT analysis. To select the best parameters that can be used for misfire detection and classification Various Decision, tree algorithms have been used. The main result was the definition of an LMT algorithm that offered a high overall classification (accuracy 100%) in differentiating between normal and fault conditions.

J Chen *et al* [16] developed an Artificial Neural Networks (ANNs)-based automated diagnostic system for misfire diagnostic combining information from torsional vibration and rotation of the engine block. They introduced a simulation model that could simulate combustion faults. The model was subsequently updated and tested by the experimental results. The ANN networks included three stages: misfire detection, misfire localization and severity identification. The feed-forward multilayer perceptron (MLP) neural networks were used to detect whether there are misfires and to define the severity. The probabilistic neural network was used to identify the misfire location. The final results showed that the torsional vibration method can efficiently diagnose misfires.

Using closed-loop control of the internal combustion engine is beneficial to reducing emission and fuel consumption. Some of the combustion parameters could be identified from the vibration acceleration signals.

Zhao *et al* [17] proposed the Empirical Mode Decomposition (EMD) method to reconstruct vibration acceleration signal from which they identified combustion parameters. They found that there were angle deviations between the combustion

parameters extracted from vibration acceleration signal and those from the cylinder pressure. In particular, they proposed algorithms to correct the angle deviation referring to the start of combustion (SOC) and the location of the maximum pressure rise rate. The angular deviation was corrected within a good error bound. Furthermore, a monitoring framework was inferred from feature point in the composite signal to evaluate combustion parameters.

Vibration methods are often used for detecting a misfire or a knock condition. In fact, when one of these particular phenomena occurs, a unique vibration pattern is created. By analyzing this pattern, it is also possible to detect in which cylinders a malfunction occurs. Vibrational measures, on the other hand, are affected by a low signal-to-noise ratio at low frequencies that influences the correct reconstruction of the engine cycle.

1.4 Crankshaft Speed Method

Techniques for the condition monitoring of the ICE utilizing crank-angle measurements are based on the angular speed and acceleration fluctuation of the crankshaft. These fluctuations are linked to the fast variation of the in-cylinder pressure for each cylinder during engine operation. The measurements of the crankshaft speed variation could be used to evaluate both engine torque and in-cylinder pressure.

For example, the study of Taglialatela *et al.* [18] proposes the use of the crankshaft speed to determine the combustion parameters. They choose to use a Multi-Layer Perception neural network to model the relationship between the engine crankshaft speed and the in-cylinder pressure. The study refers to a single-cylinder spark ignition engine. The conclusions show that it is possible, with a good accuracy for all operating conditions tested, to find the in-cylinder pressure peak and its angular location, starting from the engine angular crankshaft speed and the crankshaft speed derivative.

An investigation conducted by Johnsson [19], using as input both engine structure vibration and crankshaft speed fluctuation, performed a reconstruction of in-cylinder pressure pulse waveforms. The utilized method was a nonlinear model based on complex

radial basis function networks. This article shows that the engine structure vibration and the crankshaft angular speed are related to the cylinder pressure mainly in different frequency regions. The crankshaft angular speed fluctuation has the highest coherence with the cylinder pressure for low frequencies while the engine structure vibration has the highest coherence for high frequencies. The conclusion is that with the combination of these two parameters, the reconstruction of the in-cylinder pressure should be possible for a wide range of running conditions.

Jian Chen *et al* [20][21] proposed the use of Artificial Neural Networks (ANNs) for diagnosis of misfires in IC engines. Two methodologies were used for detecting misfires, which were based on the torsional vibration signals and the derivate of the angular speed of the engine block, respectively. The simulation model was calibrated by using real experimental data, then numerical simulation was used to recreate a different range of misfires. Results confirmed that the model can diagnose misfire, including location and severity.

Crank angle measurement-based monitoring techniques have many advantages: the availability of already used crankshafts sensors, the low-cost of the sensors, the possibility to distinguish the contribution of each cylinder and the system of measurement is nonintrusive. However one of the main disadvantages of this techniques is the poor sensitivity of the crankshaft speed, due to the high inertia of the engine, meaning that the fault has to be sufficiently severe to cause enough variation in terms of torque that has a measurable effect on the crankshaft velocity fluctuation. Another weakness of these techniques is related to the inability to identify specific component related faults [22].

1.5 Turbocharger Speed Method

As previously mentioned, this thesis wants to suggest the use of turbocharger (TC) speed measurement-based monitoring technique because of the growing use of TC in automotive, marine and power generation fields and its direct connection with the thermal and fluid-dynamic conditions at the inlet and outlet of the engine. Indeed the TC speed is strictly connected with all the important parameters of a turbocharged diesel engine (TCDE), like the EGR ratio, the fuel injection characteristics, the combustion process or

the environmental pressure, and it requires nonintrusive and inexpensive measurements. By monitoring the TC speed, as explained in following chapters, it could be possible to detect faults regarding many engine conditions in TCDE. For example, it could be possible to detect if there is a different injection mass in one cylinder and in which cylinder this difference occurs.

Regarding this aspect, a study carried out by Maciàn *et al.* [23] by using experimental and numerical data demonstrate that it is possible to detect fault related to the injectors in a diesel engine. They develop an algorithm with the aim to ensure that the same quantity of fuel is injected into each one of the cylinders. This governor can be applied to the full operating range of the engine. The injection failure detection and identification technique are based on the measurement of the turbocharger instantaneous speed and its treatment in the frequency domain. They also show the possibility to use instead of the instantaneous turbocharger speed the dynamic pressure inside of the exhaust manifold.

2 1D Numerical Model Development

The first step of the activity was to build and calibrate a numerical 1D model with the capability to correctly estimate the behavior of the turbocharger speed overall the operating range of the considered engine, by keeping several engine parameters under control, in order to perform a preliminary fault detection strategy based on 1D simulation. A first experimental campaign was conducted by Yanmar Co. Japan in cooperation with Bosch Japan with the specific aim to calibrate the numerical model mentioned.

Once calibrated, it is possible to assert that the model is able to replicate the physics behind the engine system and to simulate a wide engine operating condition. In the opening portion of this chapter, the data about the considered engine and an overview of the experimental campaign conducted by Yanmar is reported. The subsequent section provides a description of the calibration activity of the numerical model and shows the results of the calibration activity.

2.1 Preliminary Experimental Campaign

The engine selected for this work is a four-stroke turbocharged diesel engine with direct injection used for power generation. Its general characteristics are shown in Table 1

Table 1. Engine Technical Data

Engine Type	Compression Ignition
Strokes for cycle	4
Number of cylinders	4
Displaced volume	2100 cc
Stroke	90 mm
Bore	86 mm
Compression ratio	19.2:1
Number of Valves per cylinder	4
Turbocharger	Single-stage turbine with WG

In the preliminary experimental campaign, carried out by Yanmar Japan, the engine was tested at five different loads, from level 1 to level 5 (full load), and at nine engine speeds, from 1000 rpm to 3000 rpm, with steps of 250 rpm. The load levels were characterized by an imposed mass of fuel injected, constant for each angular velocity of the engine, with the exception of the full load (level 5) as shown in Figure 2.

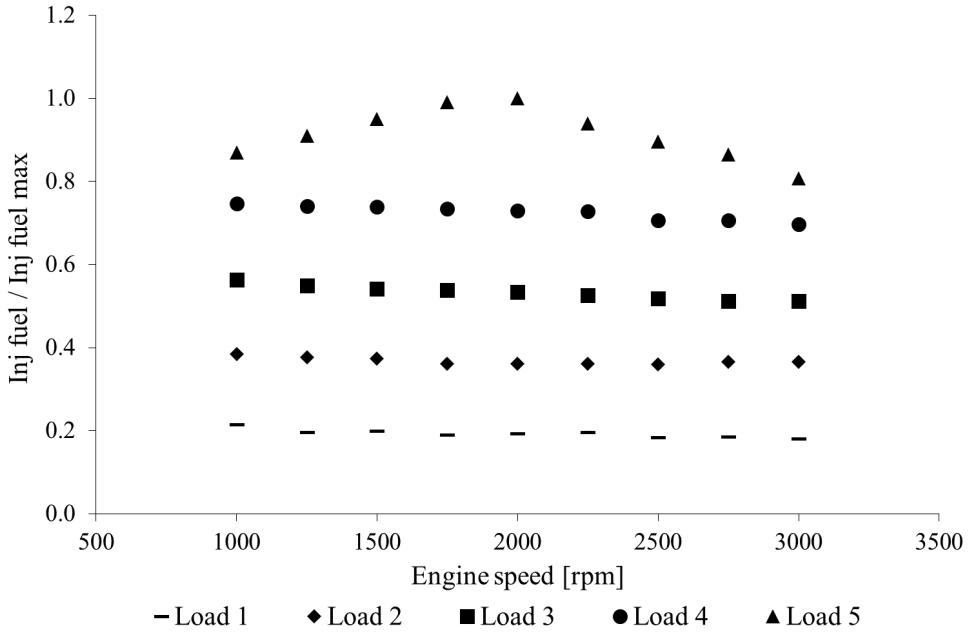

Figure 2. Experimental Test Campaign - Injected fuel quantity at five load levels and nine engine speeds from 1000 rpm to 3000 rpm; data is normalized respect to the maximum injected fuel quantity.

During the experimental tests, several data were acquired to guarantee a robust and deep calibration of the numerical model. A list of this data is reported below:

- Torque and power output
- TC average speed
- Airflow
- Fuel mass flow
- In-cylinder pressure for each cylinder
- Gas temperature in different sections
- Static pressure at different points
- Wall temperature at different points
- Data from Engine Control Unit (ECU)
- Characteristics of the Injection system

The positions of the static pressure, gas temperature and wall temperature sensors are shown with the engine scheme in Figure 3.

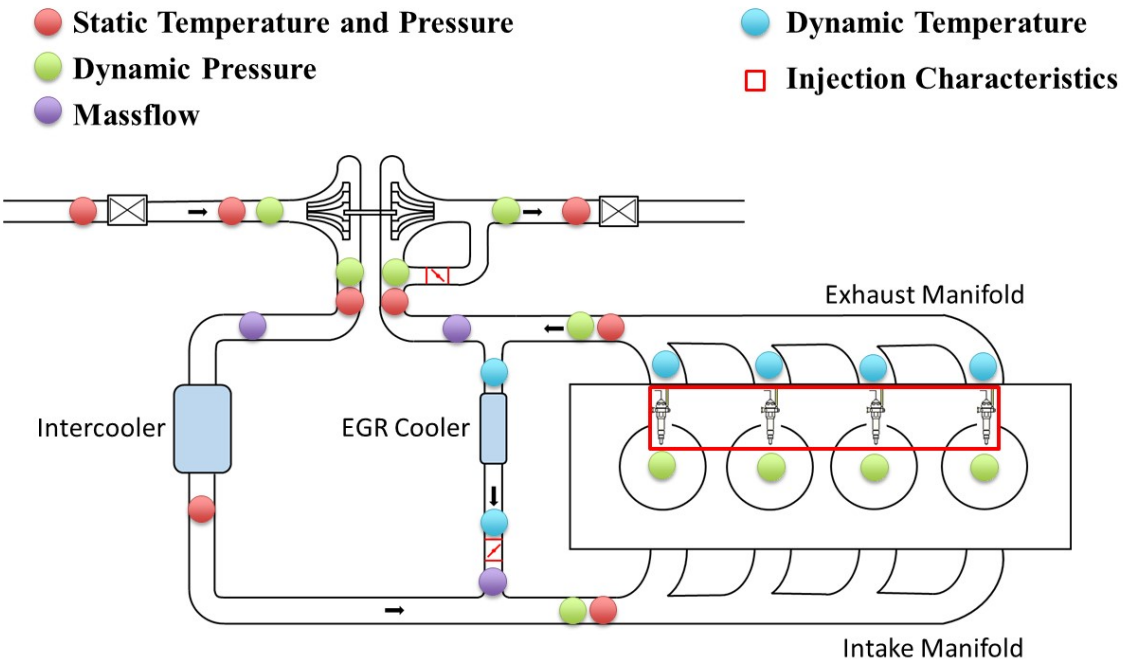

Figure 3. Engine scheme with experimental acquisition points

To measure the in-cylinder pressure, a KISTLER 6125 dynamic pressure transducer was used, whilst for the in-duct pressure, a KISTLER 4049 piezoresistive pressure sensor was used. The effect of both the inlet suction filters and the exhaust filters (associated with the exhaust gas treatment) was experimentally replicated through valves that generate a pressure drop at the compressor inlet and turbine outlet. Considering the necessity to replicate the combustion process of the engine with the model it was decided to implement

a model with a predictive combustion model, for this reason, the characteristic of the injectors was acquired.

A significant part of the experimental tests regards the turbocharger since all the research activity is focused on the turbocharger behavior. Indeed, the maps of both the turbine and the compressor, used in the engine numerical model were obtained experimentally by the industrial partner, because of the key role of the TC in this investigation. To measure the TC speed, a Hall-effect commercial sensor, faced on the compressor inducer was used (A more detailed description of the TCspeed acquisition is illustrated in the experimental validation chapter).

2.2 Numerical Model Calibration

In the first phase of the numerical activity, a numerical model with Wave®, an industrial specialized software, was built by referring to the engine data, including engine geometrical characteristics, valves lift, valve flow coefficients turbine and compressor map experimentally collected. After that, a calibration phase started with the aim to reproduce the correct experimental behavior of the engine in all its aspects, such as pressure waves, torque, volumetric efficiency and TC speed, crucial for the purpose of this research. The calibration phase was important and delicate especially by considering the complexity of the considered turbocharger diesel engine, with its EGR system, cooling systems and turbocharger. For what concern the combustion process the 1D model developed is characterized by a predictive combustion process.

The first important parameter object of the calibration was the volumetric efficiency. The key aspects related to this parameter were essentially the EGR rate, the TC and the cooling systems. In this calibration phase, due to the influence of the combustion on the charge exchange phase, a not predictive combustion sub-model was used and the experimental heat release rate was imposed.

In order to match the experimental value of the volumetric efficiency for the whole engine operating range, it was necessary to first impose the correct EGR rate and TC speed. The EGR rate was imposed with the EGR control system. The EGR control system is composed of a sensor that reads the EGR ratio inside the intake manifold and sends that value to the proportional integrative derivative controller (PIDC). The PIDC compares this value with the experimentally imposed target and, depending on this comparison, sends the adjusted value of the EGR valve effective area to the actuator or directly to the valve. The EGR valve opening is varied to obtain the imposed value of the EGR ratio into the engine. In order to match also the correct temperature and pressure of the EGR system, the calibration parameters for both the EGR cooler and the EGR ducts were the wall temperature, the friction coefficients and heat coefficients.

It is important, in this initial stage, to impose the TC speed because of its crucial influence on the volumetric efficiency. Due to the imposition of the TC velocity, it was necessary to work with a specific Wastegate control system. This control system read the value of the TC speed, from the turboshaft element, compared it with the reference one and managed the opening of the Wastegate valve to reach the correct TC speed. With this specific

control system, it was possible to have the correct value of the TC speed and consequently the correct intercooler inlet pressure needed in this phase. Once the TC speed and EGR rate were imposed, it was possible to modify the tuning parameters, wall temperature, friction coefficient and heat coefficient of ducts, intercooler and junctions of the intake system to calibrate the volumetric efficiency of the engine.

After the preliminary phase, the combustion process of the model was designed with predictive combustion sub-models. The main calibration parameters were represented by:

- Injection Profile: The fuel mass per cycle, the start and the end of the injection were experimentally measured. The instantaneous fuel mass flow was derived from these experimental data and it was imposed constantly at an average value.
- Heat Transfer Coefficient Inside the Cylinders: The Woschni heat transfer sub-model was used, It views the charge as having a uniform heat flow coefficient and velocity on all surfaces of the cylinder and calculates the amount of heat transferred to and from the charge based on these assumptions. The heat transfer multiplier coefficient inside the cylinders was changed for both the situation with closed valve and opened valve.
- Cylinder Temperatures All temperatures of the cylinders were calibrated and were different in function of both the engine load and speed. They include the temperature of the piston top, liner, head, intake valve and exhaust valve.
- Combustion Coefficients The combustion calibration parameters are related to the different distribution of the diffusive and premixed combustion and to the velocity of the combustion process.

The *Diesel Jet Combustion* sub-model was exploited for this purpose since it has the ability to predict combustion heat release rate from user-specified fuel injection rate and injector geometry. Many of the parameters available for adjustment of the jet combustion sub-model are related to the velocities, turbulence levels, and gas mixing effects in the combustion chamber. It can be assumed that heat transfer, air entrainment, and exhaust gas re-entrainment into the combustion zone can all be expected to increase as in-cylinder velocities and turbulence levels increase. Similarly, they can be expected to decrease as the cylinder conditions approach a more quiescent state. The Diesel Jet combustion model relies on the user-defined fuel mass flow profile and nozzle diameter/number of holes, experimentally evaluated, to obtain jet characteristics such as nozzle pressure drop, jet velocity, and fuel spray droplet size.

In this last calibration phase, the TC speed had not to be imposed. For this reason, it was necessary to use a control system to manage the Wastegate open area. This control system is able to replicate the real physics of the Wastegate valve, indeed it was built to open the valve when the compressor outlet pressure overcame its experimentally founded limit value. The Wastegate control system works with a sensor that reads the value of the compressor outlet pressure and sends it to a PIDC. If the read pressure is higher than the imposed limit value, the PIDC sends the needed value of the Wastegate open area to the actuator. The actuator varies the valve opening in order to limit both the TC speed and the compressor outlet pressure.

In the following figures (Figure 4 to Figure 6) the accordance between numerical and experimental results for the heat release rate, the in-cylinder pressure, the indicated mean effective pressure and the turbocharger average speed is highlighted. It is important to underline that the focus of this calibration phase was to find the tuning parameters that allow having an engine model characterized by an optimum coherence, with the experimentally tested engine, over the whole operating range.

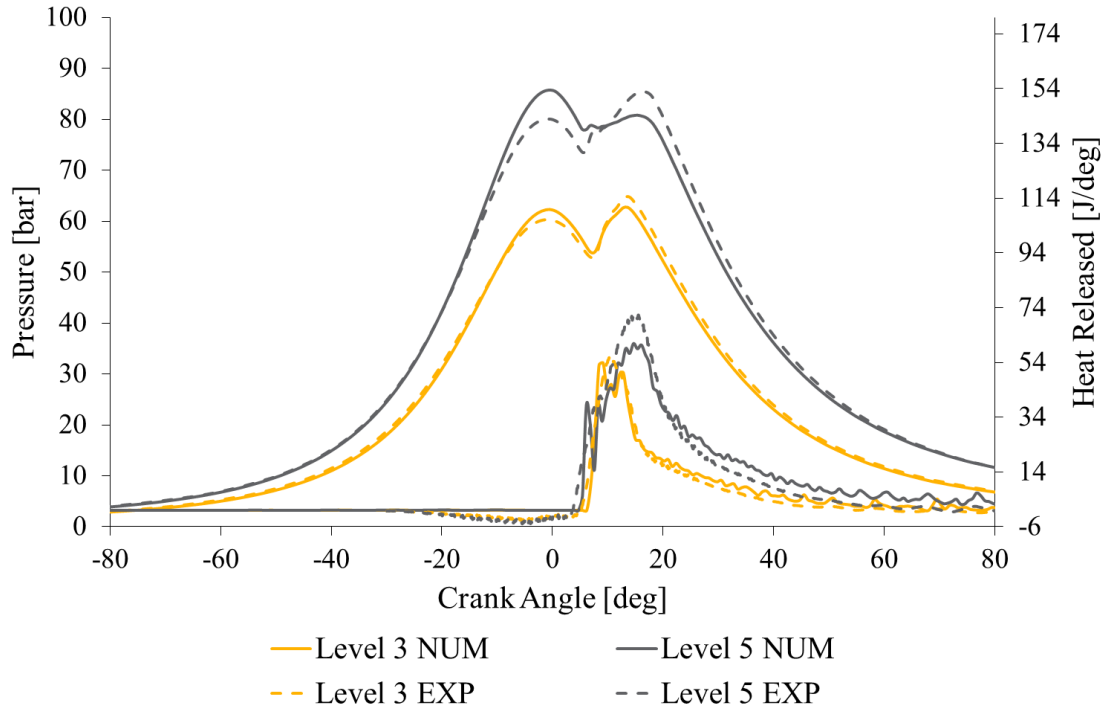

Figure 4. In-cylinder pressure/heat released at two different operating conditions (load level 3 and 5 at 1750 rpm); a comparison between numerical and experimental results.

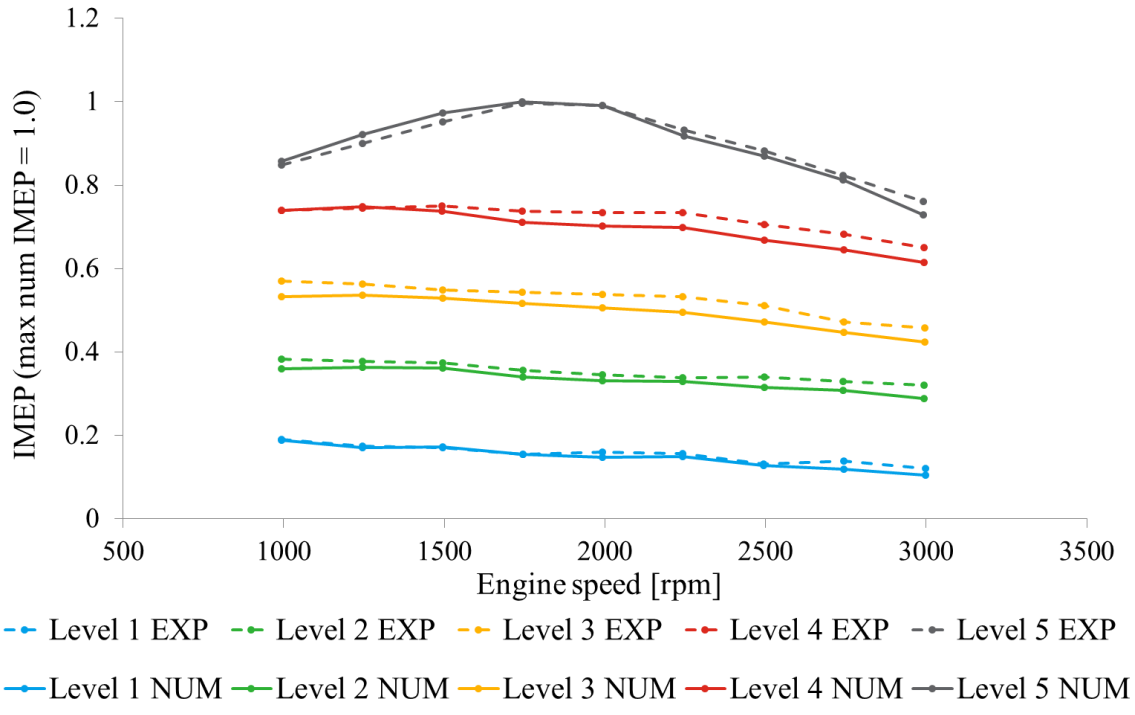

Figure 5. Indicated Mean Effective Pressure at five different load levels (numerical and experimental results); the data is normalized respect to the maximum numerical IMEP.

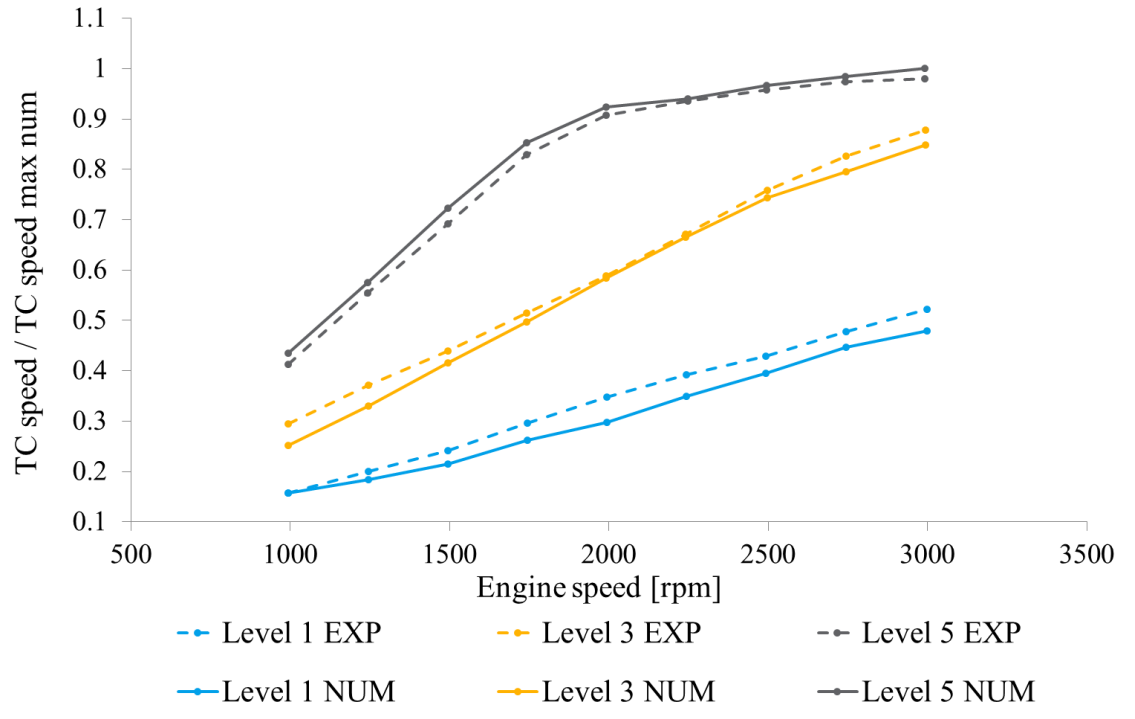

Figure 6. Average TC speed at three different load levels (numerical and experimental data); The data is normalized respect to the maximum numerical average TC speed

Very remarkable results for the calibration are represented by the instantaneous TC speed. In Figure 7-Figure 10 the agreement in terms of instantaneous TC speed variation with respect to the average values is shown.

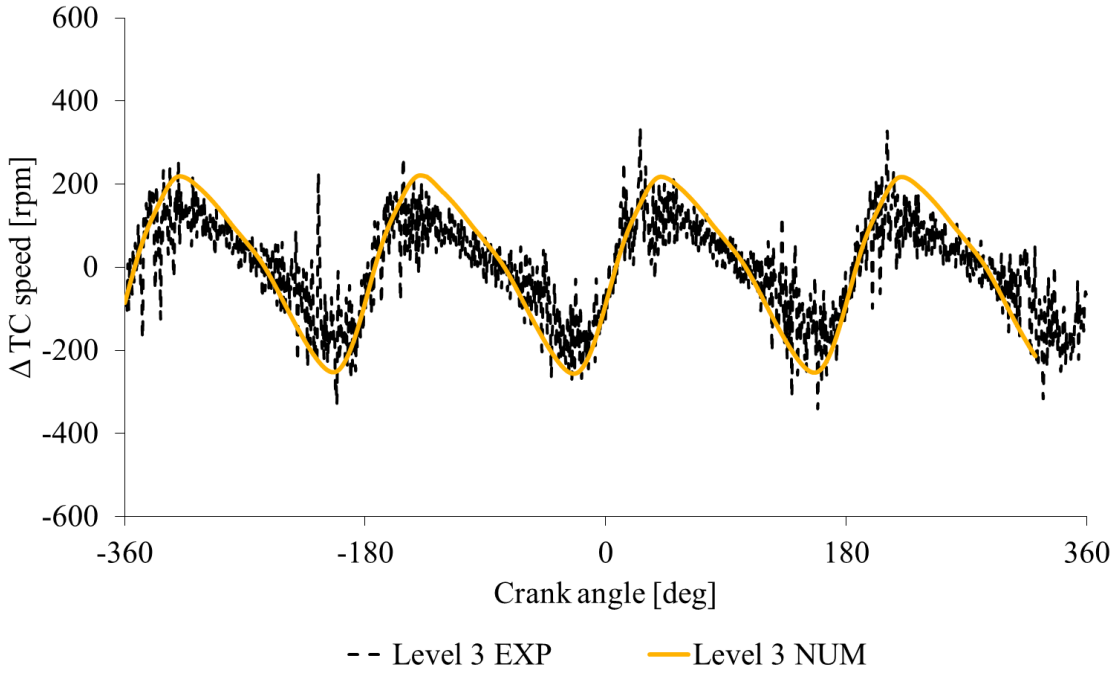

Figure 7. Instantaneous Δ TC speed function of the crank angle (numerical and experimental data); operating condition load level 3 at 1000 rpm

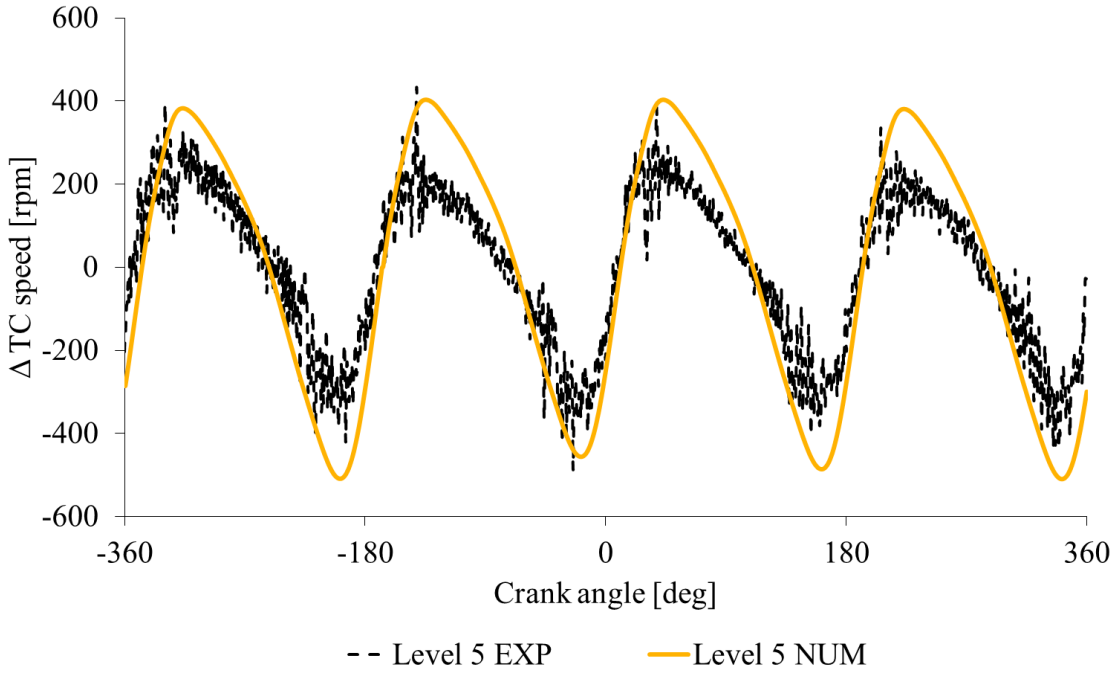

Figure 8. Instantaneous Δ TC speed in function of the crank angle (numerical and experimental data); operating condition load level 5 at 1000 rpm

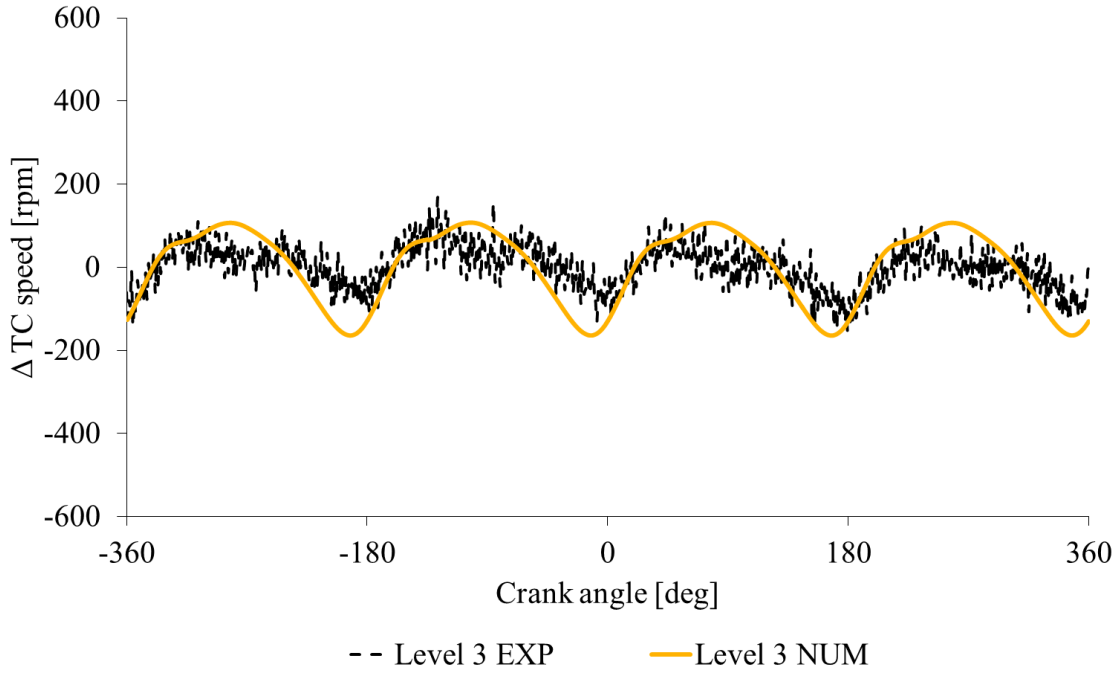

Figure 9. Instantaneous Δ TC speed in function of the crank angle (numerical and experimental data); operating condition load level 3 at 1750 rpm

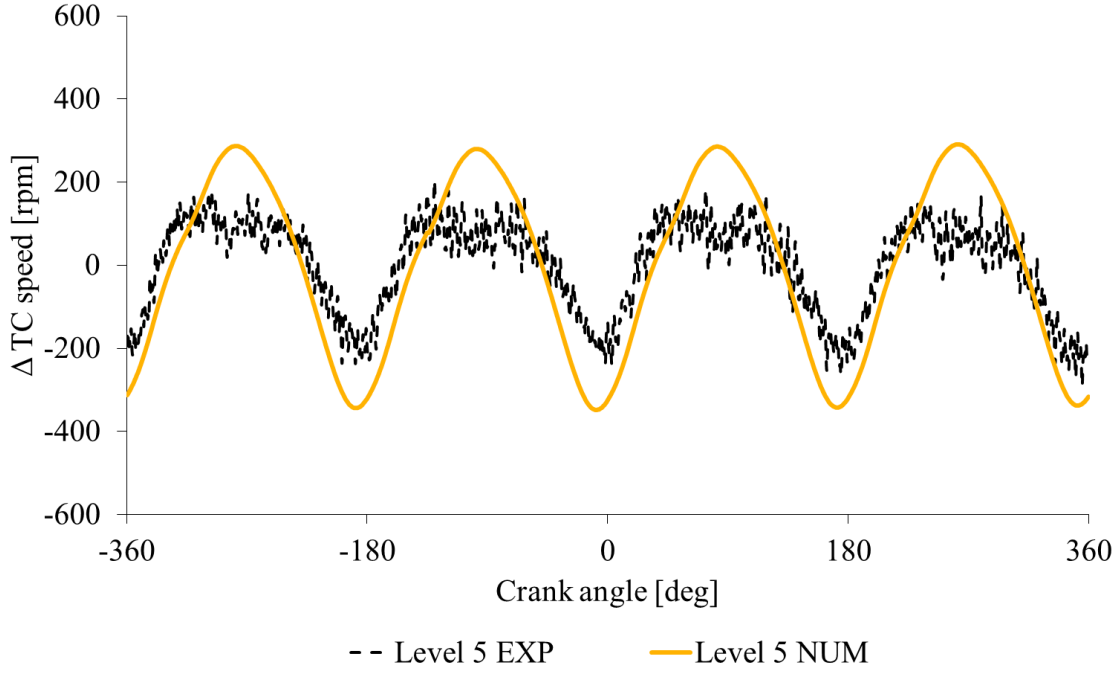

Figure 10. Instantaneous Δ TC speed in function of the crank angle (numerical and experimental data); operating condition load level 5 at 1750 rpm

The numerically and experimentally investigated cases at 3000 rpm highlight that the experimental data is affected by noise and irregularity. This issue is related to the acquisition frequency used to acquire instantaneous TC speed data. Moreover, the irregular acquisition is related to the double peaks in the instantaneous TC speed every 180° CA (Figure 11)

detected with the numerical model and consequence of the scavenging process and so to the valve overlap (strictly linked to the behavior of the inlet turbine pressure Figure 12). In the next chapter, a more detailed analysis of the TC speed behavior at 3000 rpm is discussed.

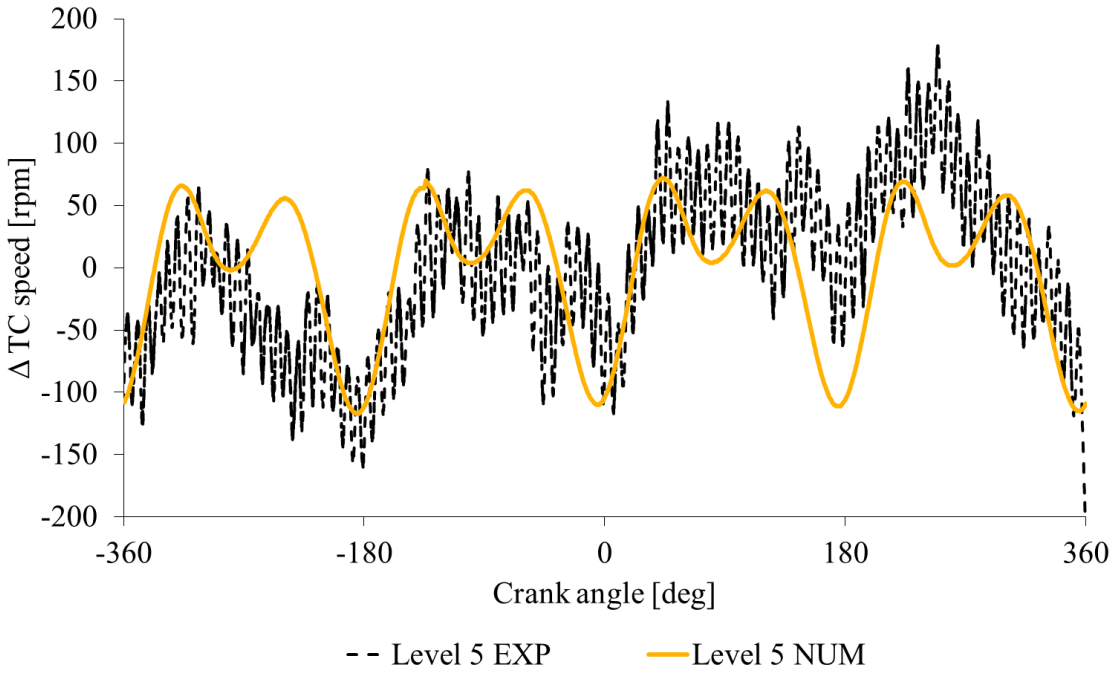

Figure 11. Instantaneous Δ TC speed in function of the crank angle (numerical and experimental data) at a specific operating condition (load level 5 at 3000 rpm)

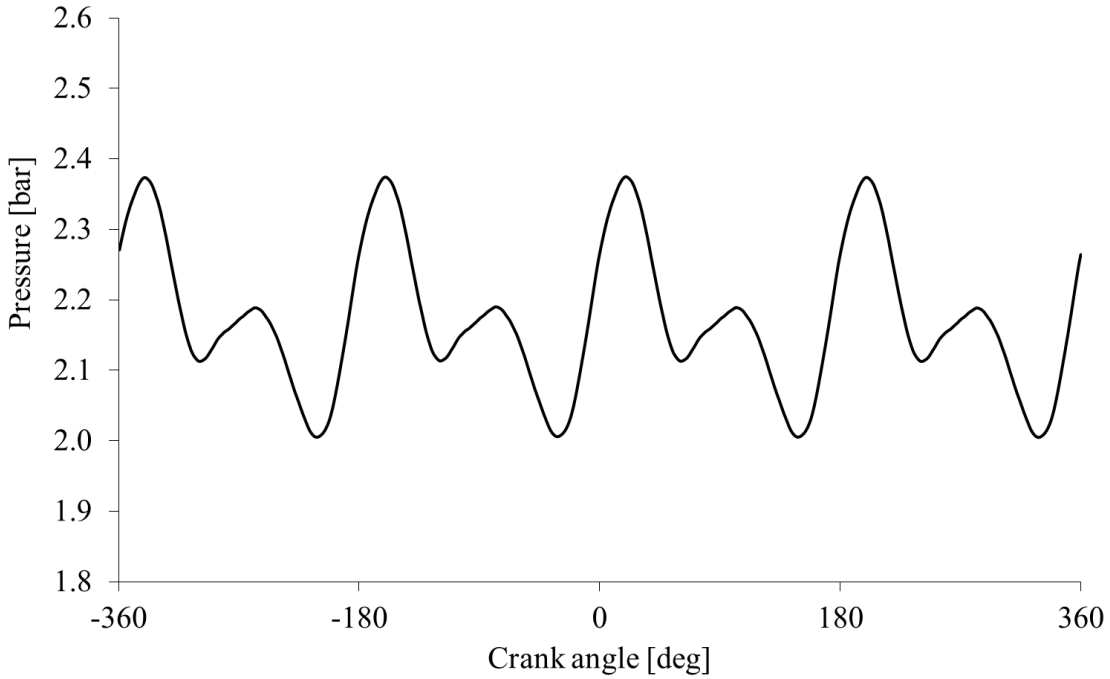

Figure 12. Dynamic pressure at the turbine inlet at a specific operating condition (load level 5 at 3000 rpm); numerical data.

3 Injectors Performance Prediction based on Turbocharger Speed

The following step of the activity, reported in this chapter, aims to assess the feasibility of the Injectors performance prediction based on Turbocharger Speed signal by exploiting the calibrated engine numerical model. With this goal in mind three numerical approaches have been developed and then experimentally validated.

The numerical activity was performed by analyzing the sensitivity of the instantaneous TC speed to the cylinder-to-cylinder and to global injection variation. Several injection variations were investigated in different engine working points. Three processing methodologies of the instantaneous TC speed signal have been developed combined with the related injection monitoring strategies with the aim to measure the actual fuel quantity injected into each cylinder. The methodologies were developed to take into account the contribution of each cylinder and are based on:

- The area subtended the TC speed signal named integral methodology
- The acceleration of the turbocharger equal to the derivative of the TC speed signal
- The frequency content of the TC speed signal analyzed by means of a Fast Fourier Transformation of the signal

3.1 Acceleration Methodology

The first methodology developed is based on the TC speed in the time domain. The acceleration methodology, as the name suggests, exploit the TC acceleration information contained in the TC speed signal. The evolution of the TC speed during an engine cycle is directly influenced by the pressure waves at the turbine inlet, indeed, the force that drives the turbocharger coming from the energy content of the flow at the engine exit. The previous statement led to consider the TC acceleration determined mostly by the exhaust pressure upstream the turbine, since this pressure, in turn, depends on the engine combustion process and so to the fuel quantity injected in each cylinder, it is reasonable to consider the TC acceleration as a fuel injection monitoring parameter.

As an example, in Figure 13 it is shown the good accordance between TC acceleration and pressure waves.

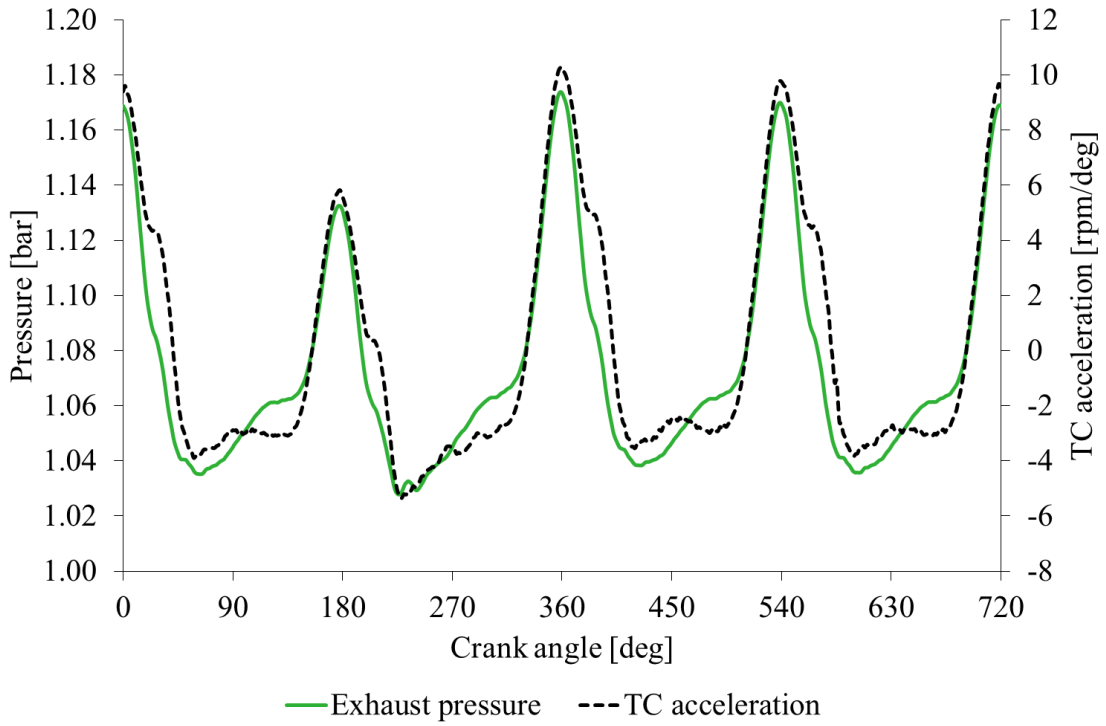

Figure 13. Pressure in the exhaust manifold VS TC acceleration. Engine operating condition: 1000rpm at Level 2 by varying the injected fuel quantity in the cylinder 1 (-3mg). Numerical results

To evaluate the possibility of determining injector performance variation through TC acceleration, cases with homogeneous and inhomogeneous injection are compared.

In Figure 14 and Figure 15, the TC acceleration in case of a cylinder-to-cylinder injection variation is compared with respect to the reference baseline case. Within a very first evaluation from the comparison discussed, it can be seen that the differences between the peaks of the two acceleration profiles allow one identifying the inhomogeneity of the injection in one or more cylinders.

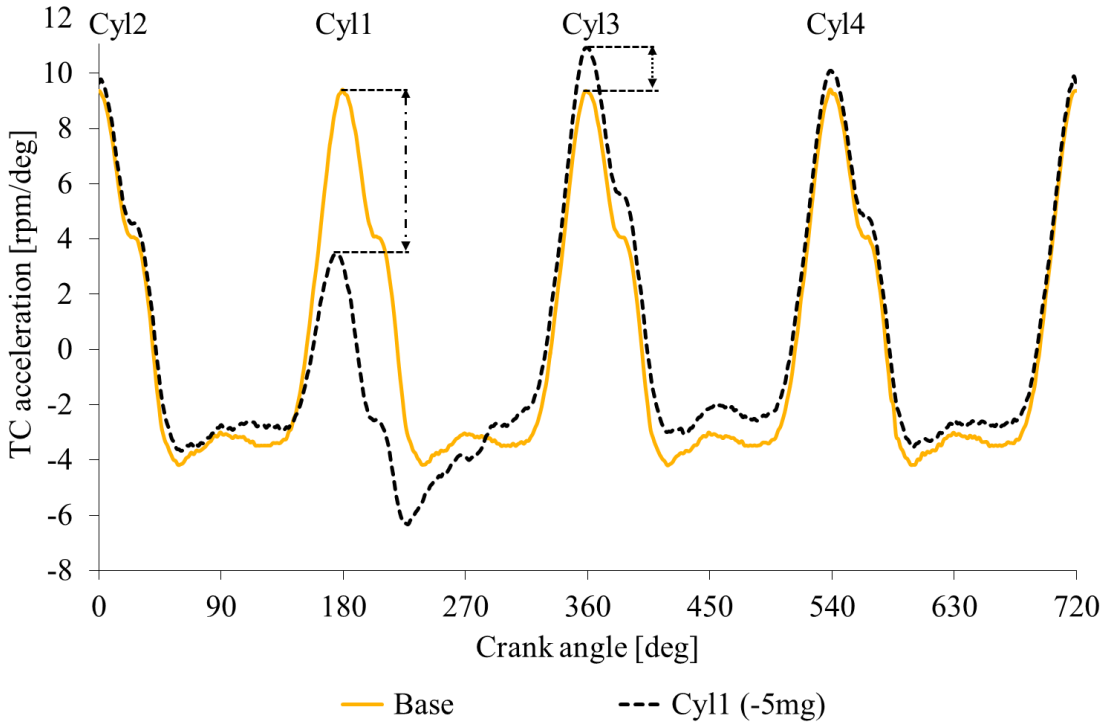

Figure 14. TC acceleration signal. Engine operating conditions: 1000rpm at Level 2, base injection and injection variation in the cylinder 1 (-5mg).

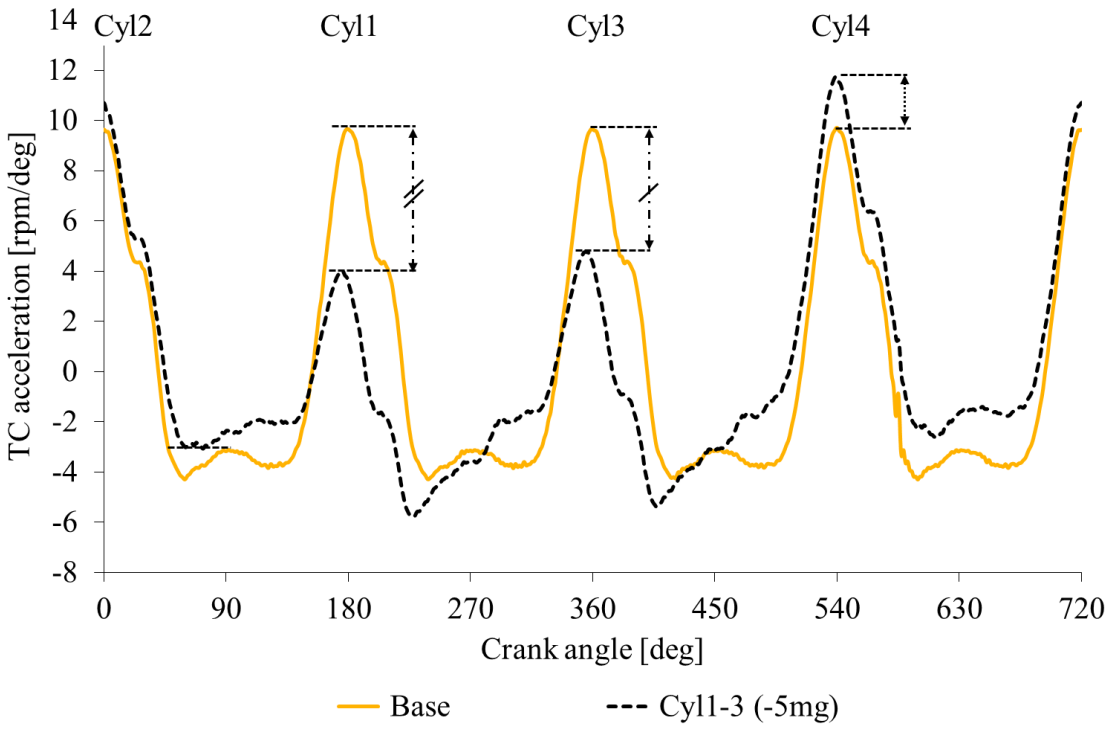

Figure 15. TC acceleration signal. Engine operating conditions: 1000rpm at Level 3, base injection and same injection variation in cylinder 1 and cylinder 3 (-5mg).

However, it can be noticed immediately that a not negligible difference in terms of acceleration peaks is experienced also for the cylinders with the regular fuel injection. Further, considering the results in Figure 15, despite the imposed injection variation in cylinders 1 and 3 is the same, the differences in the acceleration peak with respect to the reference baseline case are not equal. Consequently, it seems not possible to quantify exactly the cylinder-to-cylinder injection variations by considering only the difference in the acceleration peak linked to each cylinder.

Going one step back, to identifying the cylinder associated with the acceleration peak the whole engine cycle has to be divided into four crank-angle windows in which each cylinder gives the major contribution to the instantaneous TC speed oscillation. With this aim, it is considered the minimum value of the TC speed as the end of the contribution of one cylinder, indeed, when the pressure wave associated with one cylinder run out its influence the TC speed experiences its minimum value. Although, after the minimum value the TC speed starts to increase, this phase can be associated with the opening of the exhaust valve of the subsequent cylinder (in terms of firing order). Summing up, windows of influence are defined starting from the minimum value of the TC speed and moving by

step of 180° of CA (in case of a 4 cylinders' engine). Till now all the acceleration peaks are considered in the respective influence window of each cylinder.

Now, to overcome the issue related to the misleading differences in terms of acceleration peaks in the cylinder without injection variation or with the same injection variation, the methodology developed reckon on the evaluation of the acceleration peak subtracted to the average acceleration for each specific window. This operation is made to limit the mutual influence among cylinders that can be represented by the base average exhaust pressure and so to the average acceleration among different windows.

In Figure 16 and Figure 17, the instantaneous TC acceleration subtracted from the average value for each cylinder-window is depicted in comparison with the actual acceleration and the baseline case. Considering the actual acceleration subtracted from the average value (scaled acceleration, "Acc - avg Acc"), the difference in terms of peaks for the cylinders without any difference in terms of injection becomes negligible with respect to the baseline case. The results depicted in Figure 17 show that peaks referred to cylinder 1 and 3, in which the same injected fuel reduction is imposed, have the same value as expected.

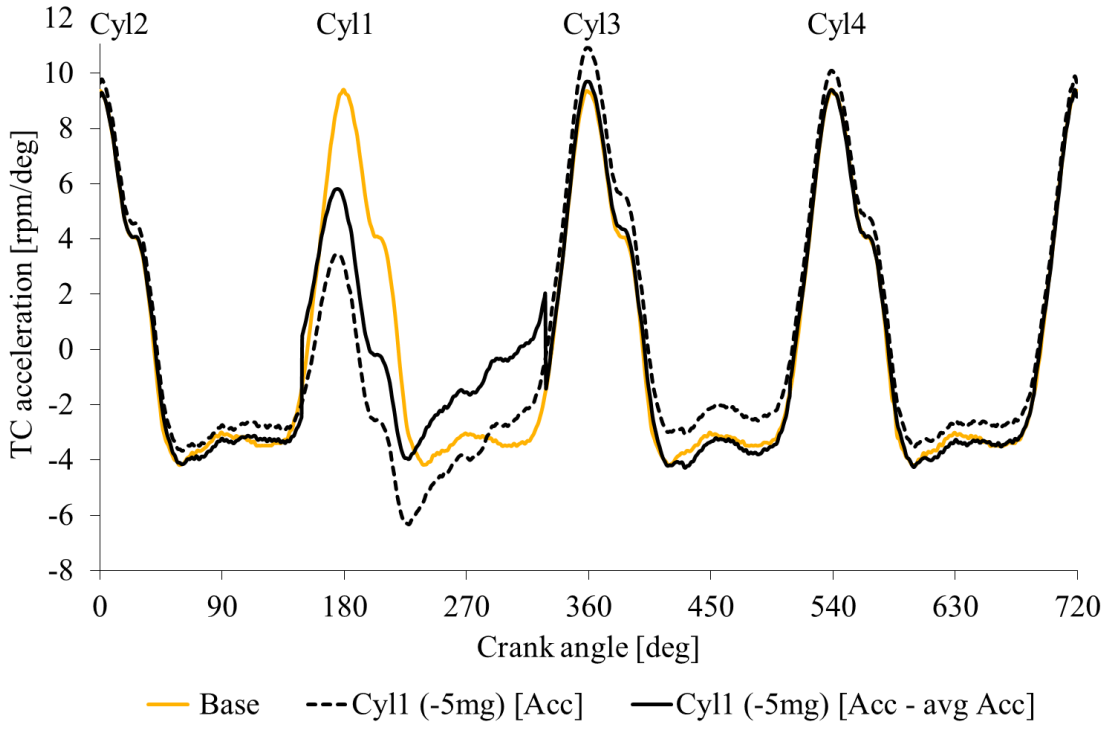

Figure 16. TC acceleration signal. Engine operating conditions: 1000rpm at Level 2, base injection and injection variation in the cylinder one (-5mg). The continuous black line is the scaled instantaneous TC acceleration reduced by the mean value for each cylinder-window.

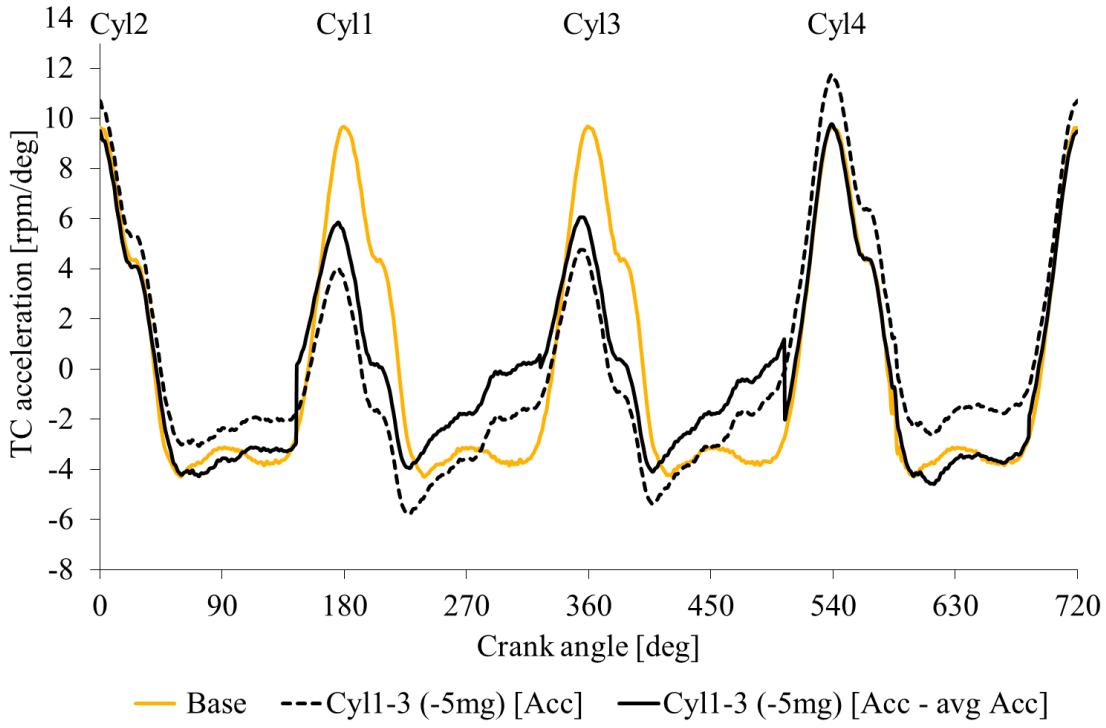

Figure 17. TC acceleration in case of two engine operating conditions: 1000rpm at Level 3, base injection and same injection variation in cylinder 1 and cylinder 3 (-5mg). The continuous black line is the scaled instantaneous TC acceleration reduced by the mean value for each cylinder-window.

To easily identify this methodology a parameter is here defined as TurboCharger Acceleration Factor (TCAF). The TCAF is defined for each cylinder as the maximum acceleration value reduced by the average one calculated in the related contribution window, which brings to the definition of two simple equation:

$$TCAF_{Cyl\ i} = acc_{peak} - acc_{avg}^{\vartheta_f,\vartheta_i} \quad (1)$$

$$acc_{avg}^{\vartheta_f,\vartheta_i} = \frac{\omega_{TC}(\vartheta_f) - \omega_{TC}(\vartheta_i)}{\vartheta_f - \vartheta_i} \quad (2)$$

The TCAFCyl i is related to the fuel quantity injected in the ith cylinder. It is noted that in case of regular injection the average acceleration of each window is zero.

To identify the variation of the injection respect to the baseline, the percentage variation is considered. In Figure 18, the acceleration processing results are shown in terms of percentage variation of the TCAFCyl i with respect to the baseline value in case of regular injection. The negligible TCAF percentage variation for the cylinders with unchanged injected fuel quantity and the negligible difference between cylinders with the same injection variation has to be underlined. The acceleration method developed shows a good reliability for the development of an injection monitoring strategy.

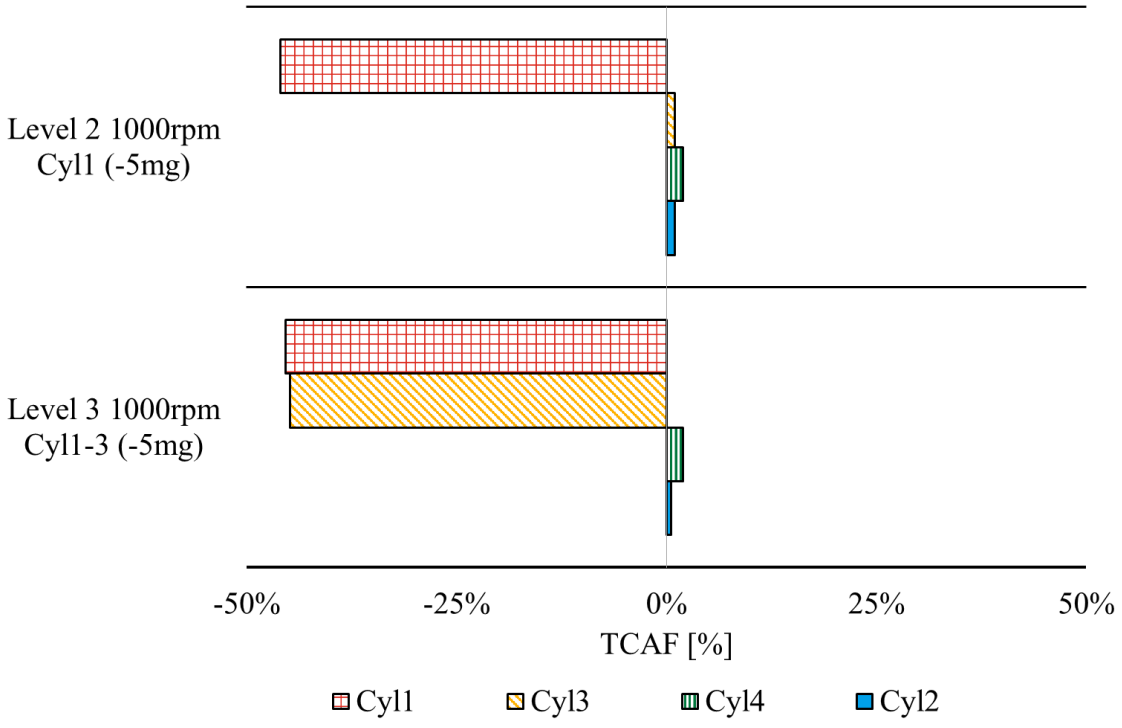

Figure 18. TCAF in percentage terms. Engine operating conditions: 1000rpm at Level 2 by varying the injected fuel quantity in the cylinder 1 (-5mg), and 1000rpm at Level 3 by varying of the same quantity the injected fuel in cylinder 1 and cylinder 3 (-5mg).

3.1.1 Engine Operating Range for the Injection Monitoring

The reliability of the acceleration methodology for the injector performance monitoring is limited by the engine speed. During the development phase engine speeds from 800rpm (idle condition) to 3000 rpm have been numerically tested. The result of the numerical test at different engine speed is reported in Figure 19 and demonstrate that at high engine rotational speed (3000rpm) the correlation between TCAF parameter and injected fuel in one of the cylinders is completely not exploitable.

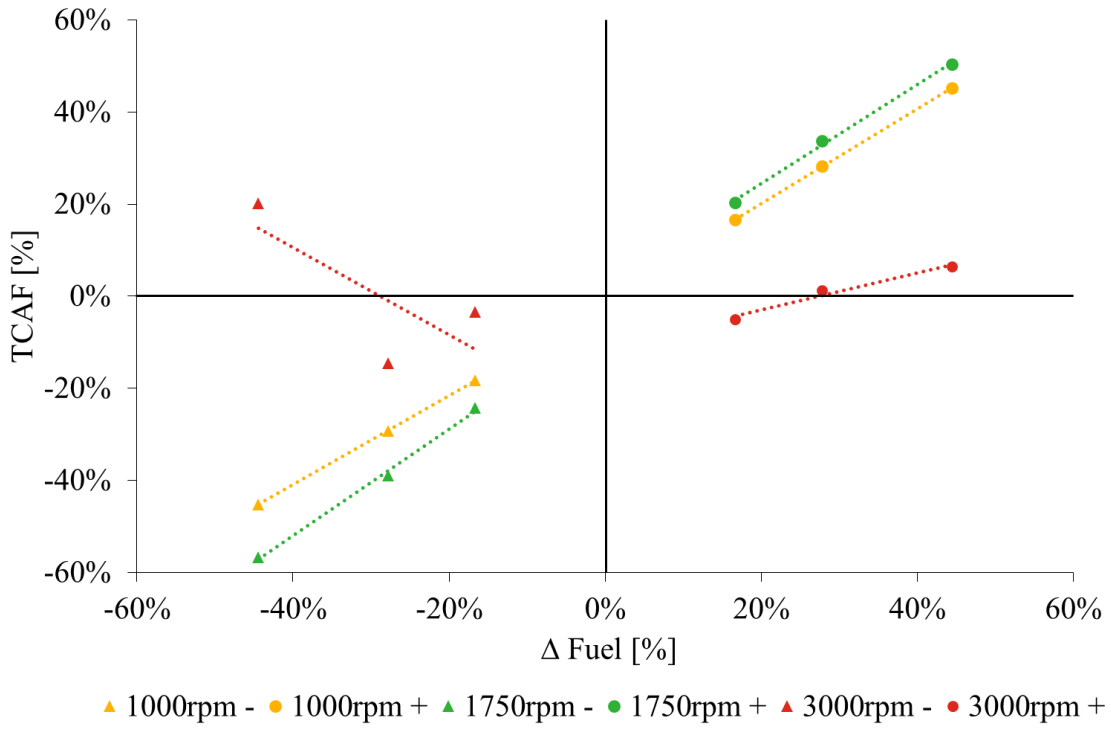

Figure 19. TCAF (as % difference with respect to the standard condition) function of the percentage fuel variation at three different engine speeds (1000rpm, 1750rpm and 3000rpm): starting from the base load 3, the fuel variations ±3mg, ±5mg and ±8mg are imposed in the cylinder 1.

The main causes that lead to this discrepancy, among different engine rotational speeds, are listed and explained above:

- At high engine rotational speed the scavenging phase managed by the valve overlap cause the pressure wave coming from the inlet duct, so from the compressor, to influence the pressure at the turbine inlet (i.e. the lower peak of the pressure oscillation subsequent to the main peak shown in Figure 20) and to affect, in not negligible way, the instantaneous TC speed (Figure 21 (a)).
- High engine speed results in pressure pulses, and consequently in instantaneous TC speed oscillations, characterized by a very high frequency (Figure 21 (b)), indeed, the frequency of the pressure pulse that drives the turbine is directly related to the engine speed as reported in eq. 3

$$f = 2\,N\,n_{cyl}\,T^{-1} \quad (3)$$

where n_{cyl} is the number of cylinders, N is the average engine speed and T is the number of strokes of the engine. This frequency is called firing frequency.

Since the turbine response is mostly affected by its inertia (for example, at fixed load without cylinder-to-cylinder injection variations the oscillation amplitude becomes lower by increasing the engine speed (Figure 21 b)) and the higher is the engine speed, the lower is the time available for the turbocharger to vary its speed, the difference between the acceleration trend and the pressure oscillation increases with respect to the low regime (Figure 22) and the TC speed signal is not able to give useful information about the cylinder-to-cylinder injection variation (Figure 23).

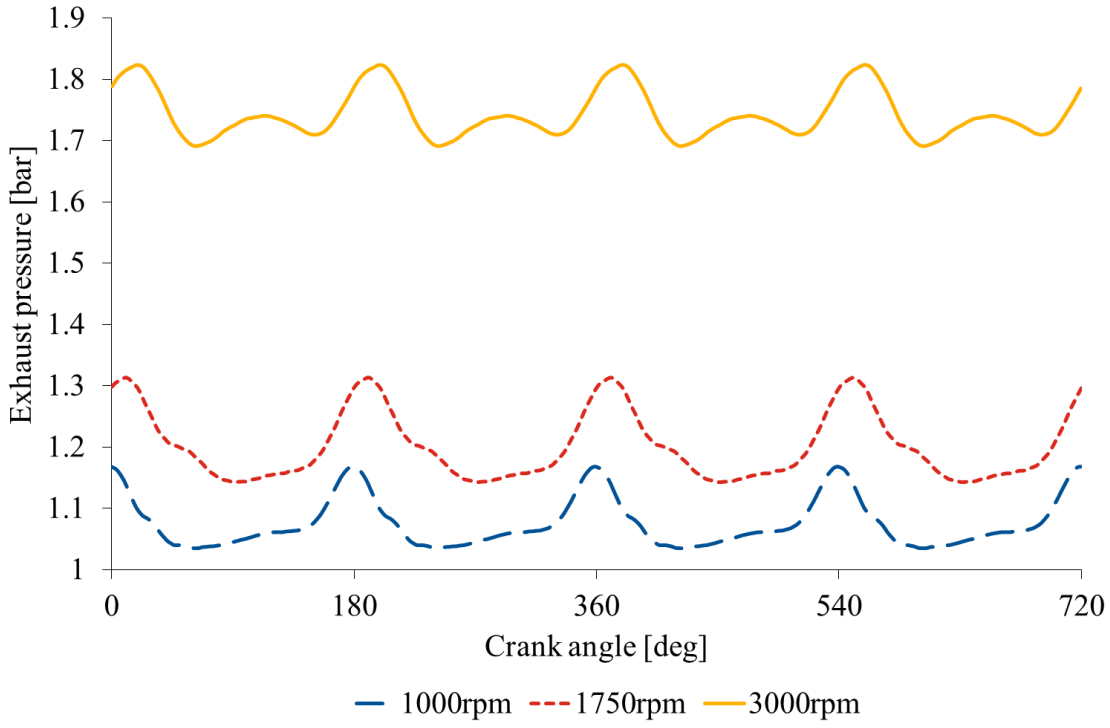

Figure 20. Pressure in the exhaust manifold. Engine operating condition at Level 3 at 1000rpm, 1750rpm and 3000rpm.

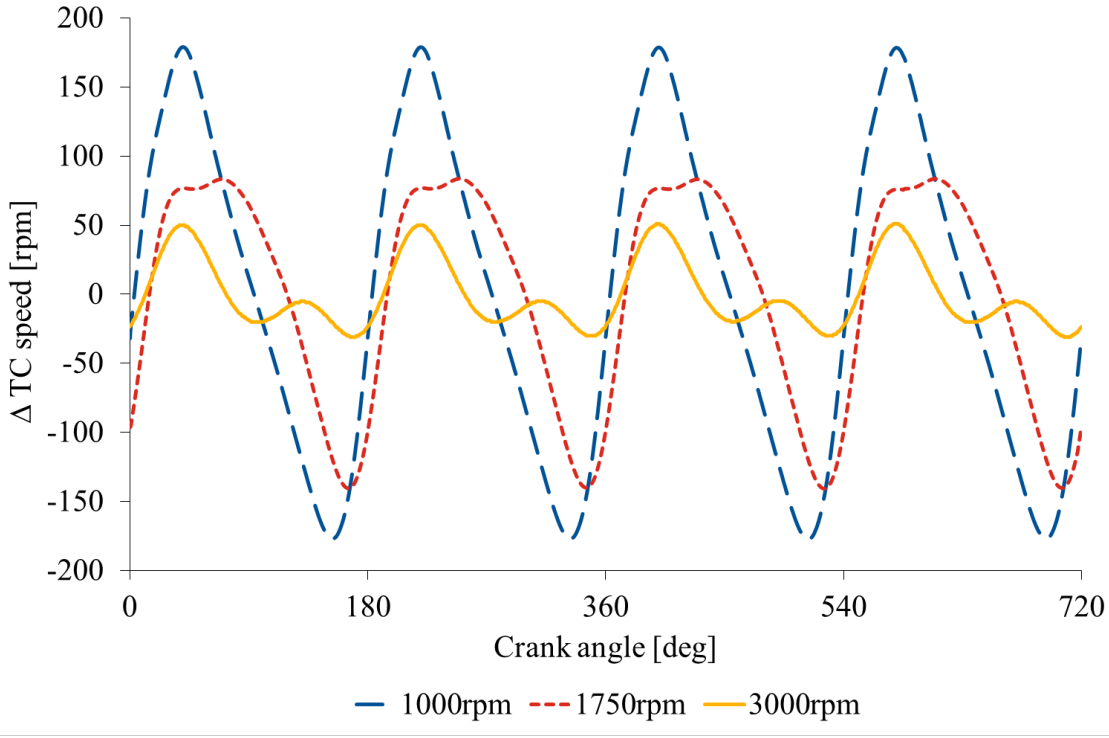

a.

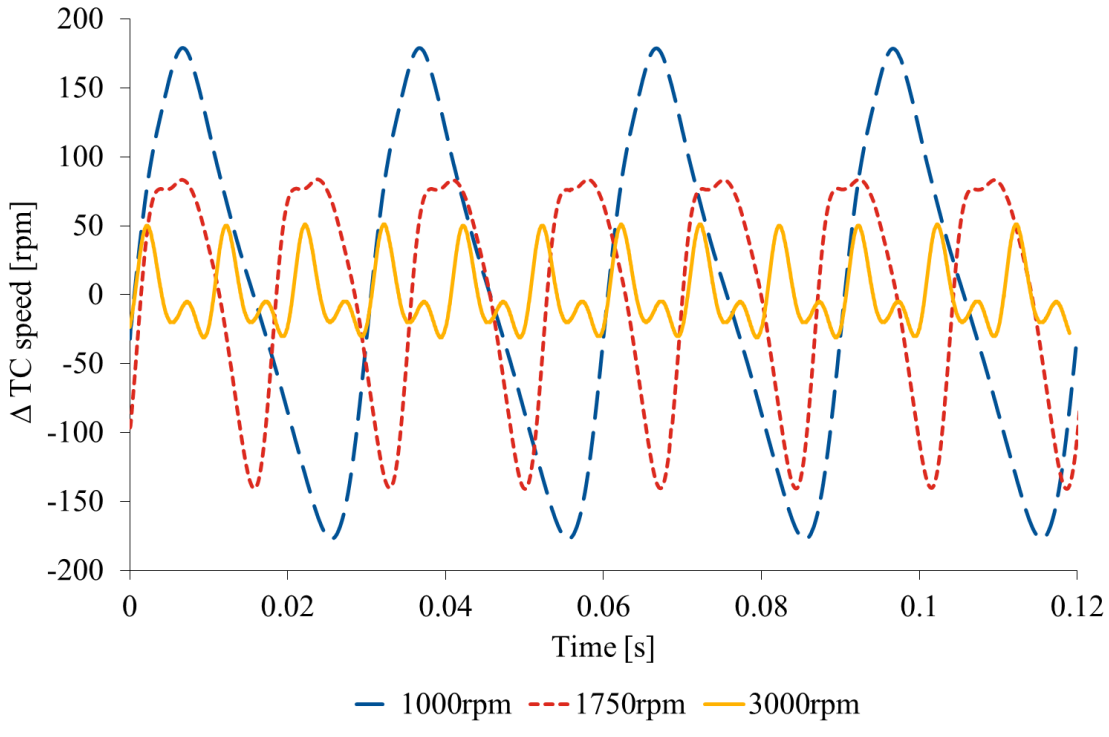

b.

Figure 21. Oscillation of the instantaneous TC speed: Engine operating condition at Level 3 at 1000rpm, 1750rpm and 3000rpm. (a) Function of the crank angle; (b) Function of the time.

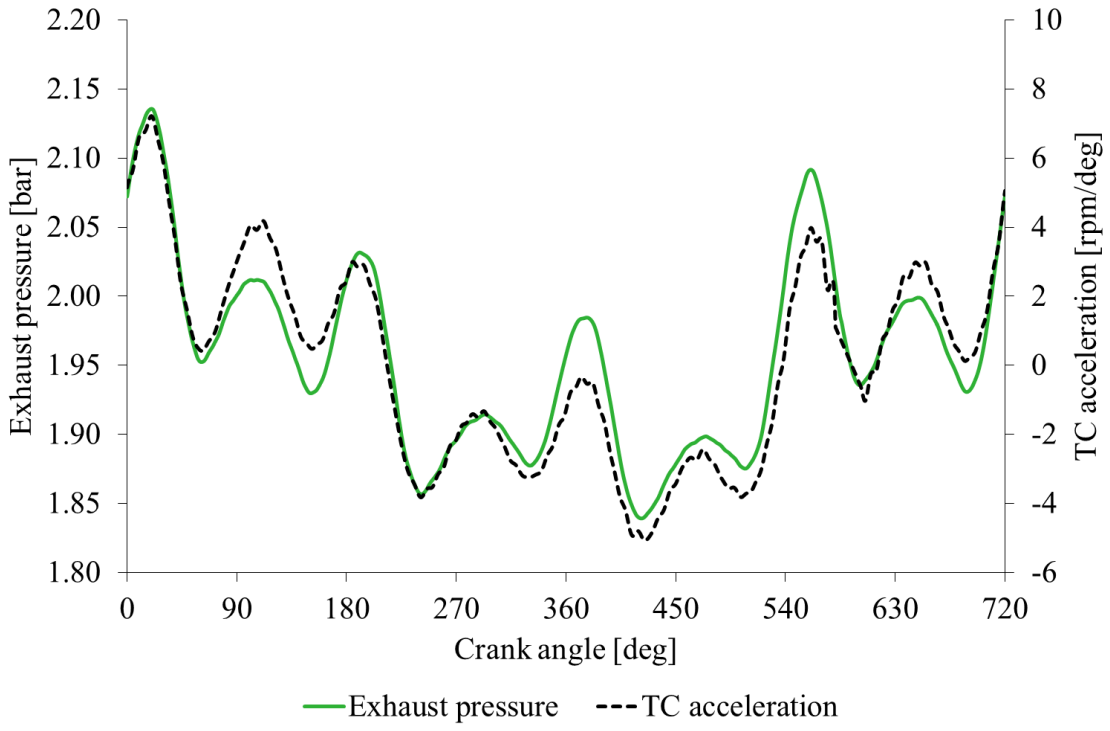

Figure 22. Comparison between pressure in the exhaust manifold and TC acceleration. Engine operating condition: 3000rpm at Level 3 by varying of the same quantity the injected fuel in cylinder 1 and cylinder 3 (-5mg).

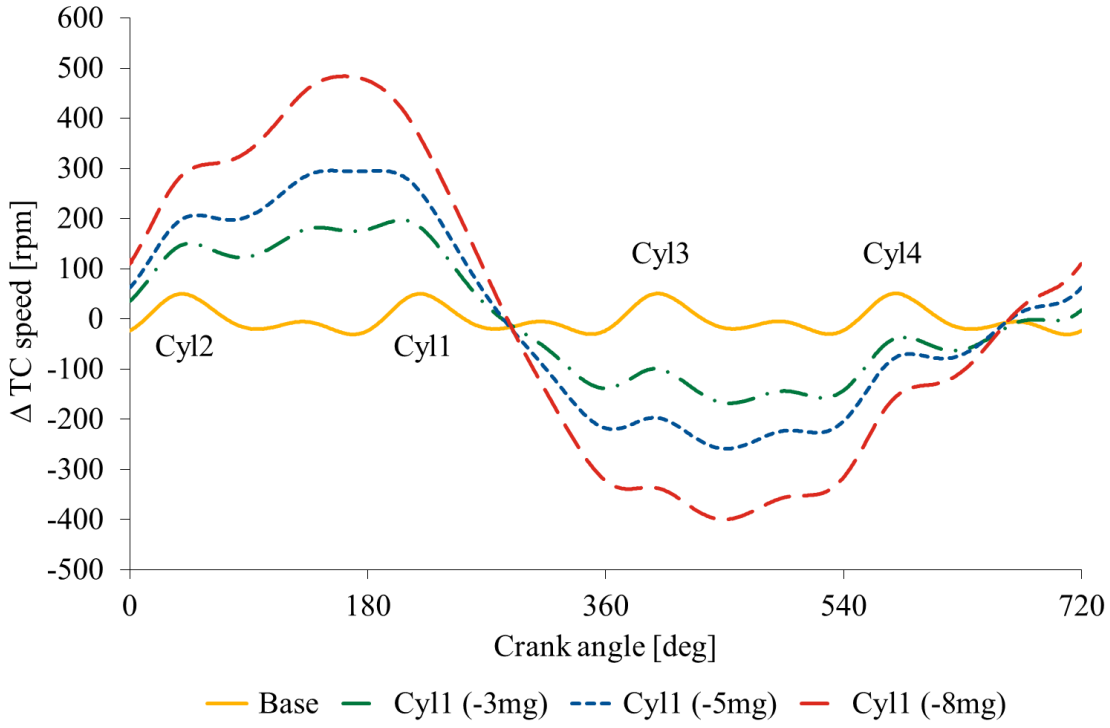

Figure 23. Oscillation of the instantaneous TC speed starting from the baseline engine operating condition at 3000rpm at Level 3 by varying the injected fuel quantity in the cylinder 1 (-3mg, -5mg and -8mg).

3.1.2 Correlation for the Injection Monitoring

A first numerical correlation to verify the possibility to evaluate the fuel injected into each cylinder exploiting the instantaneous TC speed signal is reported in this paragraph. With this aim, for each cylinder of the engine, the actual value of the injected fuel quantity and the related value assumed by the control parameter TCAF are considered.

The engine operating conditions that were considered are: 1 engine speed (i.e. 1000 rpm) at three loads (Level 2, Level 3 and Level 5) in standard configuration and by imposing a variation in the injected fuel quantity in the cylinder 1 only, in the cylinders 1 and 3, and in the cylinders 1 and 4 (±1mg, ±2mg ±3mg and ±5mg).

As mentioned before for each cylinder the actual quantity of the injected fuel and the related value of the TCAF parameter were taken into account. As shown in Figure 24 a linear correlation was found between TCAF and actually injected fuel:

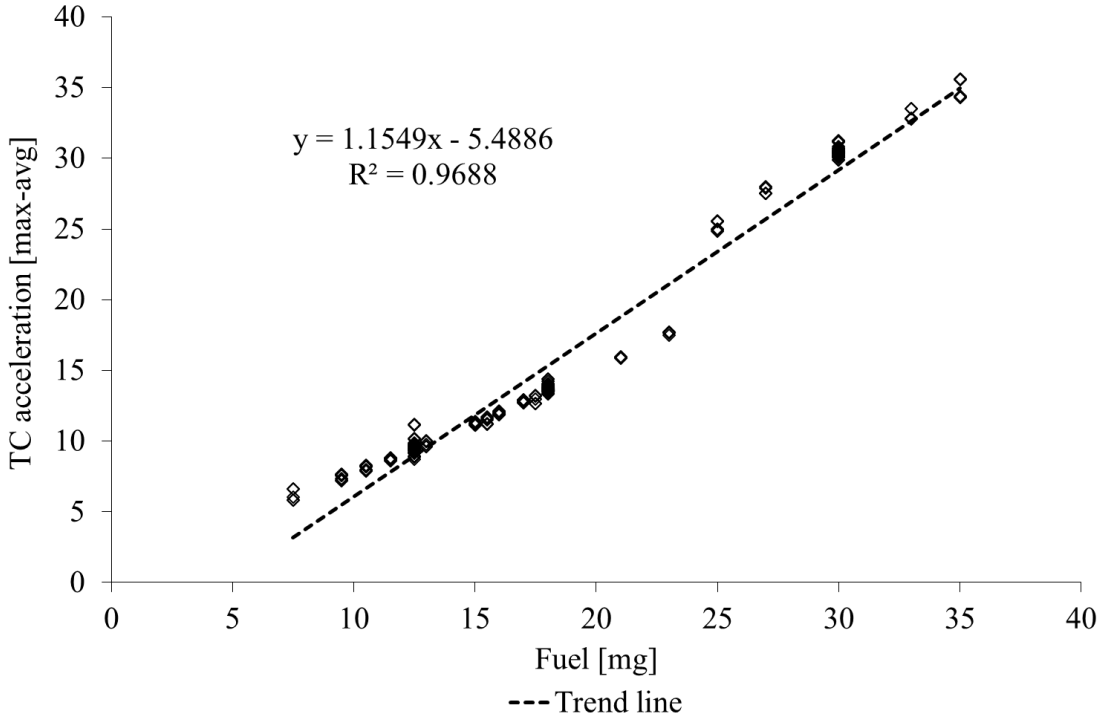

Figure 24. Correlation between injected fuel quantity in each cylinder and the related TCAF value. Operating conditions considered: fuel injection variations in cylinder 1 only, in cylinders 1 and 3, and in cylinders 1 and 4 equal to ±1mg, ±2mg ±3mg and ±5mg, at 1000rpm starting from the loads 2, 3 and 5.

The direct correlation between the injected fuel quantity in each cylinder and the related value of the monitoring parameters (TCAF) is reliable and could be exploited for the purpose of this study so, to perform the detection and eventually the correction of the injector performance in terms of fuel injected, with the exception of the engine working points at high engine speed (equal or above 3000 rpm).

3.2 Integral Methodology

The second methodology developed is based on the turbocharger speed time domain analysis. Since the already stated connection between the angular displacement of the turbocharger and the pressure boost given by each cylinder, directly dependent on the energy released in the combustion chamber and to the injected fuel quantity, the monitoring of the TC speed integral (i.e. angular displacement) was considered suitable for the injector performance estimation. With the aim to evaluate the contribution of each cylinder to the instantaneous TC speed, the cycle period was divided by the number of the cylinders. The division was made exactly in the same way respect to the acceleration methodology. As mentioned above, each cylinder affects the TC speed in a specific window of the whole engine cycle.

In order to take into consideration, the contribution of each cylinder and limiting the mutual influence among cylinders, the integral method associates for each cylinder the area limited by the instantaneous TC speed and the segment joining the initial and final values of the specific contribution window. The subtracted area depends on the contribution of the velocity that varies with constant acceleration. The graphical representation of the area described is depicted in Figure 25.

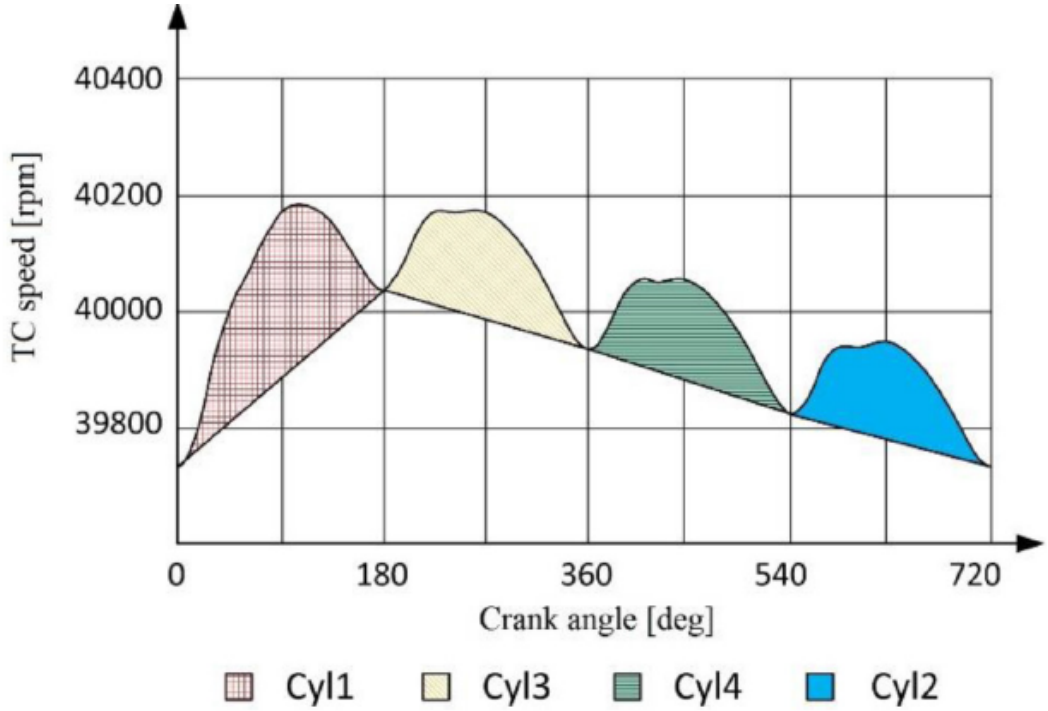

Figure 25. Integration methodology, a graphical representation

In the described methodology the name of TurboCharger Speed Factor (TCSF) was assigned to the integral value, defined as follows:

$$TCSF_{Cyl\,i} = \int_{\theta_i}^{\theta_f} \omega_{TC} \cdot d\theta_{\text{engine}} - \frac{\omega_{TC}(\vartheta_f) - \omega_{TC}(\vartheta_i)}{2} \cdot (\theta_f - \theta_i) \qquad (4)$$

The $TCSF_{Cyli}$ is related to the fuel quantity injected in the i-th cylinder.

3.2.1 Engine Operating Range for the Injection Monitoring

For what concerns the engine operating range the same consideration showed in chapter 3.1.1 for the acceleration methodology can be done. The result of the numerical test at different engine speed is reported in Figure 26 and demonstrate as for the acceleration methodology at high engine rotational speed (3000rpm) the correlation between TCSF parameter and injected fuel in one of the cylinders is not usable for the monitoring of injectors performance.

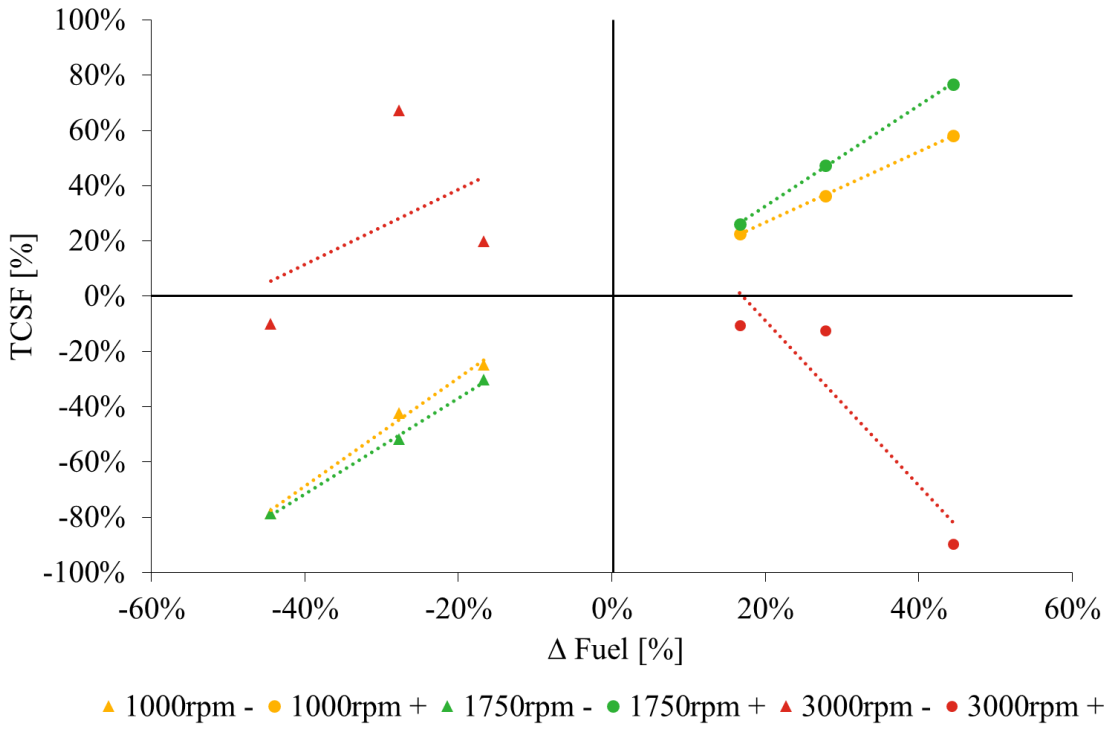

Figure 26. TCSF (as % difference with respect to the standard condition) function of the percentage fuel variation at three different engine speeds (1000rpm, 1750rpm and 3000rpm): starting from the base load 3, the fuel variations ±3mg, ±5mg and ±8mg are imposed in the cylinder 1.

3.2.2 Correlation for the Injection Monitoring

A numerical correlation to directly evaluate the fuel injected into each cylinder exploiting the instantaneous TC speed signal is reported in this paragraph. With this aim, for each cylinder of the engine, the actual value of the injected fuel quantity and the related value assumed by the control parameter TCSF are considered.

The engine operating conditions that were considered are: one engine speed (i.e. 1000 rpm) at three loads (Level 2, Level 3 and Level 5) varying the injected fuel quantity in the cylinder 1 only, in the cylinders 1 and 3, and in the cylinders 1 and 4 (±1mg, ±2mg ±3mg and ±5mg).

As mentioned before for each cylinder the actual quantity of the injected fuel and the related value of the TCSF parameter were taken into account. As shown in Figure 27 a linear correlation was found between TCSF and actual injected fuel:

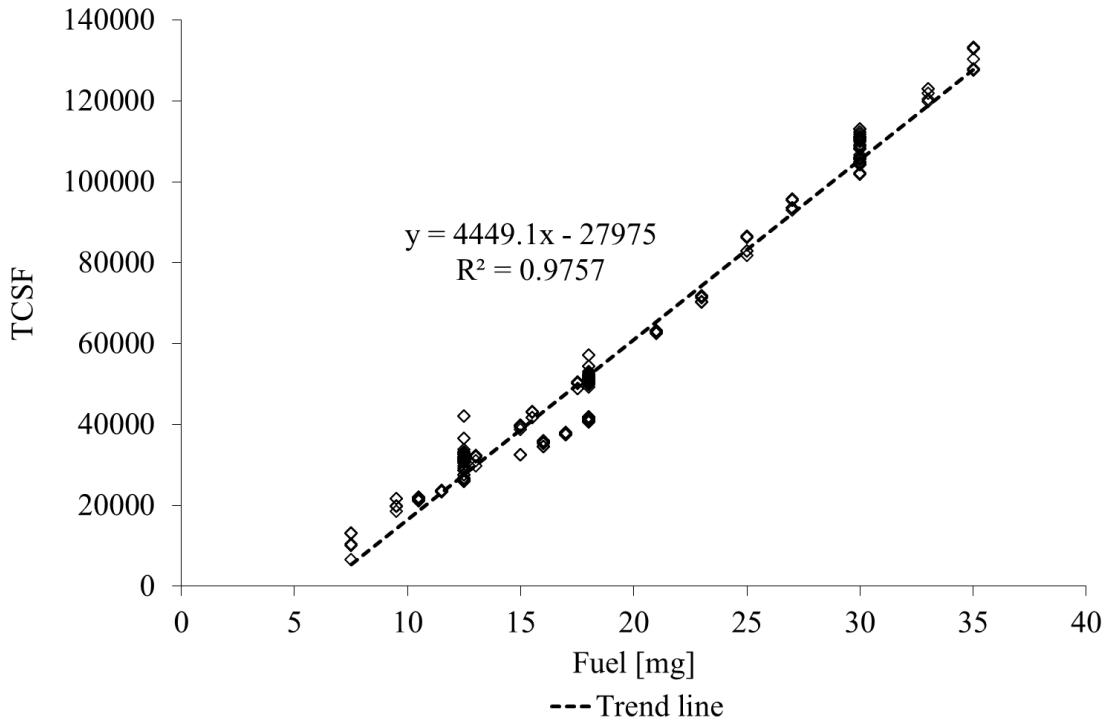

Figure 27. Correlation between injected fuel quantity in each cylinder and the related TCAF value. Operating conditions considered: fuel injection variations in cylinder 1 only, in cylinders 1 and 3, and in cylinders 1 and 4 equal to ±1mg, ±2mg ±3mg and ±5mg, at 1000rpm starting from the loads 2, 3 and 5.

The direct correlation between the injected fuel quantity in each cylinder and the related value of the monitoring parameters (TCSF) is reliable and could be exploited for the purpose of this study so, to perform the detection and eventually the correction of the injector performance in terms of fuel injected, with the exception of the engine working points at high engine speed (equal or above 3000 rpm).

3.3 Frequency Content Methodology

The preliminary numerical study on the frequency content of the TC speed is based on the periodic nature of the engine while working in steady-state condition. More in detail, when the performance of all injectors allow to supply the same fuel quantity in each cylinder most of the engine working variables, such as the instantaneous speed of the crankshaft, the intake and exhaust dynamic pressure and the instantaneous turbocharger speed, exploited in different ways for the condition monitoring of the engine, will be characterized by the same main frequency, the firing one.

Taking advantage of the engine numerical model calibrated in the first phase, the TC speed data were obtained for a whole engine cycle in steady state conditions and analyzed by means of an FFT function in MatLab code ambient. The sampling rate of the instantaneous TC speed is equal to 0.5deg in the crank angle domain.

In the performed FFT analysis, only the frequencies equal or lower than the firing one are considered as relevant, since they are the only one related to the injector performance. It is important to underline that, for this study, the frequency analysis was implemented considering not the frequencies but the orders, which consider the crank angle instead of time, by proceeding with orders it was possible comparing easily the methodology at different engine speed.

A description of each order considered is reported following:

- F1, first order: corresponds to one event for each engine cycle; it will be dominant in case of injection variation on one cylinder or in case of an equal injection variation in two cylinders consecutive in the firing order (1&3 or 2&4) (Figure 28 and Figure 29) defined as the equation 5

$$\mathrm{F1} = \frac{1}{4}\,\mathrm{f} = \frac{1}{2}\,\mathrm{N} \qquad (5)$$

- F2, second order: corresponds to two events for engine cycle; this order becomes dominant in the specific case in which there is an equal injection

for the non-consecutive cylinders in the firing order (1&4 and 2&3) (Figure 30)

- F3, third order: corresponds to three events for each engine cycle; not connected with a specific injection case

- F4, fourth order: corresponds to four events for each engine cycle; it represents the firing frequency and it is the main one in case of homogeneous injection (black columns in Figure 28, Figure 29 and Figure 30)

$$F4 = f = 2\,N \qquad (6)$$

As shown in Figure 28, the module of the first order in case of an injection variation in only one cylinder becomes the main one while the other three orders present a module not negligible.

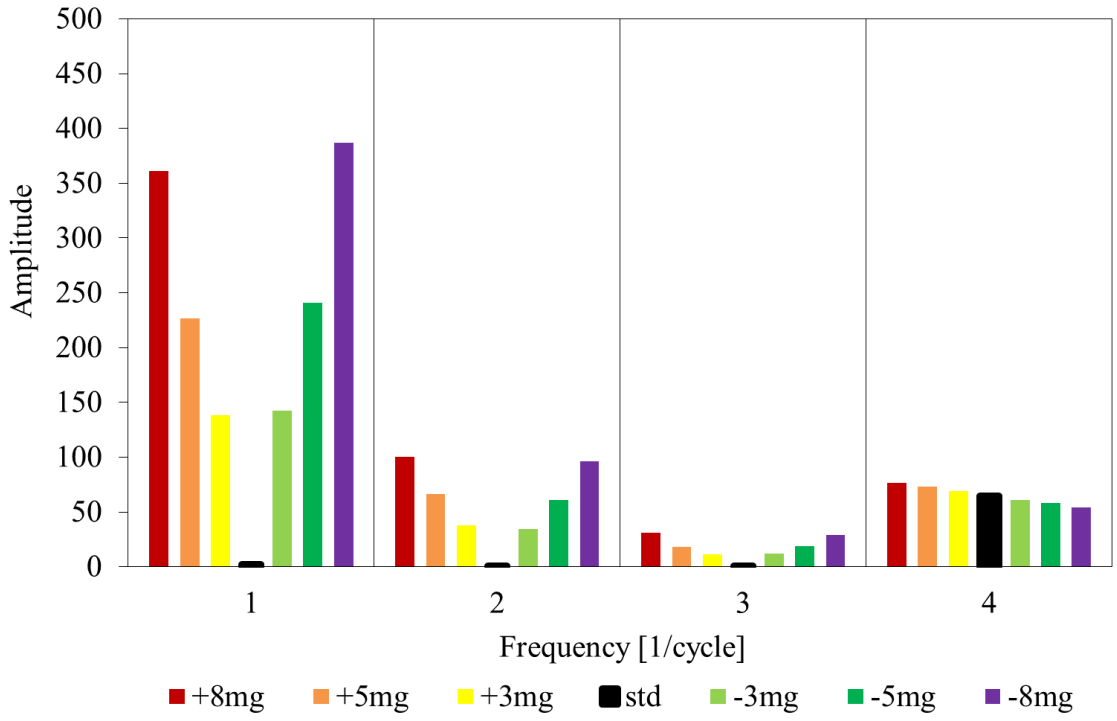

Figure 28. Modules of F1, F2, F3 and F4 in case of standard injection and several injection variations in one cylinder. Engine operating conditions: 3000rpm at Level 5.

In case of the homogeneous injection is experienced in two cylinders consecutive in the firing order at a time (1&3 and 2&4), the second order module can be neglected, indeed, in this case, the engine does not send any pressure information to the turbine with a two times per cycle frequency because of the consecutiveness of the cylinders that are functioning in homogenous condition, unless the negligible differences in the intake due to small TC speed differences. Conversely the modules of the orders F1, F3 and F4 keep a variation trend equal to the case with the injection variation imposed only in one cylinder (Figure 29). Further, even in this case, the first order module is the main one.

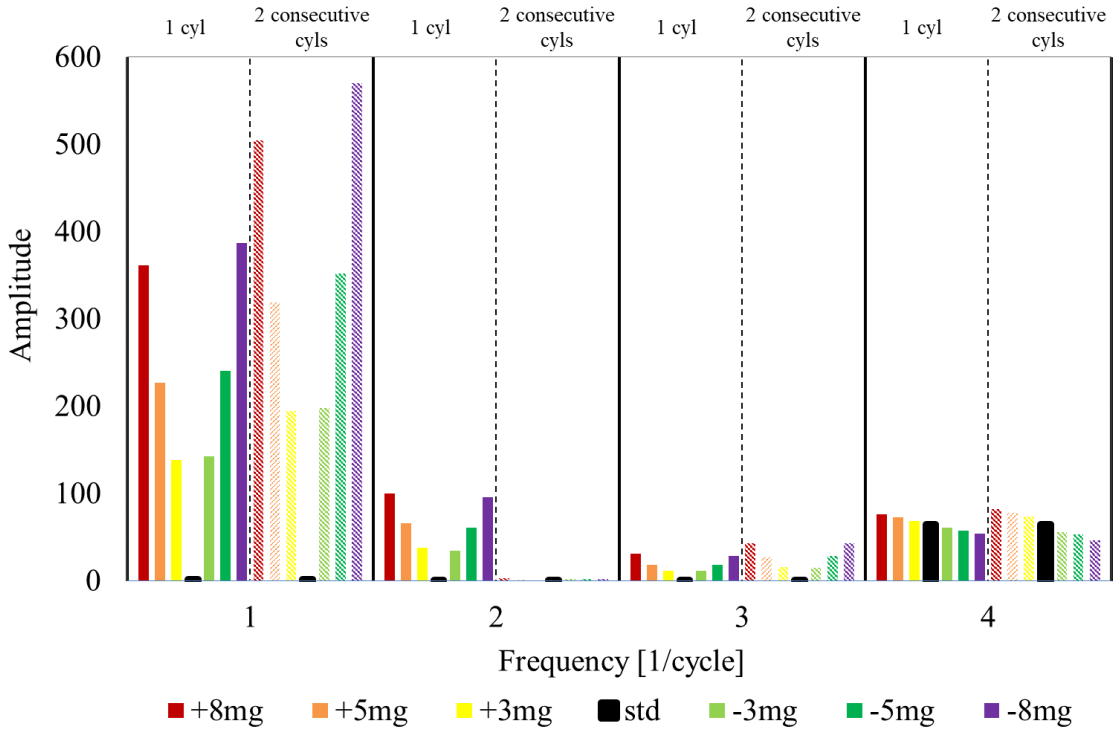

Figure 29. Modules of F1, F2, F3 and F4 in case of standard injection and several injection variations in two cylinders consecutive in the firing order (1&3 or 2&4) VS injection variations in one cylinder. Engine operating conditions: 3000rpm at Level 5.

In case of the homogeneous injection is experienced in two cylinders non-consecutive in the firing order at a time (1&4 or 2&3), the first and third order modules become negligible, conversely the modules of F2 and F4 keep the same variation trend of the case with the injection variation imposed only in one cylinder (Figure 30). The order F2 becomes the main one because of the nature of the pressure that drives the turbine is generated.

For the most common case in which injectors perform in different ways, all the modules of the four aforementioned orders present a relevant module, an example is depicted in Figure 31.

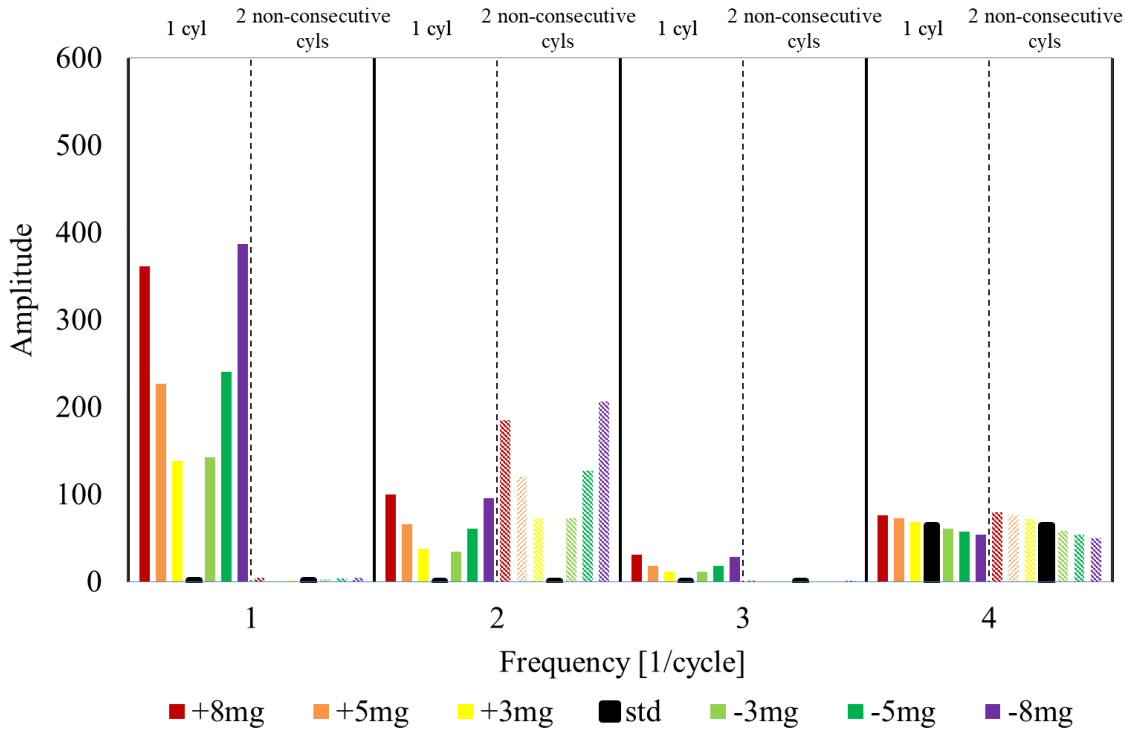

Figure 30. Modules of F1, F2, F3 and F4 in case of standard injection and several injection variations in two cylinders non-consecutive in the firing order (1&4 or 2&3) VS injection variations in one cylinder. Engine operating conditions: 3000rpm at Level 5.

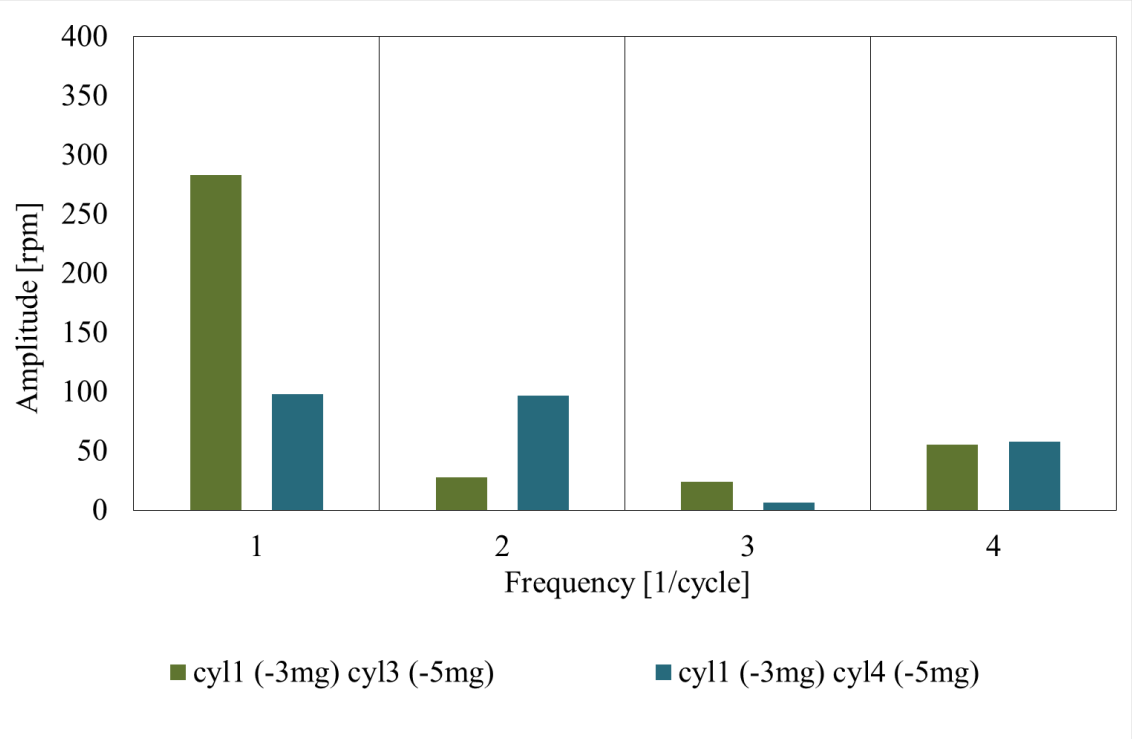

Figure 31. Modules of F1, F2, F3 and F4 in case of random injection variations in two cylinders consecutive and non-consecutive in the firing order (cylinders 1&3 and 1&4 respectively). Engine operating conditions: 3000rpm at Level 5.

3.3.1 Correlation for the Injection Monitoring

The frequency content methodology (FFT method) was developed to generate a numerical correlation to estimate the fuel injected into each cylinder exploiting the instantaneous TC speed signal and to eventually correct injection fault. In this paragraph was presented the correlation and a first algorithm for the correction of the fault.

3.3.1.1 Evaluation of the total amount of fuel

The fourth order module is associated with the base oscillation amplitude of the instantaneous turbocharger speed that in turns is directly linked to the total amount of injected fuel. In fact, an increase in the total injected fuel, maintaining constant the rotational engine speed, leads to an increase in the oscillation amplitude of the TC speed. For this reason, the F4, and in particular its module, is the order that allows one to correctly monitor the total quantity of the injected fuel.

However, the module of the fourth order, cannot be used for determining in which cylinder occurs the injection fault, indeed, as can be observed in Figure 32, if the same

change in the injected fuel is imposed in the cylinder 1 only or in the cylinders 1&3 (consecutive cylinders) and 1&4 (non-consecutive cylinders) the F4's module results is very different. Conversely, the total injected fuel in the engine can be correlated linearly to the fourth order, also in case of strong variation of the engine load (Figure 33).

In fact, as aforementioned, the order F4 characterizes the behavior of all the four cylinders, thus, the total injected fuel in the engine has to be considered in relation to the F4 module.

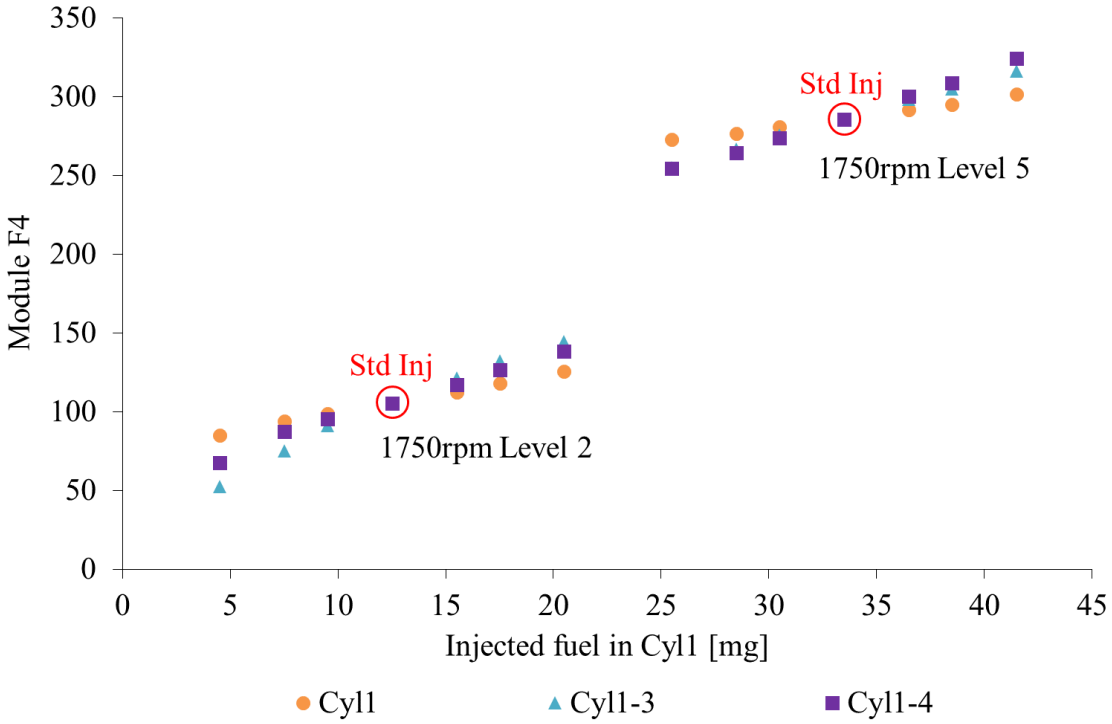

Figure 32. F4's module in case of standard injection and several injection variations in Cyl1, Cyl1-3 (same variation) and Cyl1-4 (same variation) as a function of the injected fuel quantity in the cylinder 1. Engine operating conditions: 1750rpm at Level 2 and 5.

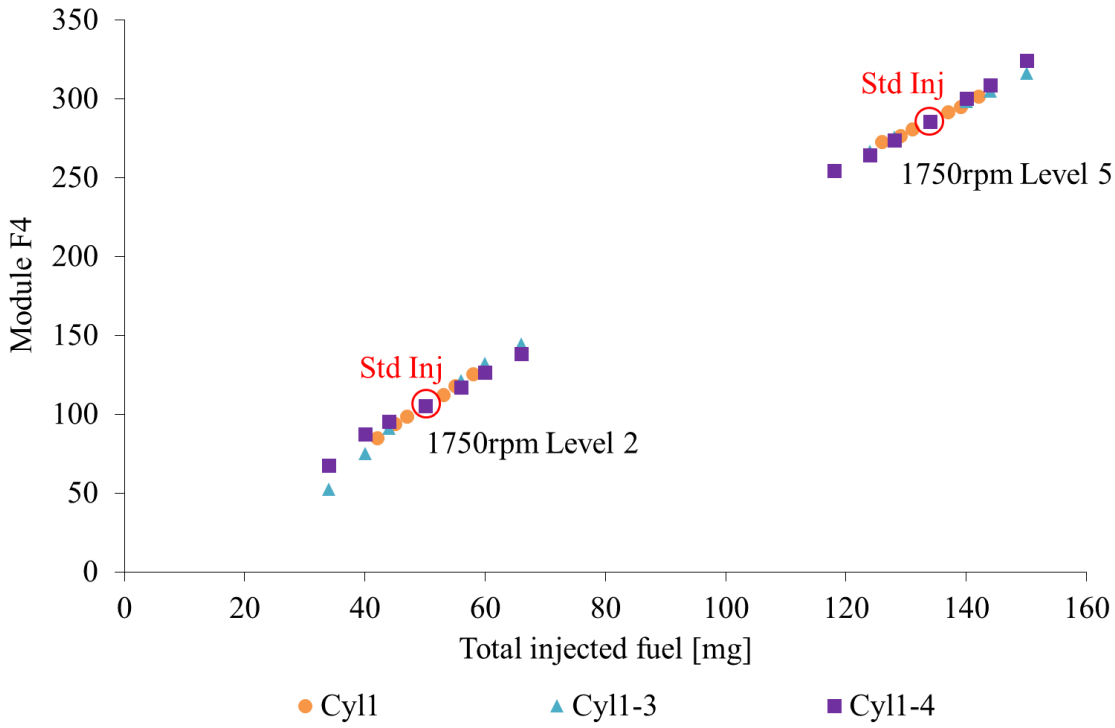

Figure 33. F4's module in case of standard injection and several injection variations in Cyl1, Cyl1-3 (same variation) and Cyl1-4 (same variation) as a function of the total injected fuel quantity in the engine. Engine operating conditions: 1750rpm at Level 2 and 5.

Starting from the results of the simulation test it can be assessed that the module of the fourth order is linearly correlated with the fuel injected in all cylinders by maintaining constant the engine speed, by the way, the coefficient of the linear correlation change by varying the engine rotational speed. The change in the coefficient is explained by the variation of the oscillation amplitude at different engine speeds (Figure 21) due to the different time frequency of the driving force (pressure in the exhaust manifold) and to the TC inertia.

With the aim to obtain a correlation that can be applied at any engine speeds so that consider the engine speed variation (Figure 35) a correction parameter is applied (Figure 36). The correction parameter depends only on the engine speed difference between a specific case take as a reference and the specific case under investigation.

The analysis of the numerical results shows that at high engine speed there is a much higher dispersion of the data respect to the case at low engine speed for the reason discussed in the previous paragraph, further, the sensitivity of the F4's module grows by reducing the engine speed (Figure 34 and Figure 35).

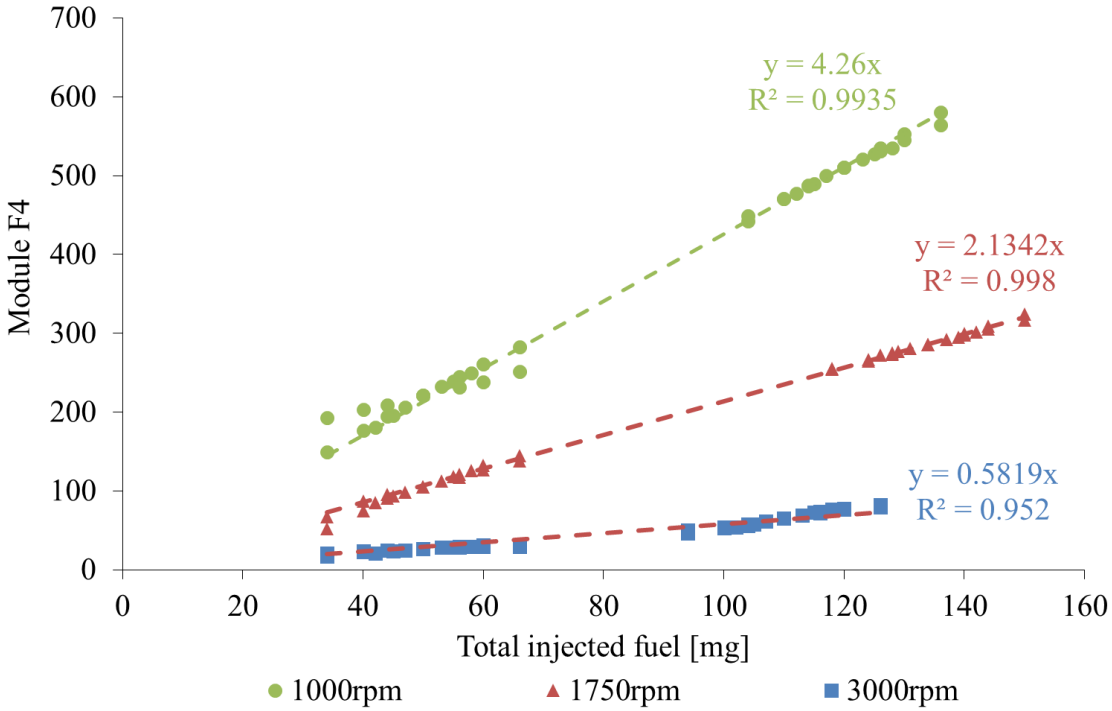

Figure 34. F4's module in case of standard injection and several injection variations in Cyl1, Cyl1-3 (same variation) and Cyl1-4 (same variation) as a function of the total injected fuel quantity in the engine. Engine operating conditions: 1000rpm, 1750rpm and 3000rpm at Level 2 and 5.

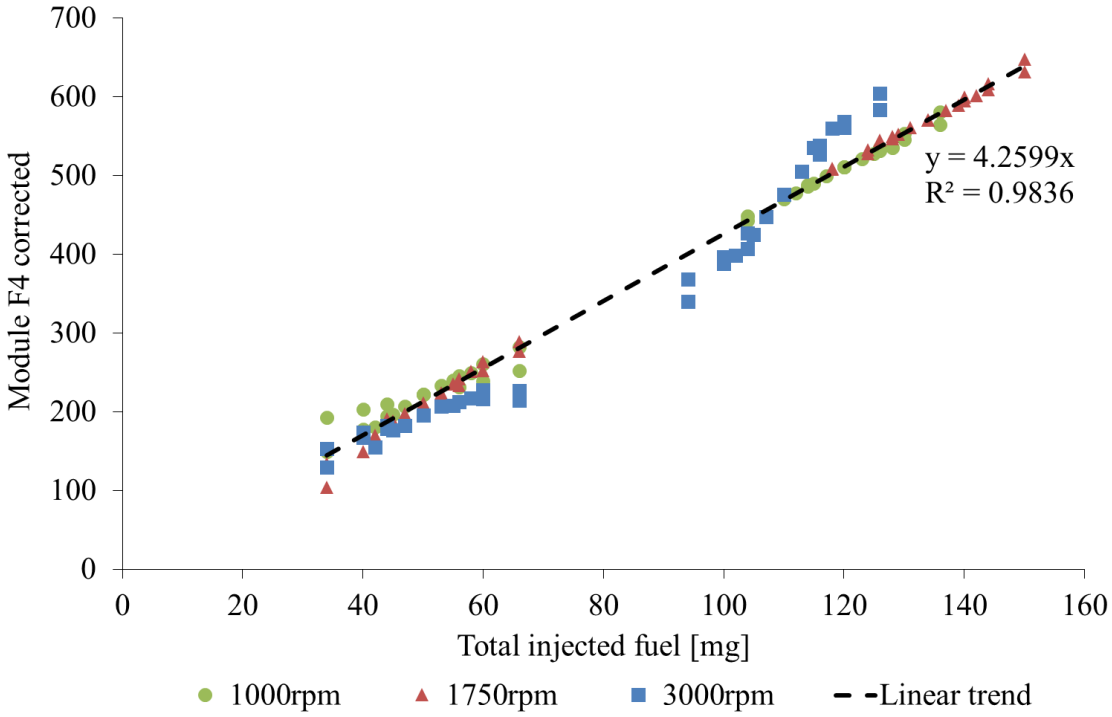

Figure 35. F4's module in case of standard injection and several injection variations in Cyl1, Cyl1-3 (same variation) and Cyl1-4 (same variation) as a function of the total injected fuel

quantity in the engine. The F4's module is divided by a correction parameter that is a function of the engine speed. Engine operating conditions: 1000rpm, 1750rpm and 3000rpm at Level 2 and 5.

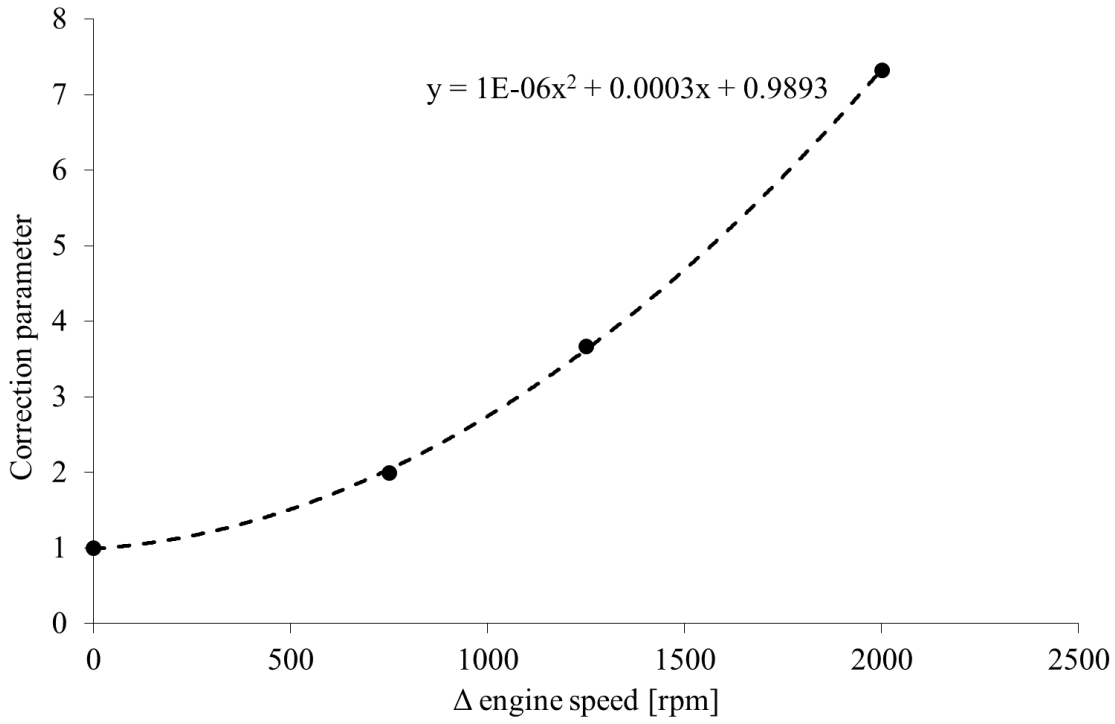

Figure 36. Correction parameter for the F4's module as a function of the engine speed difference with respect to a defined reference condition of speed.

By monitoring the fourth order module of the TC speed is possible to quantify the total injected fuel in the engine. Nonetheless, to detect the eventual cylinder's injection inhomogeneity the complex forms of first and second orders have to be taken into account.

3.3.1.2 Evaluation of Injection Inhomogeneity

In addition to the detection of the total amount of fuel, the possibility to use the frequency content of the TC speed for the detection of the fuel injected into each cylinder was investigated and described in this paragraph.

For the detection of the fuel injected into each cylinder, it has to be considered the complex form of the first and second order. In Figure 37 a simple representation of a sinusoidal signal respect to the crank angle and in the complex plan is reported. In the next figures, the orders will be represented in the complex plan because it is crucial to consider the phase of the order to understand the methodology developed.

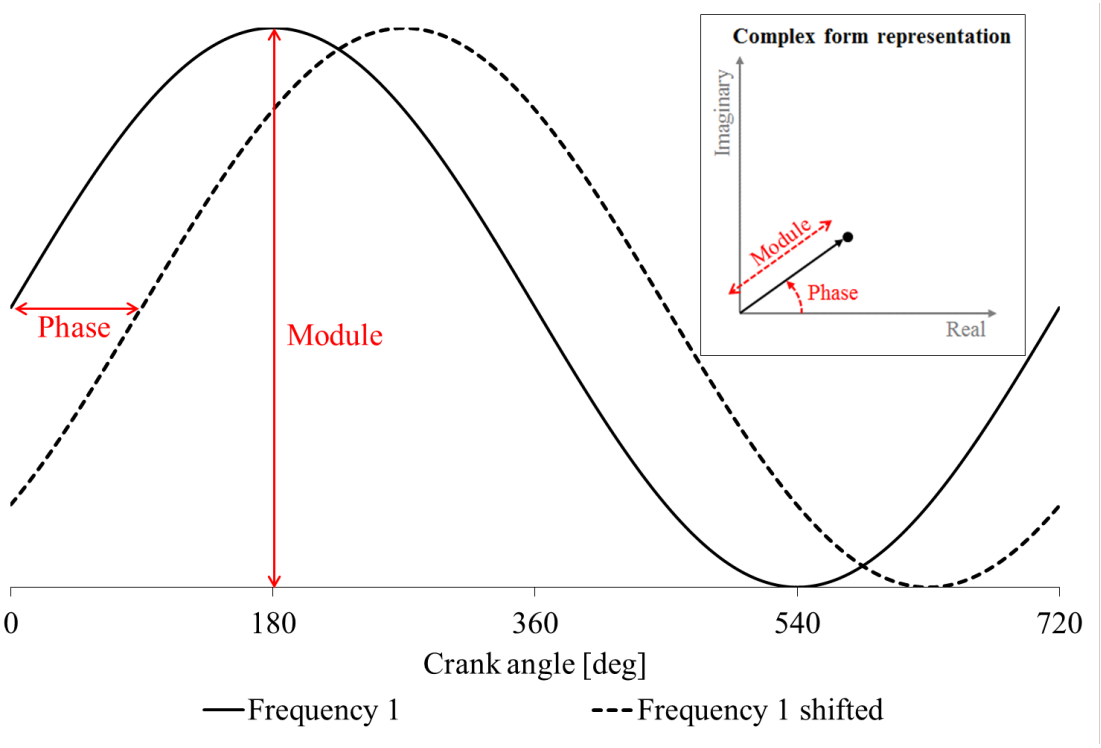

Figure 37. Complex form representation of a sinusoidal signal.

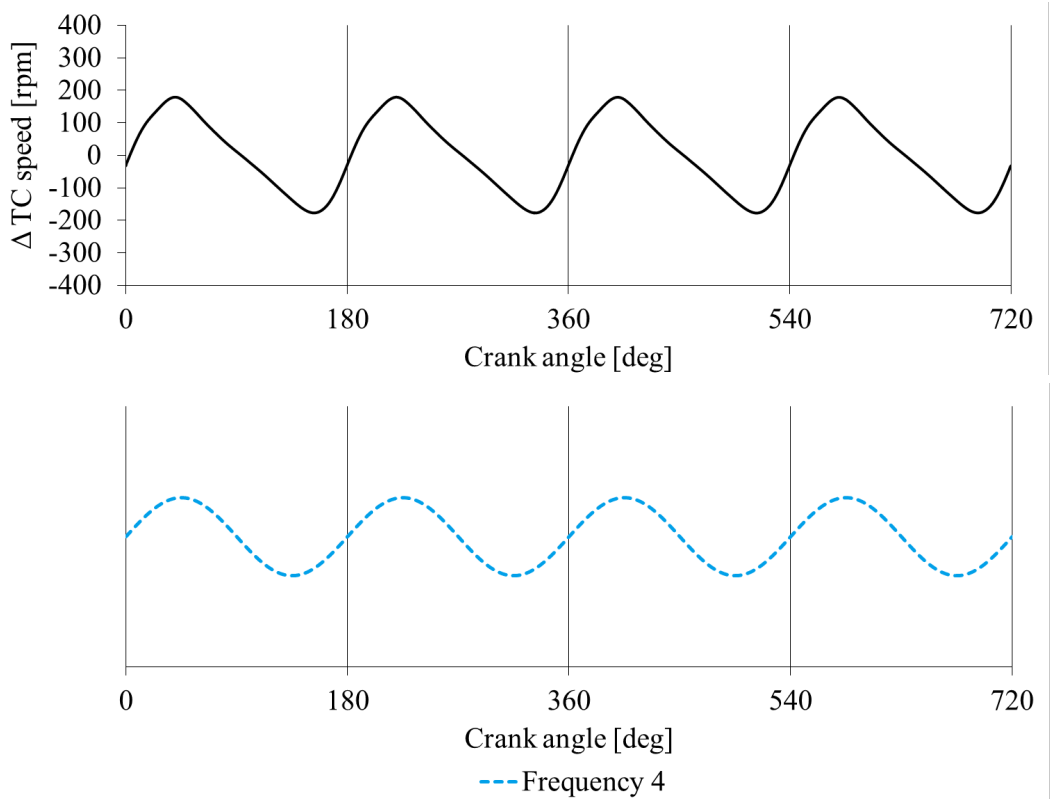

Figure 38. Instantaneous TC Speed and its frequency content in case of homogeneous injection

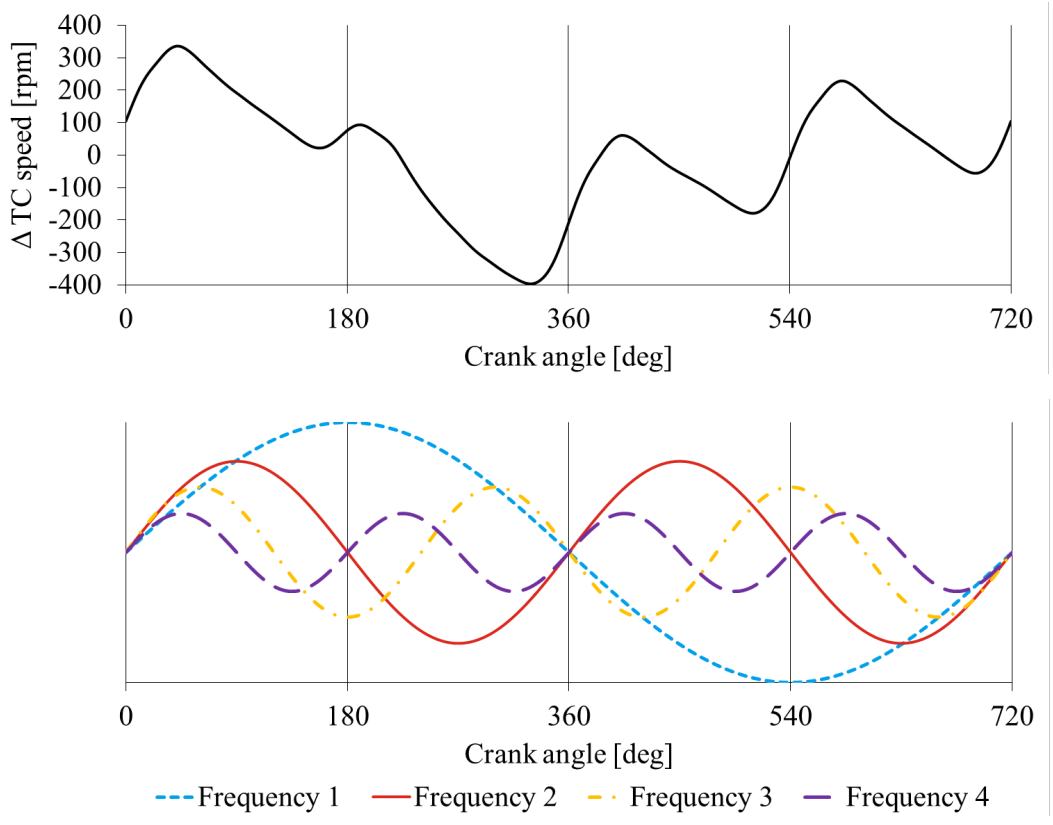

Figure 39. Instantaneous TC Speed and its frequency content in case of injection variation in 1 cylinder

By taking advantage of the F4's module and the orders F1 and F2 (Figure 37) it is possible to analyze and evaluate the injection inhomogeneity among the cylinders and to quantify the actually injected fuel in each one.

First, each cylinder is characterized by a specific oscillation of the TC speed and thus to a determined phase of the first order, in case the cylinder under investigation is experiencing a different amount of fuel injected. This phase is defined as a characteristic F1 phase of each cylinder. As an example in Figure 40, dots representing the head of the vector of the first order in the complex plan are depicted in case of injection variation in only one cylinder for all the cylinders of the engine. As can be seen, if both the imaginary and real part of the F1 are positive, so if the phase of the F1 is included between 0 and 90 degrees, it can be assessed either that there is an increased amount of fuel injected into the cylinder 3 or a decrease in the cylinder 2. To quantify the injection variation and to distinguish whether there is an increase or a decrease in the injection, the F4's module is monitored, indeed, if the F4's module increases with respect to the expected value, the injected fuel in the cylinder 3 is higher with respect to the other cylinders otherwise the injected fuel in the cylinder 2 is lower.

Further, it is possible to take into consideration engine rotational speed variation that affects the first order phase. As shown in Figure 41, where a variation of the injection in the cylinder 1 was imposed at different engine loads and speeds, the phase changes linearly in function of the engine speed, because of the differences in terms of time available for the pressure wave to reach the turbine.

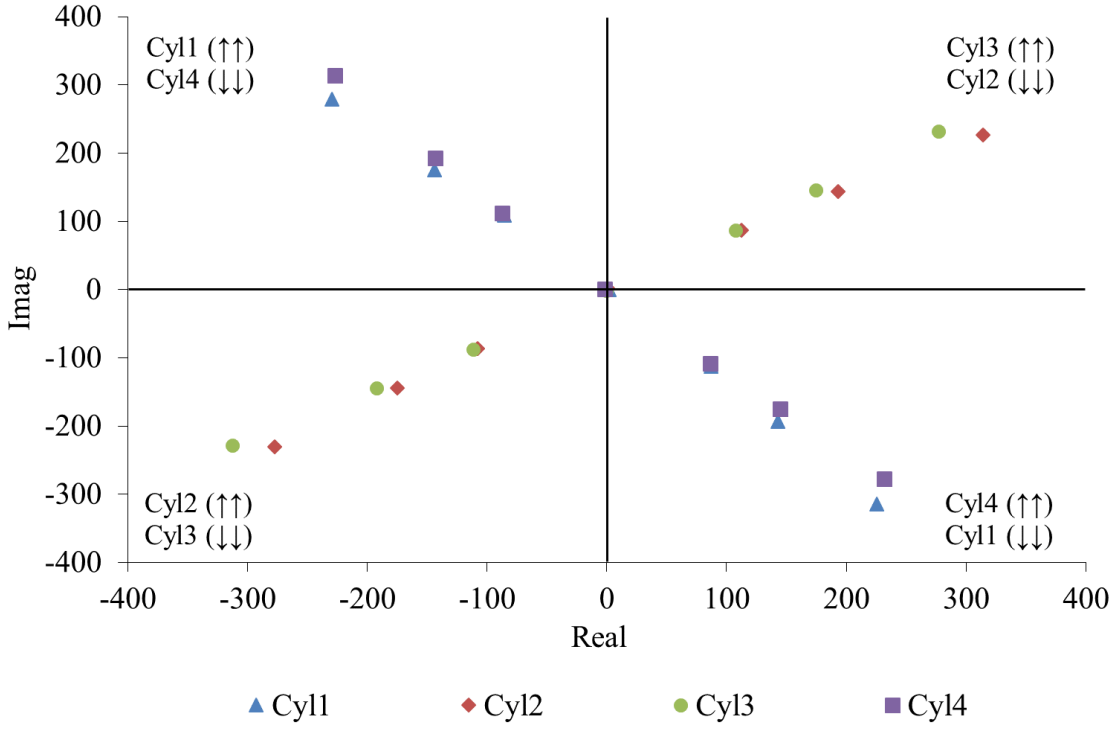

Figure 40. Representation in the complex plan of the order F1 in case of injection variations in each cylinder singularly. Engine operating conditions: 3000rpm at Level 5.

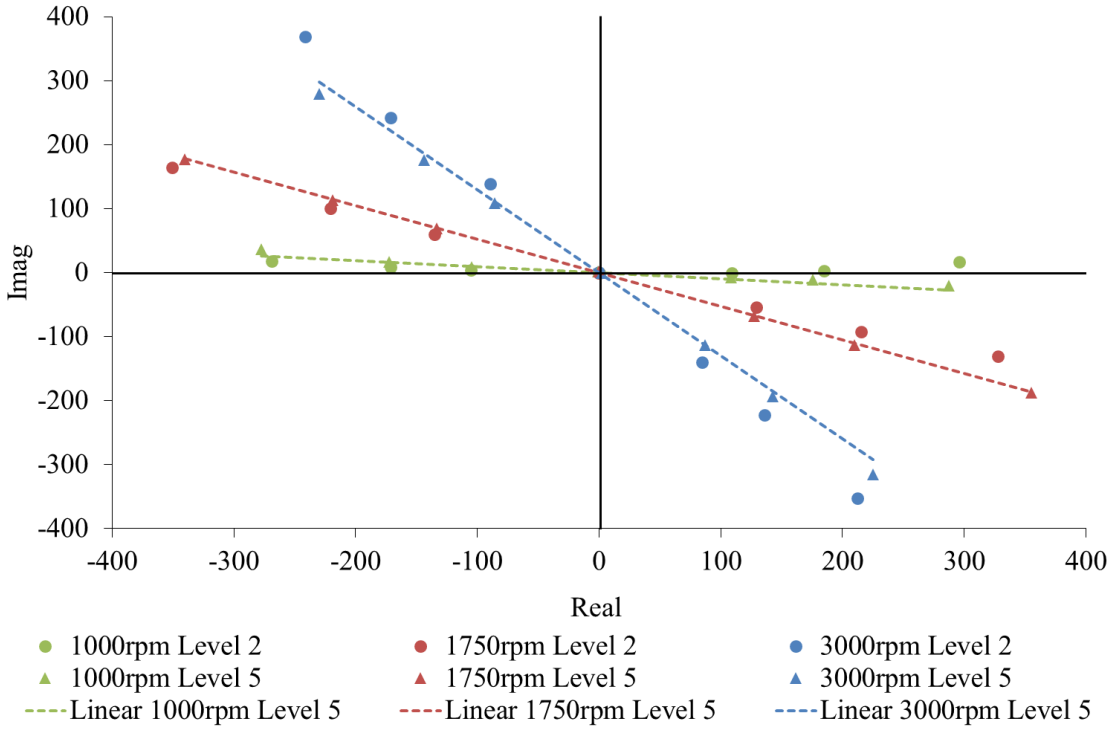

Figure 41. Representation in the complex plan of the order F1 in case of injection variations in cylinder 1. Different engine loads and speeds.

By keeping constant the engine rotational speed and the base engine load (as for example 3000 rpm and load 5) test had been performed to demonstrate the correlation

between first order and the distribution of the injection variation. A specific test is reported in Figure 23, in case of inhomogeneous variation in cylinder 1 and 3, a decrease of 3 and 5 mg respectively, the F1's phase is in between the characteristic phase of cylinder 1 and cylinder 3 and it is closer to the one of the cylinder 3 than the cylinder 1. The opposite results in terms of first order phase were obtained by switch the injection variation between cylinder 1 and 3. The same consideration could be done in case of bigger inhomogeneity among injection variation (cylinder 3 -1 mg, cylinder 1 -5mg). In the case of homogeneous injection variations in two cylinders consecutive in the firing order (1&3 or 2&4), the F1's phase is an average value of the characteristic phase of cylinder 1 and cylinder 3. Also for the case of homogenous injection in two consecutive cylinders with only the first order is not possible to make a distinction between the cylinders 1 and 3 or 2 and 4 (Figure 42).

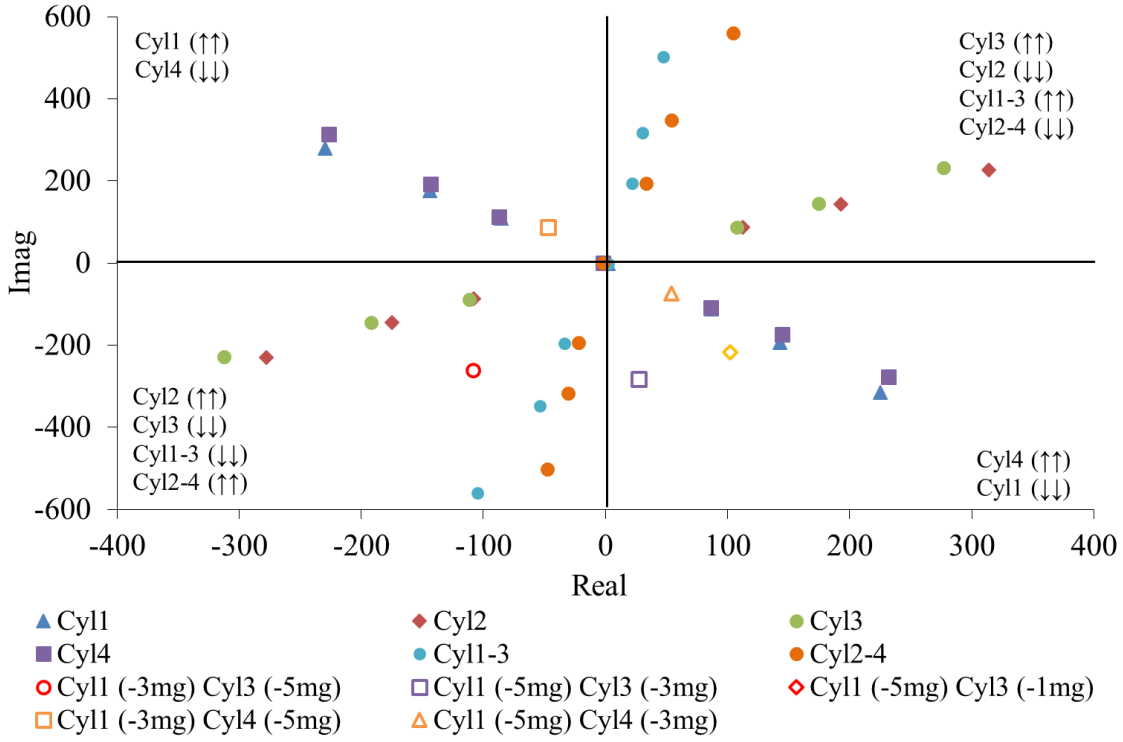

Figure 42. Representation in the complex plan of the order F1 in case of injection variations in each cylinder singularly, in case of same injection variations in two cylinders consecutive in the firing order and in case of random injection variations in two consecutive and non-consecutive cylinders in the firing order. Engine operating conditions: 3000rpm at Level 5.

Summing up, the distribution of the total variation among the cylinders can be reconstructed by the first order phase variation with respect to the characteristic phase of one of the cylinders affected by the injection variation. As an example, in Figure 43 and

Table 2 is reported the methodology results related to generic injection variations in the cylinder 1 and cylinder 3. To determine the total injection variation fourth order module has been exploited. The injection variation imposed in a specific cylinder leads to a first order phase equal to the specific one related to that cylinder. In case the total injection variation involves two cylinders, the percentage variation of the phase with respect to the characteristic phase of the cylinder 1, take as a reference, is equal to the percentage distribution of the total fuel variation between the two cylinders. This consideration is valid for the case in which the cylinders involved in the variation are consecutive in terms of firing order.

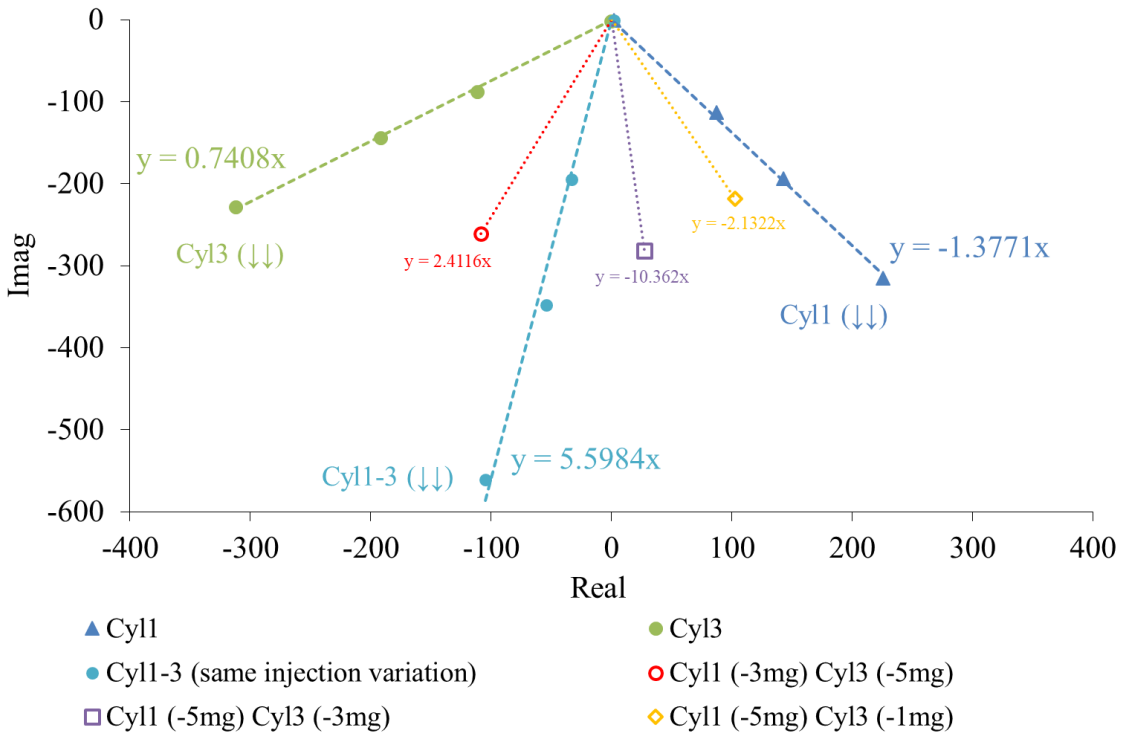

Figure 43. Representation in the complex plan of the order F1 in case of injection variations in each cylinder singularly, in case of same injection variations in two cylinders consecutive in the firing order and in case of random injection variations in two cylinders consecutive in the firing order (focus on the negative imaginary part). Engine operating conditions: 3000rpm at Level 5.

Table 2. Imposed and calculated variation of injected fuel in one cylinder and in case of random injection variations in two consecutive cylinders in the firing order.

Imposed fuel variation [% distribution of the total fuel variation]		Fuel variation ***evaluated with F1*** [% distribution of the total fuel variation]	
Cyl 1	Cyl 3	Cyl 1	Cyl 3
-3.00 mg [50%]	-3.00 mg [50%]	-2.91 mg [48.5%]	-3.09 mg [51.5%]
-3 mg [37.5%]	-5 mg [62.5%]	-2.77 mg [34.6%]	-5.23 mg [65.4%]
-5 mg [62.5%]	-3 mg [37.5%]	-5.27 mg [65.9%]	-2.73 mg [34.1%]
-5 mg [83.3%]	-1 mg [16.7%]	-5.27 mg [87.9%]	-0.73 mg [12.1%]

In case of injection variations in two non-consecutive cylinders, the related first order phase does not change with respect to the characteristic phase of the cylinders affected by the injection variation. In Figure 42, the first order phase in case of the inhomogeneous fuel injection variation in two non-consecutive cylinders is reported (orange points). When the variation in the cylinder 4 is greater, the F1's phase corresponds to the characteristic phase of the cylinder 4 the opposite results are obtained when the variation is imposed greater in the cylinder 1. These considerations highlight the issue related to distinguish the case in which the injection is changed in just one cylinder or in two non-consecutive cylinders, to overcome these issue, the second order is considered useful for the detection of events related to non-consecutive cylinders that have, for their disposition, the order two as the main frequency.

More in detail, it was observed that in case the injection variation involves two non-consecutive cylinders the module of the second order become greater than the first one, allowing one to distinguish these two cases (Figure 44), the opposite results in terms of modules are verified when the injection fault involves just one cylinder.

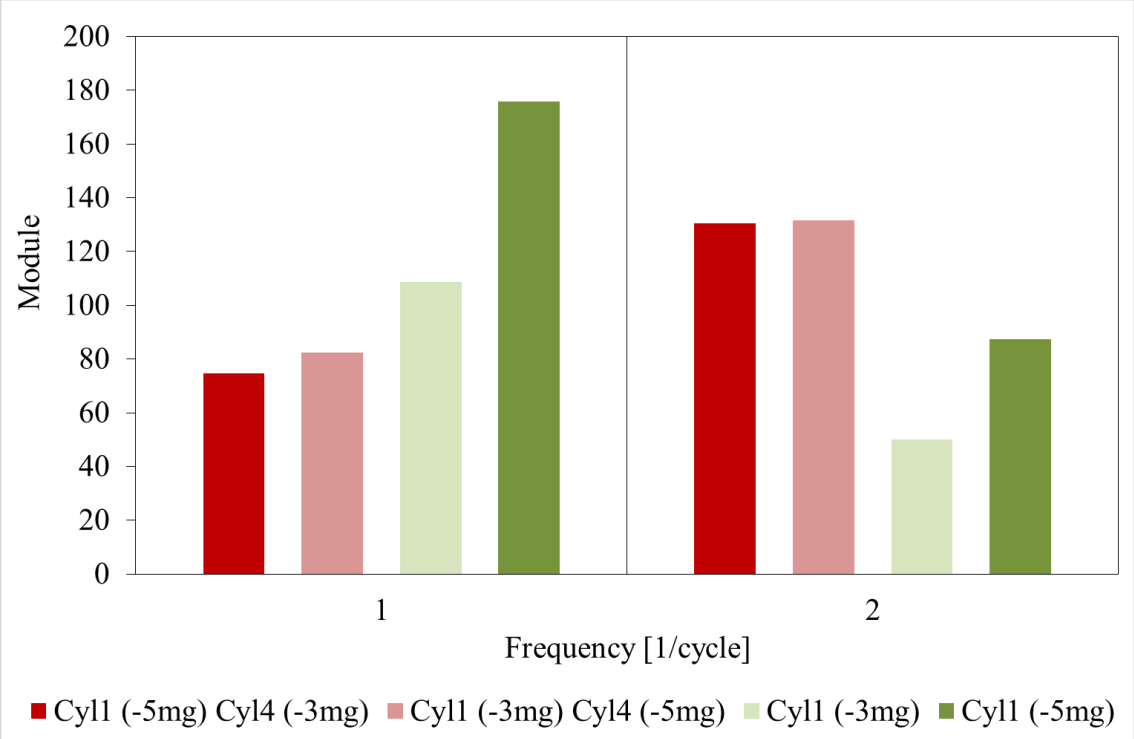

Figure 44. Modules of F1 and F2 in case of injection variations in one cylinder and non-homogeneous injection variations in two cylinders non-consecutive in the firing order. Engine operating conditions: 1000rpm at Level 5.

An exceptional case is represented by a homogeneous injection variation in two non-consecutive cylinders. When this event was imposed numerically, the FFT results show that there is no content for the first order. By the way, to distinguish which of the cylinders couple (1-4 and 2-3) is involved in the injection variation, the phase of the second order has to be considered. More in detail, if the phase is included between 0 and180 degrees the variation could be associated with the increase of the injected fuel in the cylinders 1 and 4.

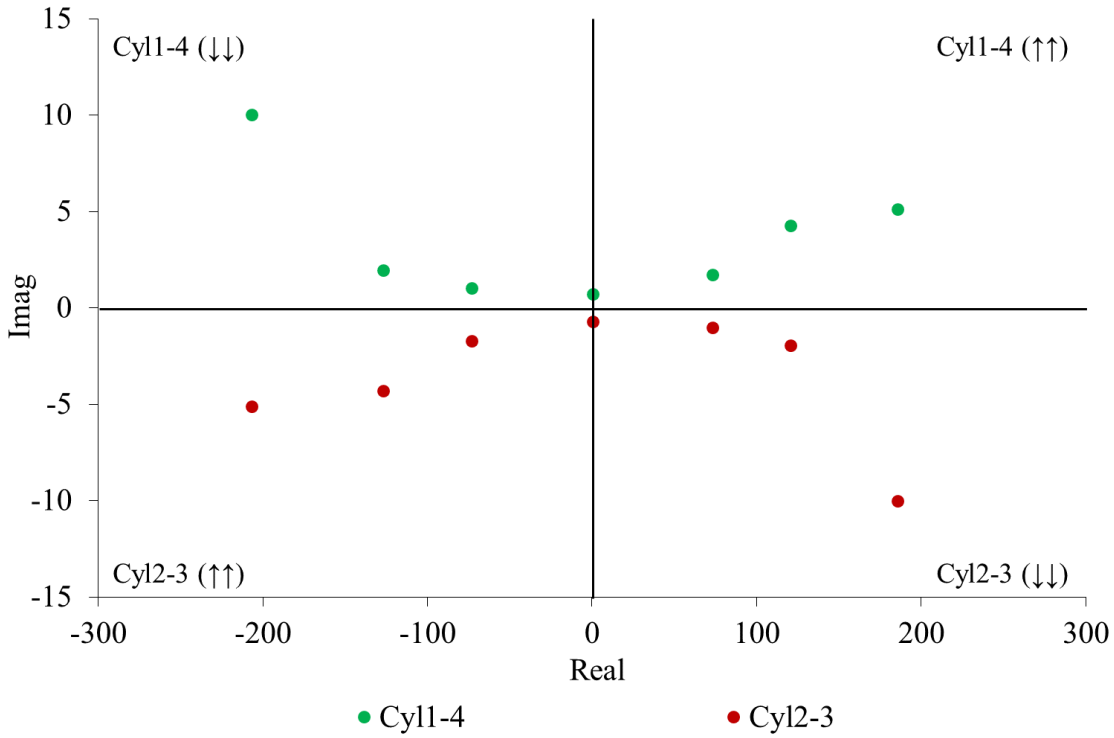

Figure 45. Representation in the complex plan of order F2 in case of a variation in two cylinders non-consecutive in the firing order (same variation in both the cylinders 1&4 and 2&3). Engine operating conditions: 3000rpm at Level 5.

Considering all the statements of the previous paragraphs, a preliminary algorithm based on numerical results was implemented with the aim to detect eventual injector fault and to correct it. The data necessary for this algorithm are:

- Module of the 4th order
- Phase and Module of the 1st order
- Phase and Module of the 2nd order

The algorithm scheme is reported in Figure 46

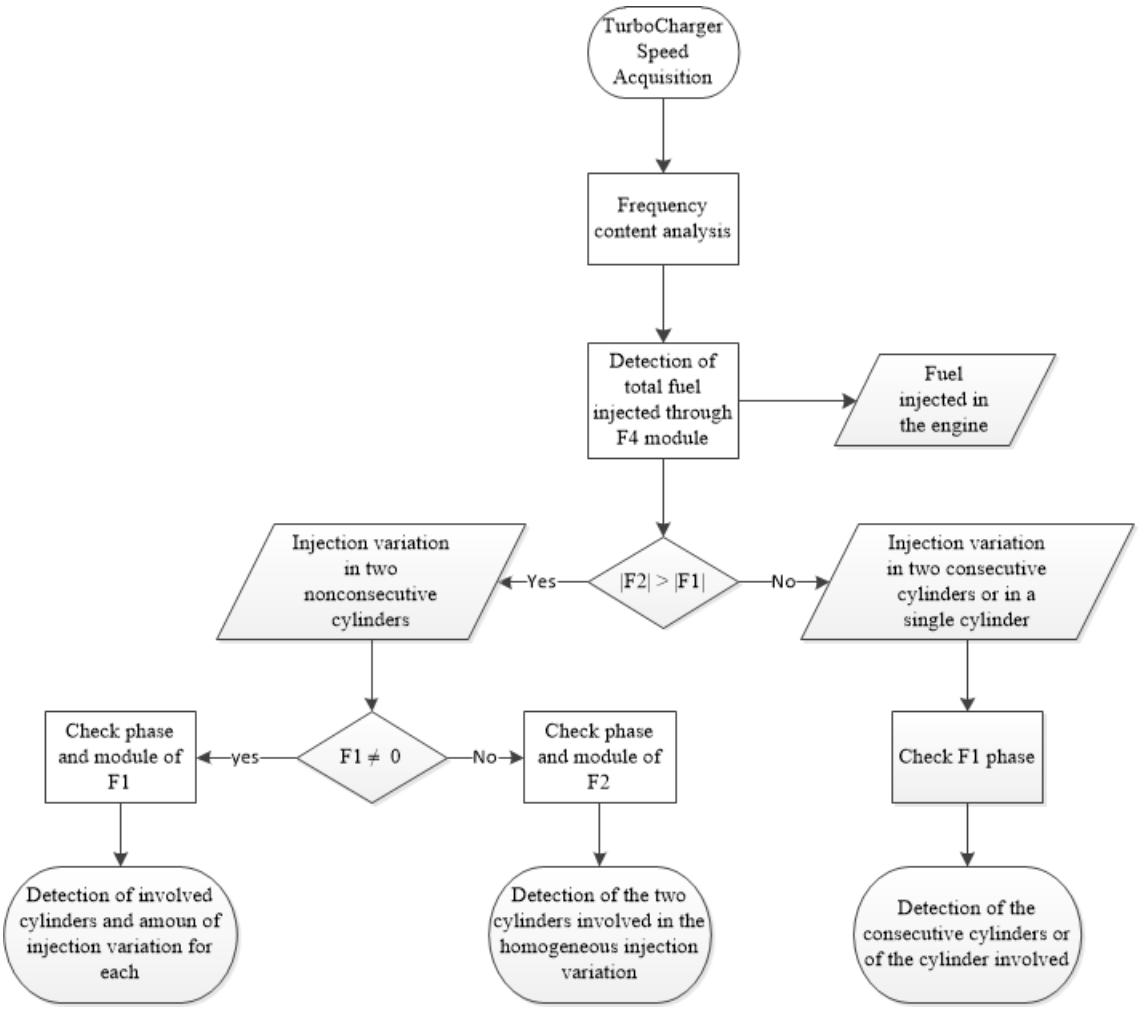

Figure 46. Block scheme of the algorithm for the detection and correction of injectors fault based on FFT methodology.

4 Experimental validation of the monitoring methodologies

In this chapter, the experimental activity carried on with the aim to validate the monitoring methodology developed during the numerical test is presented. Yanmar R&D as industrial partner of the activity provided the four cylinders' engine object of the analysis. First of all, the experimental setup will be presented with a detailed explanation of the turbocharger speed signal acquisition, following this section, the validation of the numerical methodology developed through the experimental data collected will be reported. The following part is focused on an experimental application of the methodologies proposed in case of deteriorated injectors and a comparison among all the developed methodologies. The last part of this chapter shows the possibility to use the turbocharger speed to detect misfiring events.

4.1 Experimental setup

All the experimental activity was performed on a Yanmar 4-stroke 4-cylinders turbo-diesel engine with a displacement of 2100cc for heavy-duty application. The engine was installed at the test bench of the Department of Industrial Engineer of Florence University, Figure 47.

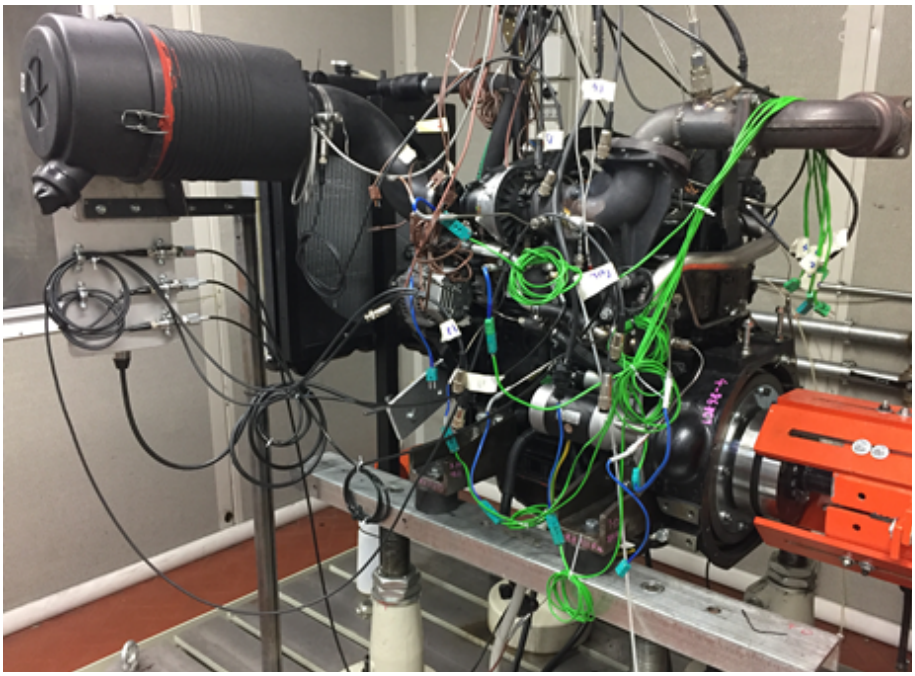

Figure 47. Engine on the test bench.

The engine was completely instrumented in order to monitor the engine operating parameters. The measured signals can be divided into dynamic and static typology.

Dynamics signals:

- In-cylinder pressure in all the cylinders
- Pressure in the exhaust manifold upstream the turbine
- Injection phasing
- Crankshaft angular position and TDC reference
- Compressor blade passage (turbocharger speed)

Static signals:

- Torque and power of the engine
- Exhaust temperature of each cylinder
- Temperature and pressure at the compressor inlet

- Temperature and pressure at the compressor outlet
- Temperature and pressure at the turbine inlet
- Temperature and pressure at the compressor outlet
- Fuel and air mass flow
- Liquid and oil temperature of the engine
- Temperature and pressure of the test cell

All the dynamic signals were simultaneously acquired with the AVL IndiMicro device on time base with a sampling frequency of 1MHz. It was chosen to not sample the compressor blade passage on crank angle base because it causes a poor instantaneous TC speed signal resolution.

The crankshaft angular position is acquired with the AVL 365C optical encoder with a resolution of 0.5deg.

The sensor used to acquire the compressor blade passage in order to measure the instantaneous TC speed is a hall-effect sensor (eddy current principle) which detect the existence or non-existence of ferromagnetic bodies. It is a screw-shaped sensor, with a diameter of 5mm and a length of 75mm, the sensing element is in the tip. In Figure 48 it is depicted the TC speed sensor coupled with its electronic unit.

Figure 48. TC speed sensor and an electronic unit for raw signal conditioning.

To properly acquire the blade passage, the sensor is flush mounted on the compressor case, Figure 49. The passage of each compressor blade (made in steel) causes the excitation of the hall-effect sensor, which gives an electric output signal. The sensor is connected to a dedicated signal amplifier, which converts the raw voltage signal of one blade in a TTL 0-5V signal. In this specific case, the compressor is provided with 10 blades, consequently, for a single TC revolution, there is a square wave with 10 periods.

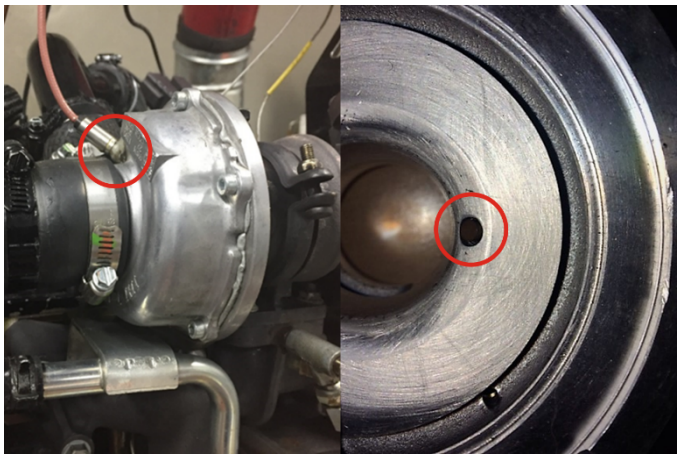

Figure 49. Hall-effect sensor installed on the compressor case.

4.2 Turbocharger speed acquisition

The present chapter proposes a methodology to correctly measure the instantaneous TC speed signal triggered with the engine cycle by exploiting the maximum acquisition frequency usually used at the engine test bench or onboard the vehicle (equal or lower than 1MHz). The same acquisition frequency is used to acquire simultaneously the crankshaft angular position.

In this work, a hall-effect sensor acquires the instantaneous rotational speed. In the turbocharger case, the hall-effect sensor acquires the compressor blade passage on time base. The sensor, coupled with its amplifier, produces a square wave signal of constant amplitude in which every period is related to the passage of one compressor blade (Figure 50).

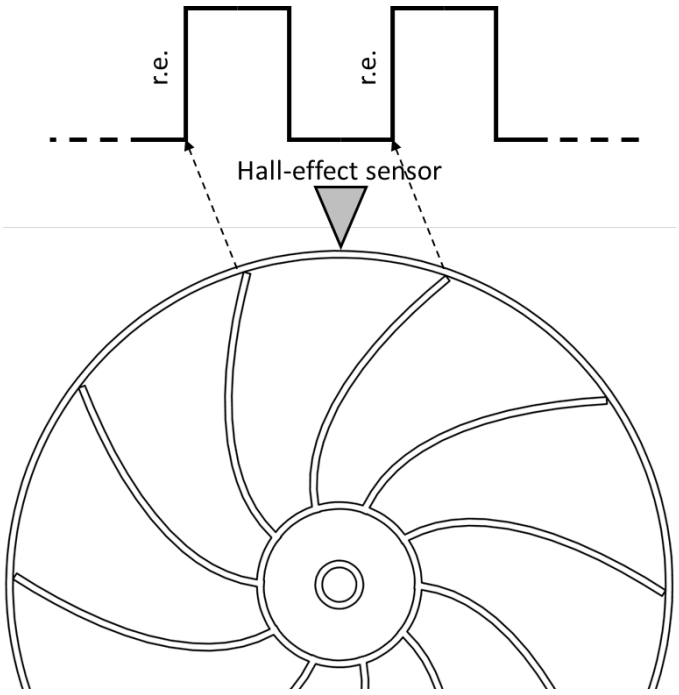

Figure 50. Schematic representation of the operation of the hall-effect sensor mounted on the compressor.

The instantaneous TC speed on time base is obtained from the time interval (ΔTime) between two consecutive rising edges (or falling edge) of the signal and it is associated to the average time of the interval.

$$TC_{speed}[\text{rounds}/sec] = \frac{1}{\Delta Time * N_{blades}} \quad (7)$$

Where N_{blades} is the total number of compressor blades.

This approach is theoretically the most accurate way to obtain the instantaneous TC speed. However, the results are unsuitable due to the excessive error related to the acquisition frequency and to the deviation caused by the compressor wheel tolerances and inconsistent blade-to-blade distances.

With an acquisition frequency equal to 1MHz, it is possible to appreciate a phenomenon with the time resolution of 1 μs. Taking into account a high TC speed, i.e. 150000rpm, and a compressor constituted by 10 blades, the passage of the blade occurs in around 40 μs. Consequently, the acquisition system is able to correctly measure the average turbocharger speed. However, the acquisition frequency of 1MHz allows one to appreciate a difference in time of 1 μs between two rising edges (r.e.) corresponding to an excessive difference in speed (in the previous example, 150000rpm, the maximum resolution will be almost 4krpm). In the case of a compressor with 10 blades, the maximum accuracy with 1MHz acquisition frequency in function of the average turbocharger speed is reported in Figure 51. In the same figure is reported the maximum resolution with a 375MHz acquisition frequency that guarantees an accuracy of 10rpm at the average TC speed of 150000rpm.

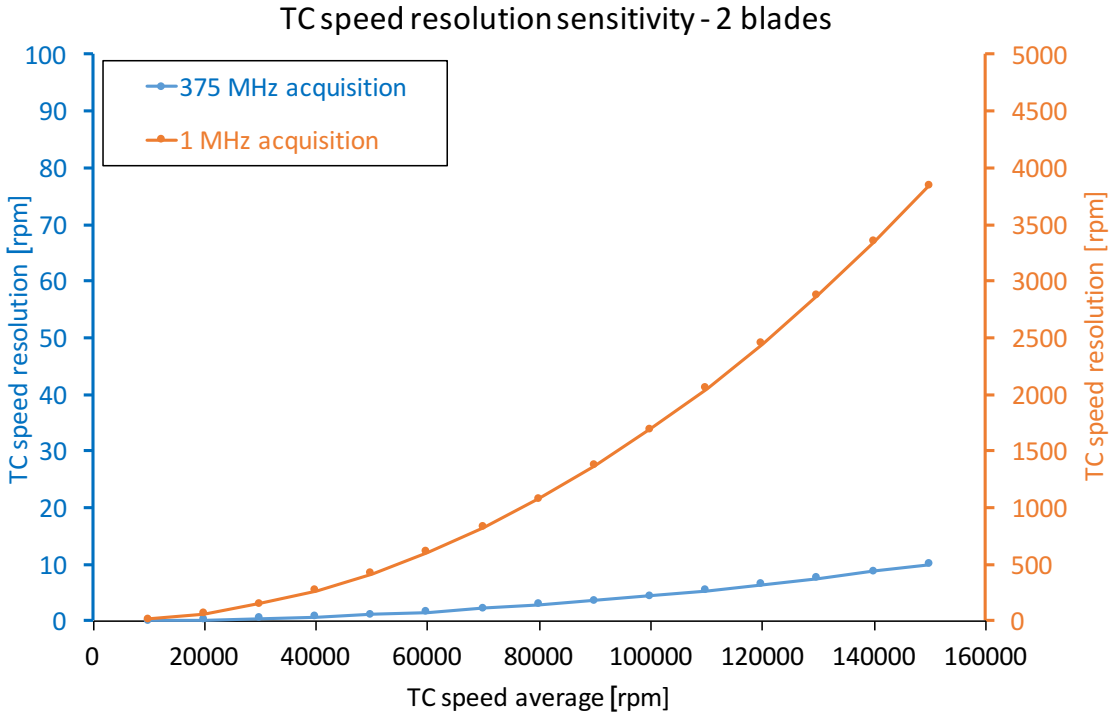

Figure 51. Maximum accuracy of the instantaneous TC speed with two different acquisition frequencies (the considered compressor has 10 blades): 1MHz (usually installed at the test bench – orange line) and 375MHz (that guarantee an accuracy of 10rpm at an average TC speed of 150krpm – blue line).

As shown in Table 3, at the TC speed of 100000rpm the interval between two rising edges is equal to 60 μs. With an interval time of 59 μs, the TC speed results equal to 101695rpm. Consequently, the resolution is too poor to appreciate during the engine cycle the instantaneous TC speed oscillation that usually is lower than 500rpm in all the engine operating range and decreases by increasing the engine speed and/or by decreasing the load.

Table 3. Example of instantaneous TC speed accuracy with an acquisition frequency of 1MHz and a compressor with 10 blades.

TC speed [rpm]	[blade / s]	[μs / blade]	ΔTC speed [rpm]
100000	16666.6	60	1695
101695	16949.2	59	

The schematic description of the error is reported in Figure 52, where a hypothetic signal of the hall-effect sensor, theoretically acquired with an infinite acquisition

frequency, is compared with the signal acquired with a defined acquisition frequency. The derived two ΔTimes are different and consequently, the TC speed values are different.

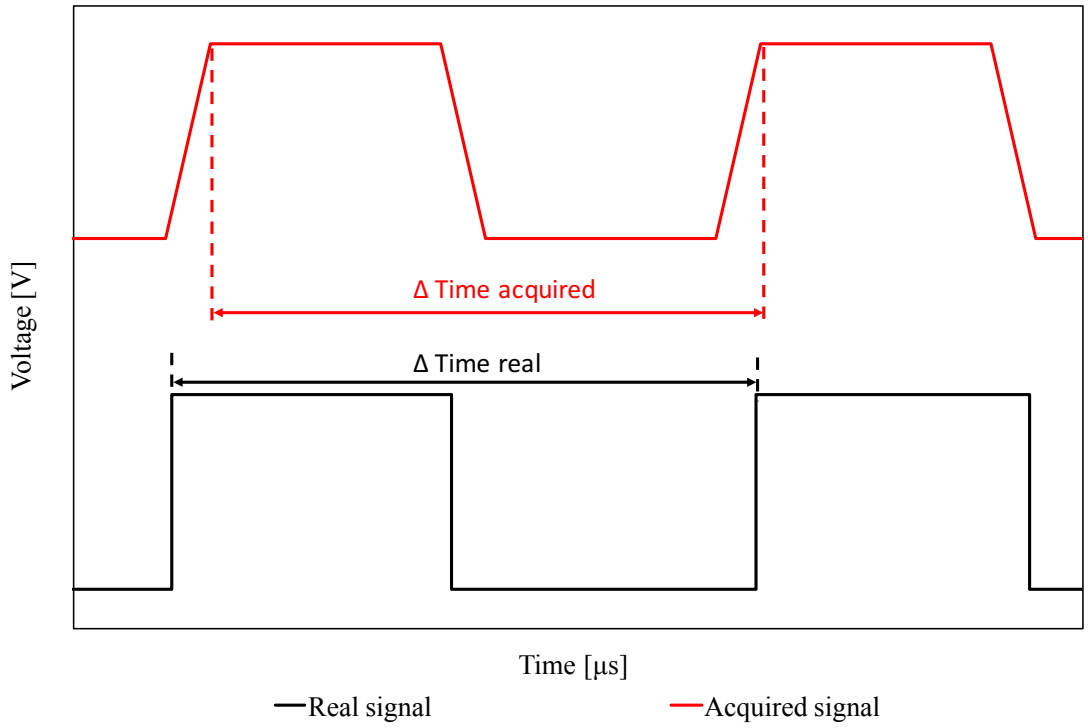

Figure 52. Comparison between the hall-effect signal derived from an infinite acquisition frequency (black line) and the one derived from a defined acquisition frequency (red line).

Once the instantaneous TC speed has been triggered with the engine cycle, the errors due to the low acquisition frequency and to the constructive tolerance of compressor blades are both distributed randomly in the cycle. Consequently, the error is reduced by applying an average on multiple engine cycles.

4.2.1 Low and High pass frequency filters

It is worth noting that the instantaneous TC speed signal is affected by a high-frequency noise due to the electrical apparatus installed inside the test cell. To reduce the contribution of this type of noise, a low-pass frequency filter is applied. The Fast Fourier Transform is applied to the TC speed signal, derived from the square one, which is converted from the crank angle domain to the frequency domain.

To conclude the discussion about the acquisition methodology of the instantaneous turbocharger speed, it is necessary to underline that during the experimental test at the

engine dyno it was experimented a macro oscillation that afflicts all the acquired engine working parameters. The macro oscillation is due to the control system of the static test bench that operates to maintain to constant value the engine speed or the engine torque. By considering the non-instantaneous action of the PID control, an oscillation at low frequency around the imposed speed or torque of the engine occurs. Because of its low frequency content, a high-pass frequency filter is applied in order to eliminate the contribution of this oscillation from all the acquired signals, among which the instantaneous TC speed. To avoid cutting of useful signal information in the whole engine operating range, the cut-on frequency of the high-pass filter must be lower than the first order frequency of the engine at the idle condition. For example, if the idle condition of a 4S engine is 600rpm, the cut-on frequency of the high-pass filter must be lower to 5Hz to eliminate only the macro oscillation due to control system of the test bench. In Figure 53, the advantage of applying the high-pass frequency filter is shown for a generic signal acquired for 100 consecutive cycles.

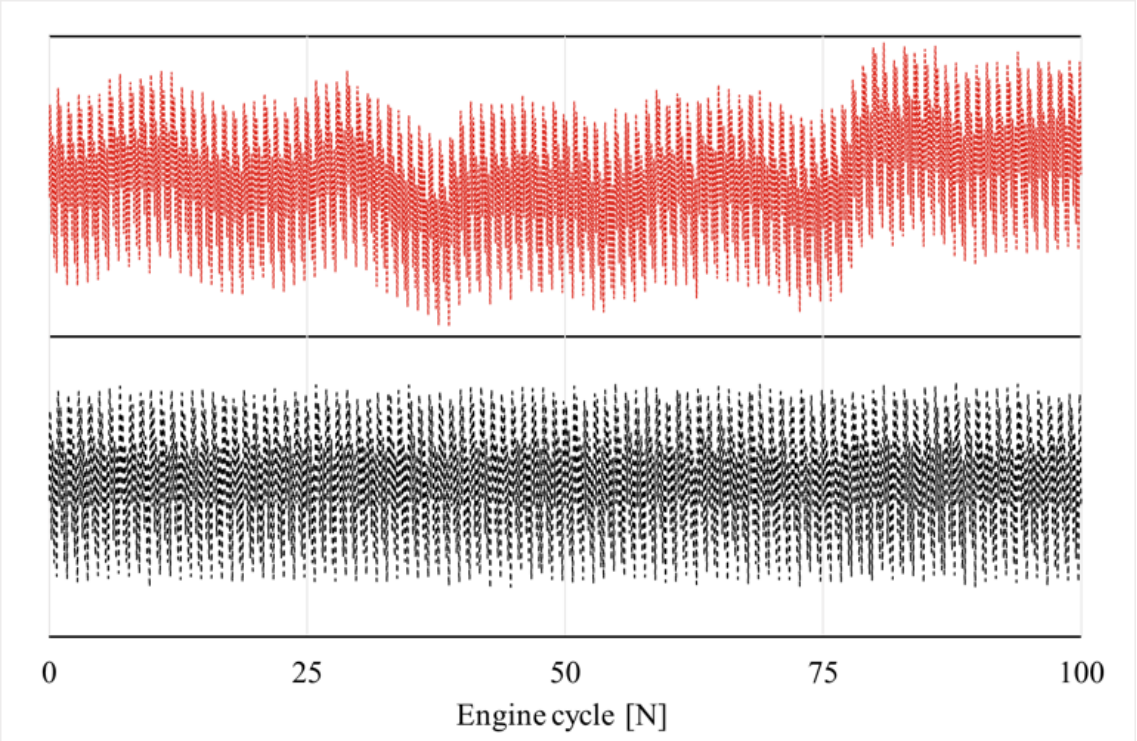

Figure 53. Engine working parameter (e.g. instantaneous TC speed) before and after the application of the high-pass frequency filter for 100 consecutive engine cycles.

4.3 Validation of the methodologies

The experimental validation of the methodologies, developed during the numerical activity, for the monitoring of Diesel engine based on TC speed is discussed in this chapter.

During the experimental tests two sets of injectors have been tested, one new set with homogeneous performance (unless constructive tolerance) and one old set with deteriorated performance, useful to test the capability and reliability of the methodologies under discussion. The first section of this chapter is focused on the validation of the methodologies carried out with the new set of injectors by imposing different engine condition. The last section reporting about test of detection and correction of inhomogeneity of deteriorated injectors.

4.3.1 Experimental validation of monitoring methodologies

First, the correlation between the F4 module and the total injected fuel mass flow (evaluated with the flow meter) was investigated. As described in the previous chapter, the fourth order, in particular its module, is the best order to continuously monitor the total quantity of injected fuel.

The experimental campaign involved the whole engine working area starting from low load and low speed to maximum speed and load as reported in Figure 2. For each engine condition tested with homogeneous injection, the correlation between the module of the fourth order and the total injected fuel was verified. As reported in Figure 54, the linearity between the F4 module and the injected fuel is completely confirmed, as expected from the numerical activity, in all the operating condition of the engine.

As expected, at high engine speed the sensitivity of the fourth order module is lower with respect to the medium-low engine speed, this is mainly due to the lower amplitude of the TC oscillation at high engine speed that in turns depend directly to the limited time available among pressure impulse coming from a different cylinder. Confirming the numerical results, the F4 module is linearly dependent on the injected fuel while maintaining the same rotational speed of the engine. In case of changing the engine speed

the linear coefficient correlating F4 module and injected fuel changes too. These differences are due to the variation of the oscillation amplitude at different engine speeds caused by the different time frequency of the driving force (pressure in the exhaust manifold) and to the TC inertia.

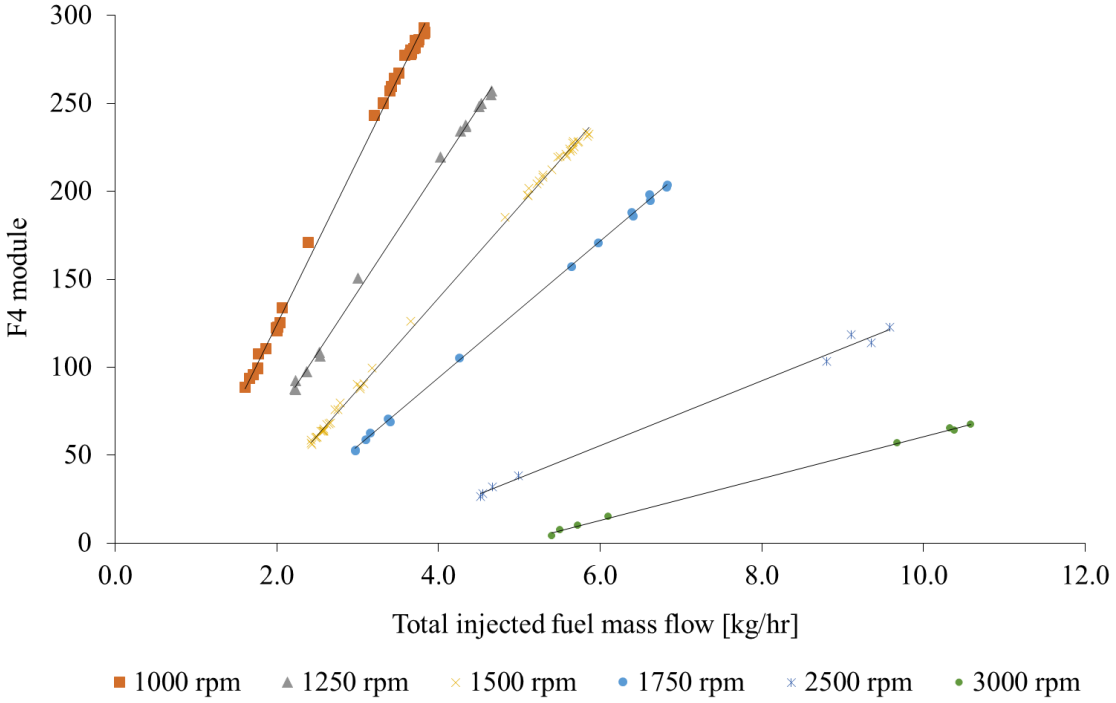

Figure 54. Correlation between F4 module and total injected fuel mass flow at different engine speed and load, in case of homogeneous and non-homogeneous injection

Once stated that the fourth order module can be used to detect and measure indirectly the total injected fuel, dedicated tests were performed to analyze and verify the reliability of the frequency content methodology to detect injection performance of each cylinder.

Variations of the injected fuel for each cylinder from 1 to 8 mg per cycle, both increasing and decreasing, were imposed. In Figure 55 and in Figure 56, the characteristic phases of each cylinder obtained by imposing injections variation in one cylinder at a time at 1750 and 1500 rpm at Load 3 (APPr ~ 40, blue point) and full load (black point), are represented.

Confirming the results of the numerical analysis, the characteristic phase of each cylinder is not affected by the load. This aspect is very important for this kind of approach

since a change in the injection in one cylinder correspond to a change in the load of the engine.

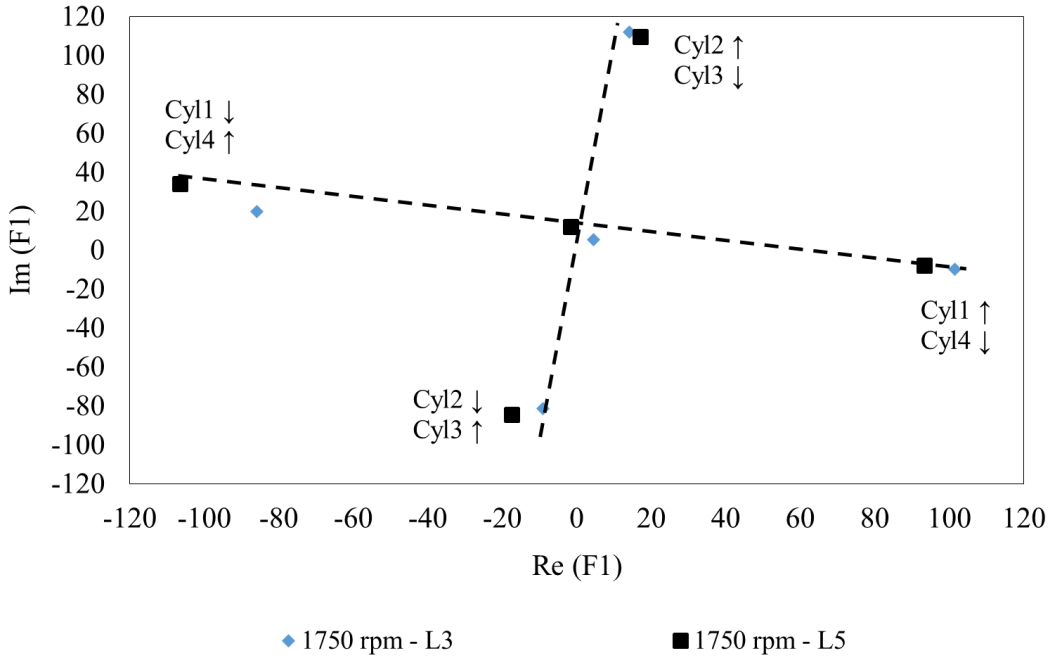

Figure 55.Representation in the complex plan of the F1 order at 1750 rpm and two loads for several injection variations

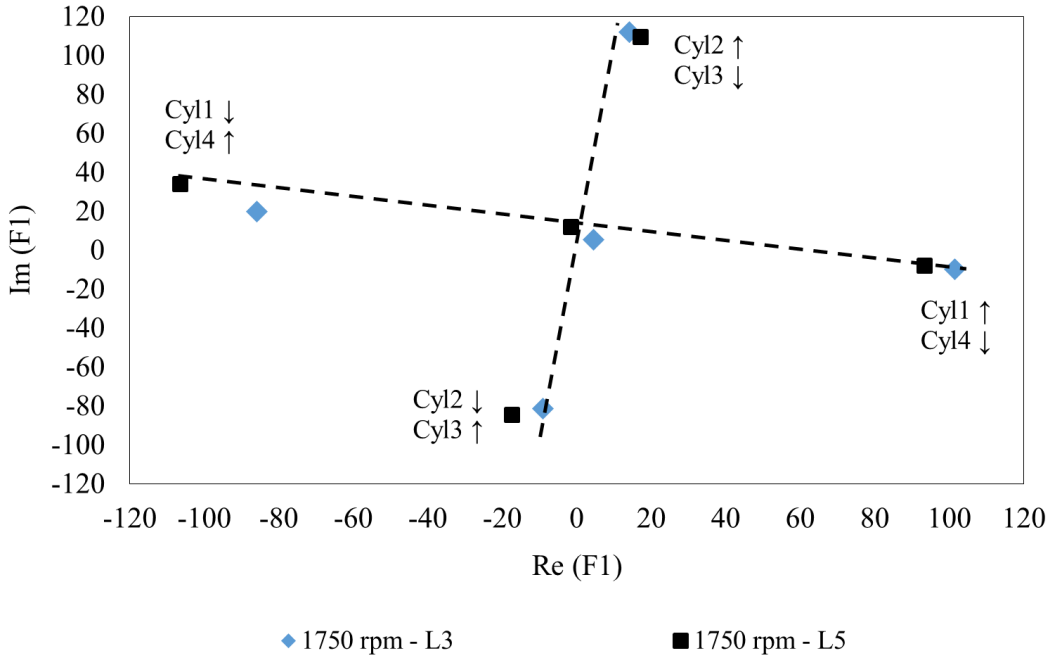

Figure 56. Representation in the complex plan of the F1 order at 1500 rpm and two loads for several injection variations

By changing the engine rotational speed, the characteristic F1 phase of each cylinder rotates in the complex plane according to previous analysis.

The behavior of the first order phase was further investigated, in order to verify the possibility to use it for detecting multiple injection variations, by imposing injection variations in multiple cylinders. Indeed, as mentioned in the numerical activity section, when the injection variation interests two cylinders at the same time it is possible to associate the exact quantity of the injection variation to each cylinder by evaluating the percentage variation of the phase between the two characteristic phases.

First, In Figure 57, the results of the experimental test with injection variation in two non-consecutive cylinders (cylinders 1 and 4) is depicted. The phase of the first order in case of injection variation in non-consecutive cylinders results in negligible variation respect to the case with injection variation in only one cylinder. More in detail, the resulting first order phase falls along the characteristic phase of these cylinders. In case of homogeneous injection variation between the two interested cylinders (grey point), the first order becomes negligible respect to other orders.

These results were expected since between cylinder 1 and 4 there is a 180°phase shift of the characteristic phase. In case of different injection variations in the cylinders 1 and 4 (green point and orange point of Figure 57), the resulting point is located in the side of the characteristic phase related to dominant variation. For example, in case of negative variations, the resulting point is located in the positive real part of the complex plane if the highest variation is in the cylinder 4 (orange point), in the negative real part of the complex plane in case the highest variation is in the cylinder 1 (green point).

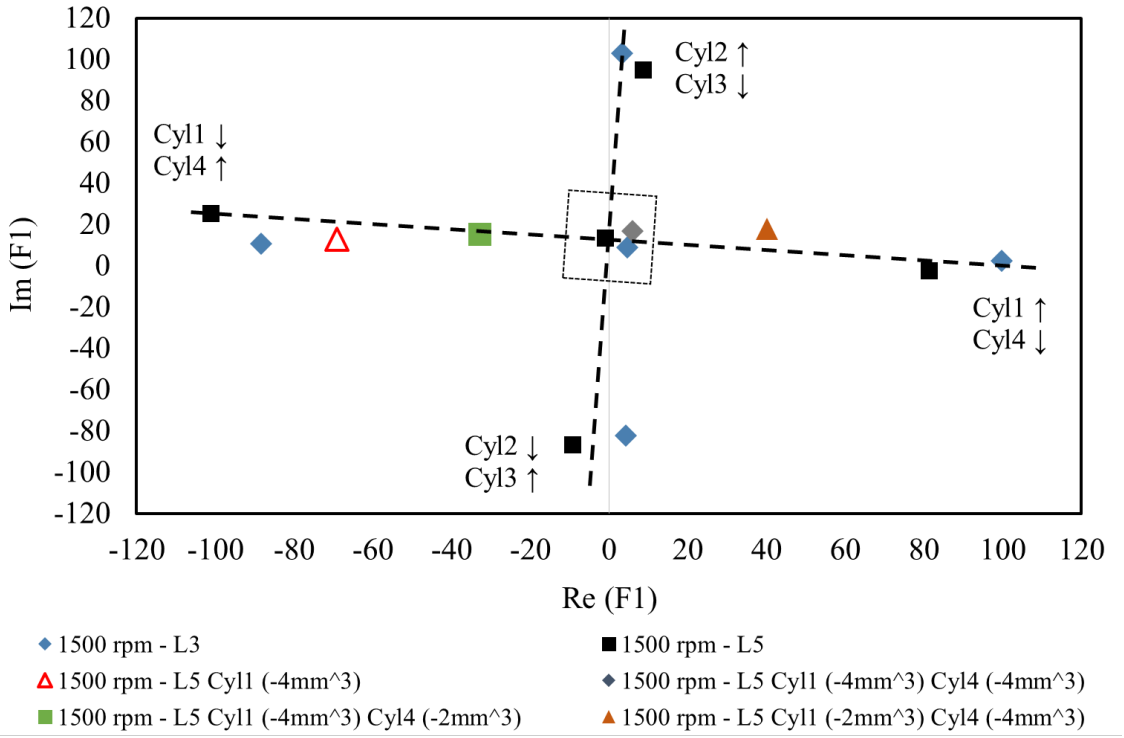

Figure 57. Representation in the complex plan of the F1 order at 1500 rpm and two loads for several injection variations

For the case in which the cylinders involved in the injection fault are consecutive in terms of firing order, the F1 response was investigated. In Figure 58, results in case of injection variations imposed in the cylinders 1 and 3, consecutive in the firing order, are depicted. When equal injection variation (green point) is imposed, the phase falls in the middle of the characteristic phases of the cylinder 1 and 3, while considering different injection variations in the cylinders 1 and 3, also in this case, the resulting point (yellow and light blue points) is closer to the characteristic phase related to the cylinder of a greater variation (cylinder 1 or cylinder 3, depending of the considered case). These results confirm the numerical results obtained and described in the numerical section.

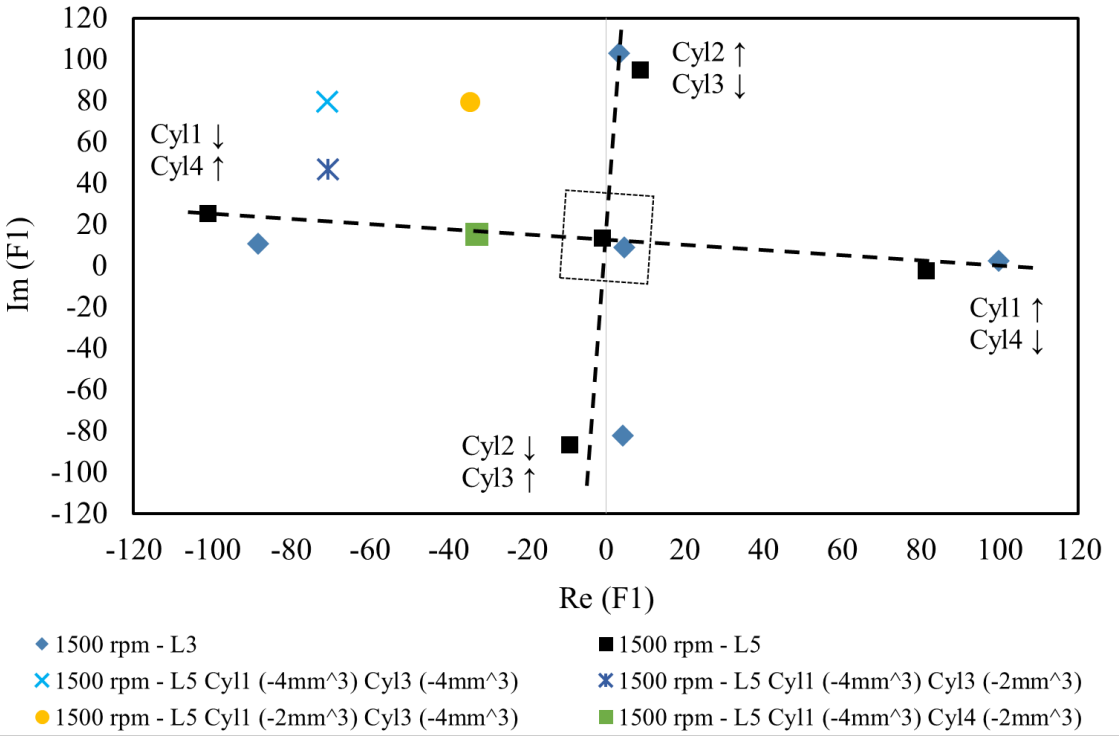

Figure 58. Representation in the complex plan of the F1 order at 1500 rpm and two loads for several injection variations.

In the last condition tested, injection variations were imposed in three different cylinders at the same time (Figure 59). Even in this case, considering the position of the resulting points it can be seen that the first order phase is closely linked to the imposed injection variations. The example reported in the figure shows the case of an imposed negative injection variation of $4mm^3$ in cylinders 1 and 4 and a negative variation of $2mm^3$ in cylinder 3. If we consider as a representative point the one related with an homogeneous injection in cylinders 1 and 4 and a different injection variation in cylinder 3 it can be seen that the variation imposed in cylinders 1 and 4 results in a first order close to the origin (the equilibrium point), while the variation in cylinder 3 shifts the point far from the origin and in phase with the cylinder 3, as expected.

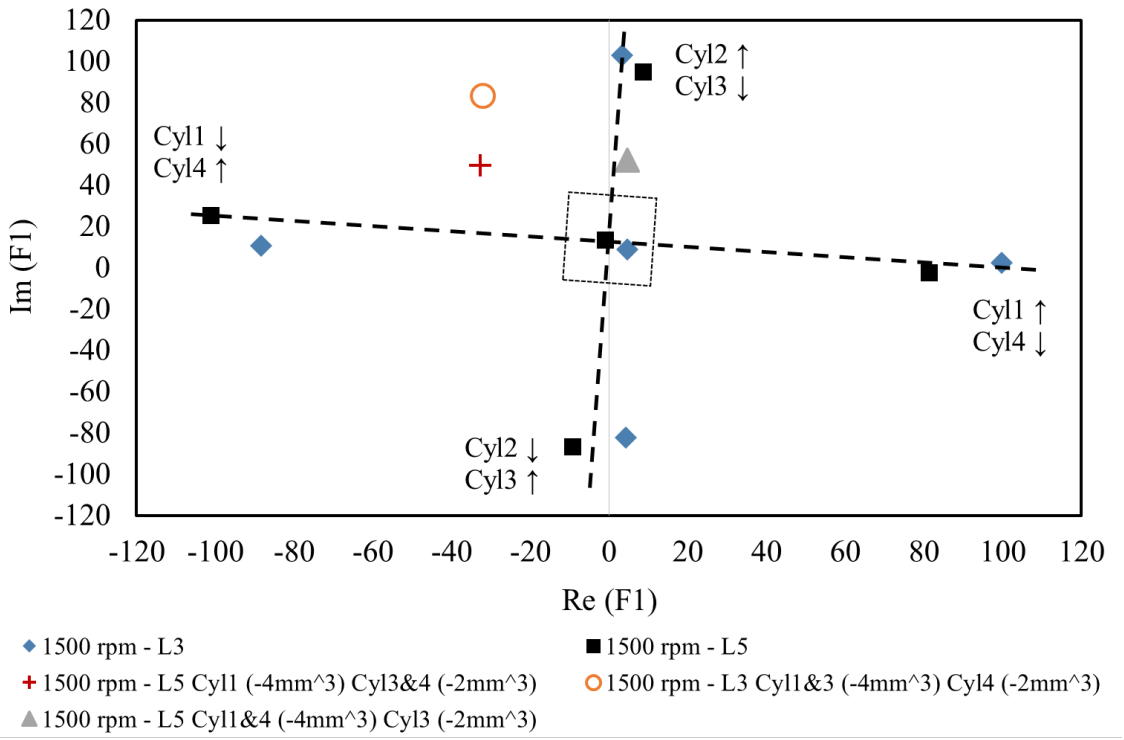

Figure 59. Representation in the complex plan of the order F1(Engine operating conditions: 1500 rpm at full load) by imposing different injection variations in three cylinders

A technique, to distinguish between the very exceptional case of identical injection variation in two non-consecutive cylinders was developed. This technique consists in monitoring the second order phase that in case of cylinder 1 and 4 results in a positive real part and the opposite in case of cylinder 2 and 3. In Figure 60, the characteristic phases of the F2 in case of several injection variations are represented. The F2 frequency corresponds to two events for each engine cycle; this order becomes dominant when there is an equal injection variation with respect to the standard condition in two cylinders non-consecutive in the firing order (1&4 or 2&3). When the module and phase of F1 are negligible but there is a variation in terms of fourth order module and a non-negligible value of the second order, an equal injection variation in two cylinders non-consecutive in the firing order occurs. In this case, by checking the phase of F2 the involved cylinder can be detected and the injection variation in each cylinder can be evaluated.

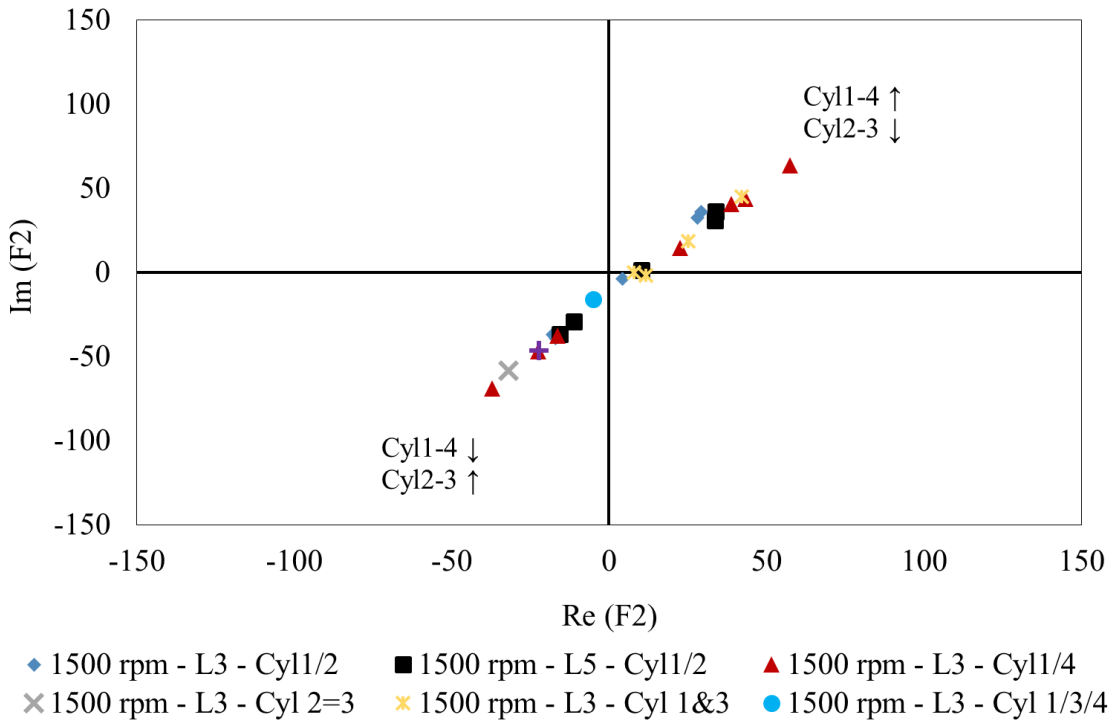

Figure 60. Representation in the complex plan of the F2 order at 1500 rpm and two loads for several injection variations

The experimental results confirm that a robust and physical correlation between the real and imaginary part of the first four orders (in particular F1, F2 and F4) and the cylinder-to-cylinder injection is present. From the analysis of the performed experimental tests, it can be concluded that the control strategy proposed in Figure 46 in case of a four cylinder engine can be used for a real operative engine.

Considering the TCAF methodology, in Figure 61 are reported the sum of the TCAF related to each cylinder for many different working points starting from high engine speed and full load to idle condition. As highlighted in the numerical study there is a linear correlation between TCAF and fuel injected into the engine, the coefficient of linearity changes with the engine speed as mentioned in chapter 3.1. For the amount of fuel injected into each cylinder the experimental test performed leads to the results depicted in Figure 62, that demonstrate the good reliability of the implemented monitoring system. As can be noticed, the results in terms of actual injected fuel in each cylinder are affected by a non-negligible data dispersion, this is mainly due to the injected fuel data in each cylinder that is not measured but it is collected through the installed ECU. Consequently, the uncertainty of the ECU data leads to a non-negligible dispersion.

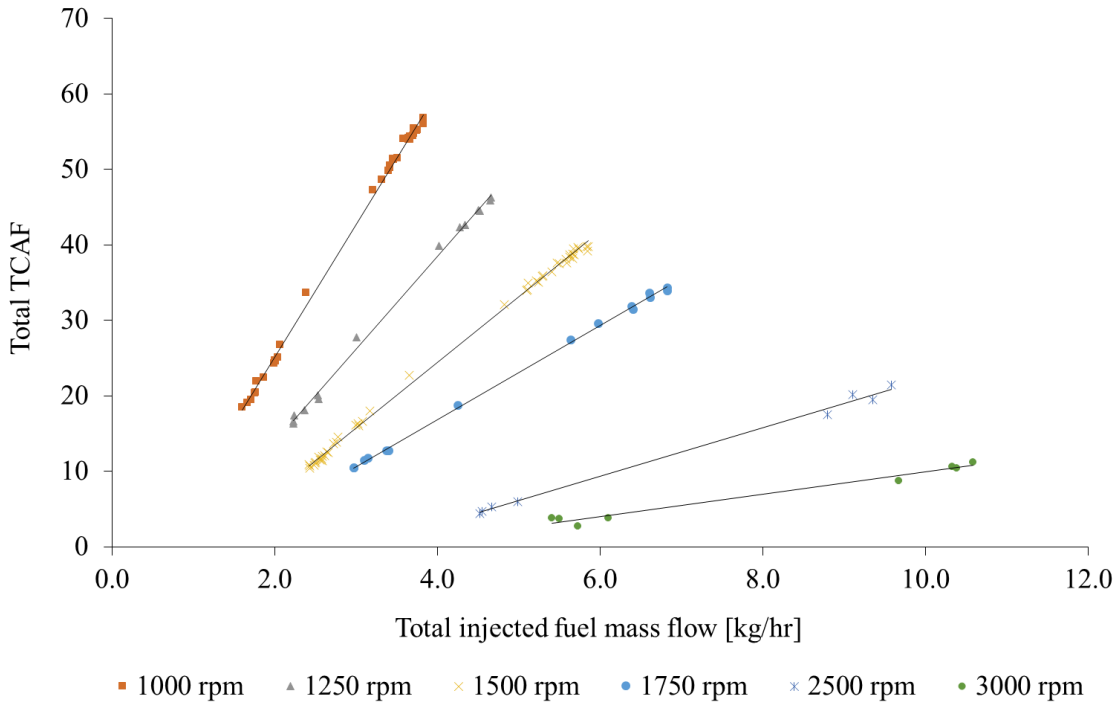

Figure 61. Correlation between total TCAF and total injected fuel mass flow at different engine speed and load (homogeneous and non-homogeneous injections are considered)

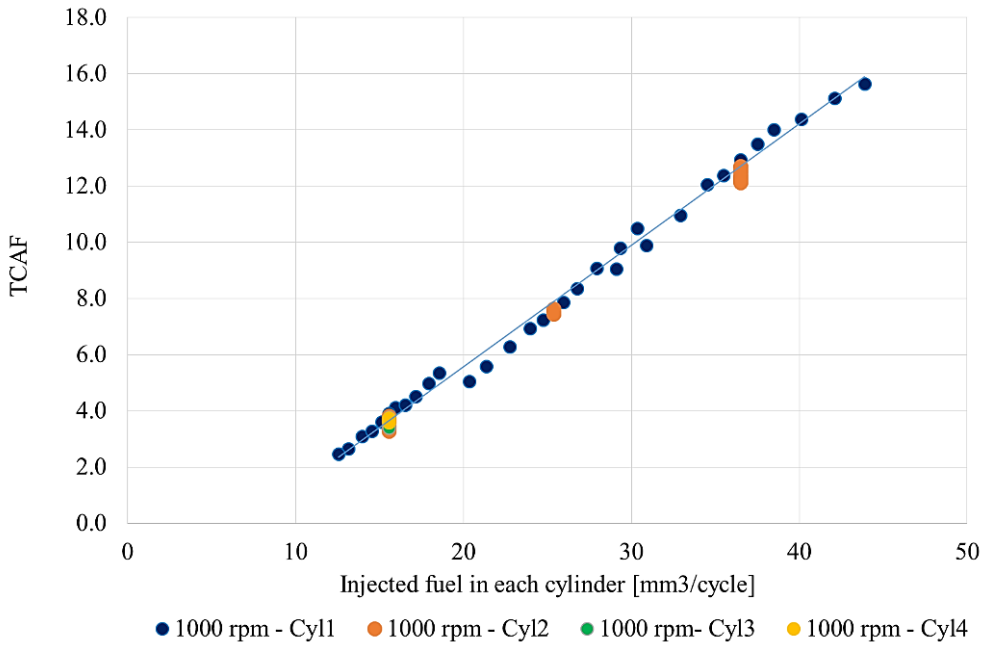

Figure 62. Correlation between TCAF and injected fuel quantity in each cylinder. Engine speed:1000 rpm from load 1 to full load

The experimental results of TCSF parameter for the total amount of fuel are depicted in Figure 63. More in detail, the sum of TCSF parameter for each cylinder respect to the total amount of fuel injected measured, validate the predictability of the fuel injected throw this specific monitoring parameter. Indeed, a linear correlation between TCSF and total fuel injected is experimentally confirmed.

Further, the amount of fuel in each cylinder respect to the related TCSF is depicted in Figure 64, more in detail, the TCSF's trend related to the injected fuel mass in each cylinder and the related fuel injected, at the engine speed of 1000 rpm for several load condition (from lowest load to full load). Despite the confirmation of the linearity found during the numerical activity, a data dispersion can be highlighted. It has to be underlined again, that it was not possible to measure the fuel injected in each cylinder so the dispersion of the data is affected by the uncertainty of the data coming from the ECU, as mentioned for the TCAF methodology.

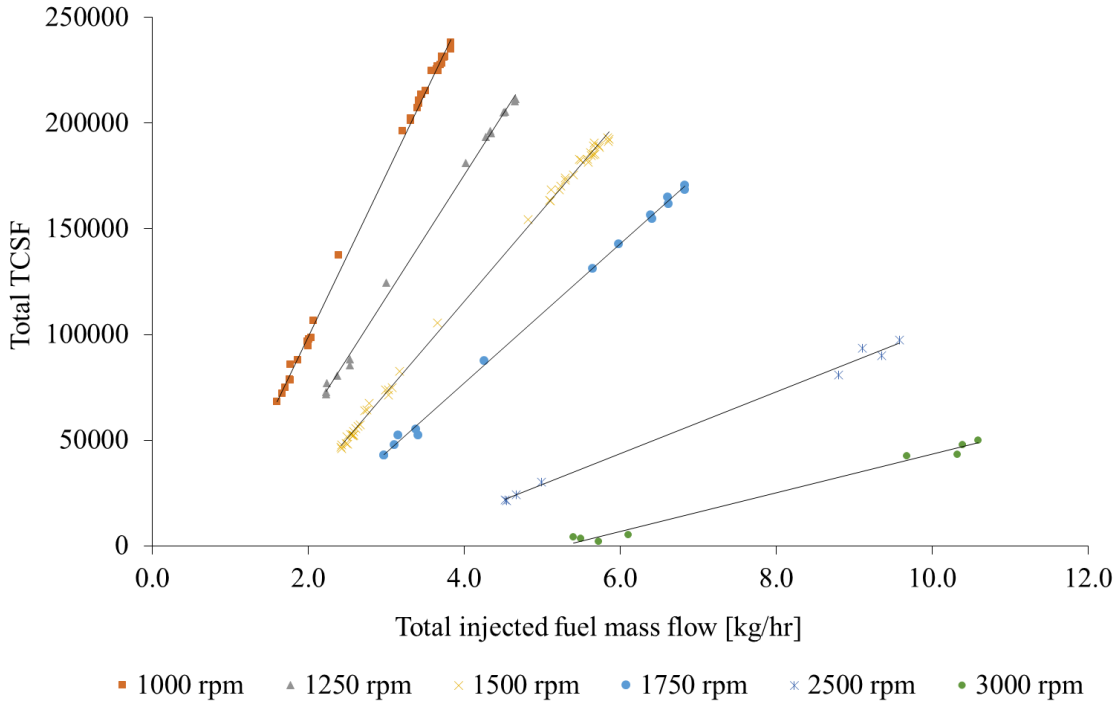

Figure 63. Correlation between total TCSF and total injected fuel mass flow at different engine speed and load (homogeneous and non-homogeneous injections are considered)

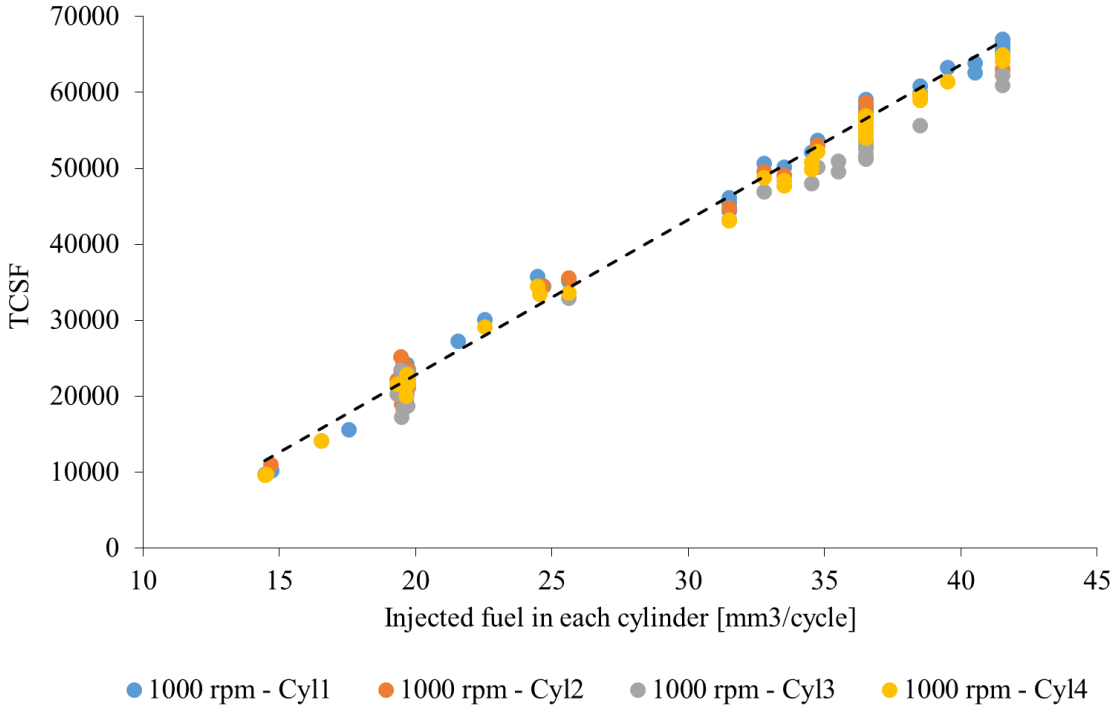

Figure 64. Correlation between TCSF and injected fuel quantity in each cylinder. Engine conditions: 1000 rpm from load 1 to full load

As highlighted during the numerical activity both the TCSF and TCAF methodology becomes not reliable when applied to engine working point at high revolution speed, so, the correlation is consistent at medium and low engine speed (up to 2000 rpm), where it is possible to apply a strategy for correcting the cylinder-to-cylinder injection variations by using information coming from the TCSF or TCAF. For brevity reason, in Figure 65 and Figure 66, only TCSF correlation at 1500 and 1750 rpm related to the cylinder 1 is reported, in order to highlight the reliability of the correlation at low engine speed.

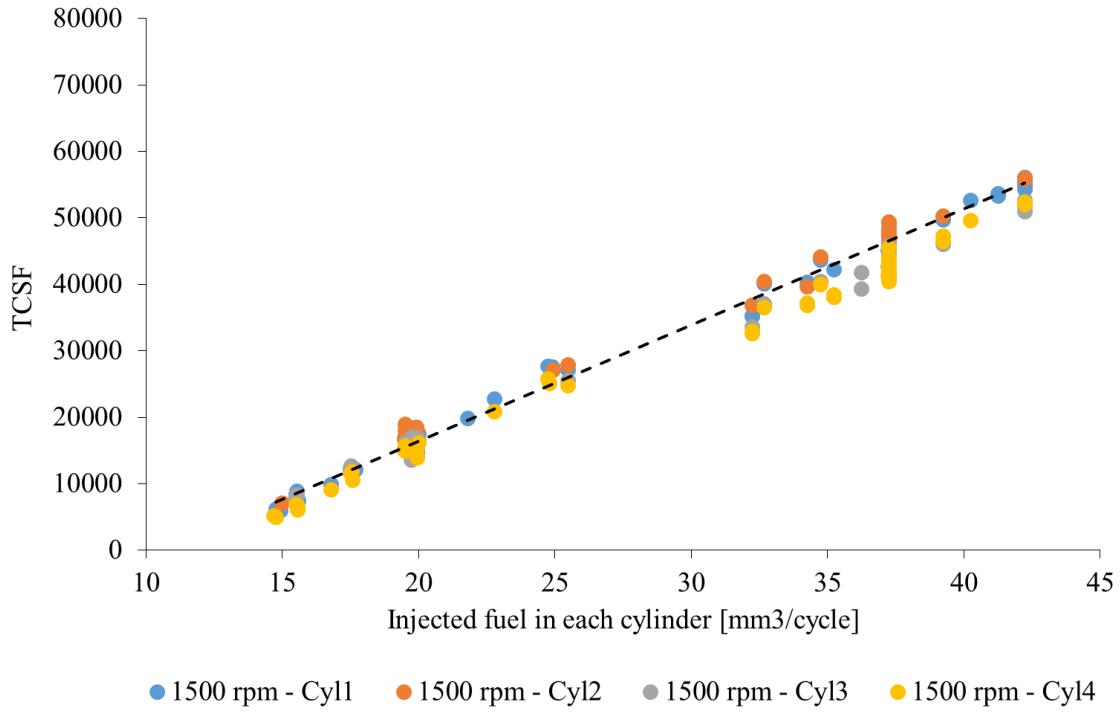

Figure 65. Correlation between TSF and injected fuel quantity in each cylinder. Engine condition: 1500rpm from load 1 to full load

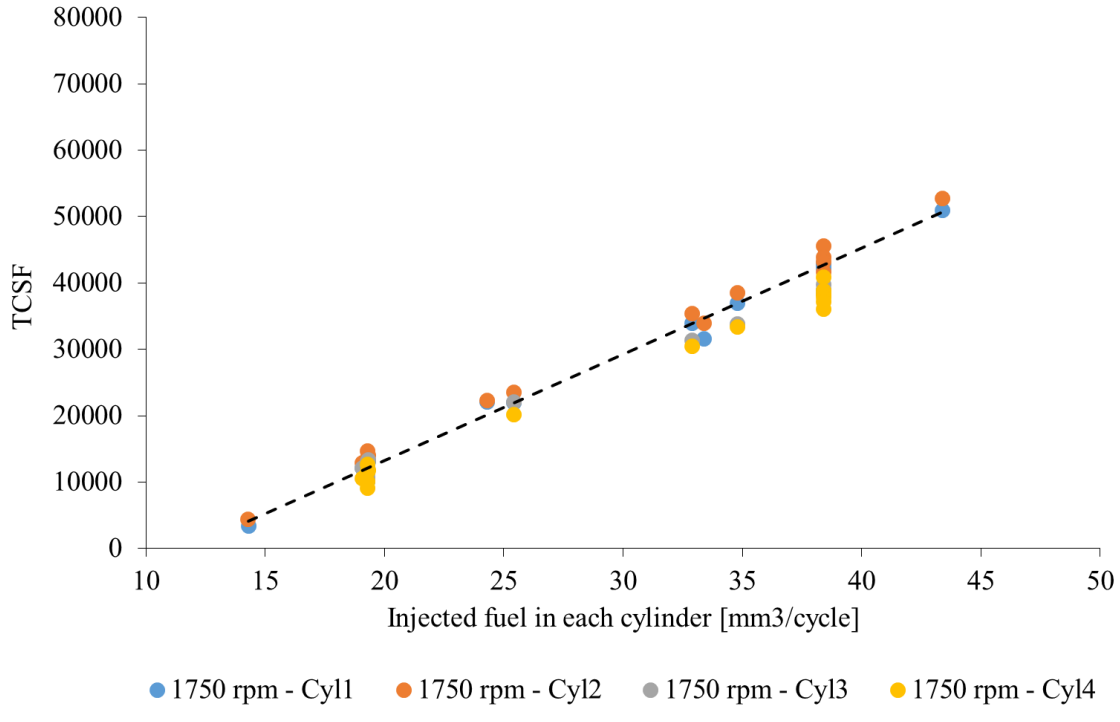

Figure 66. Correlation between TCSF and injected fuel quantity in each cylinder. Engine condition: 1750rpm from load 1 to full load

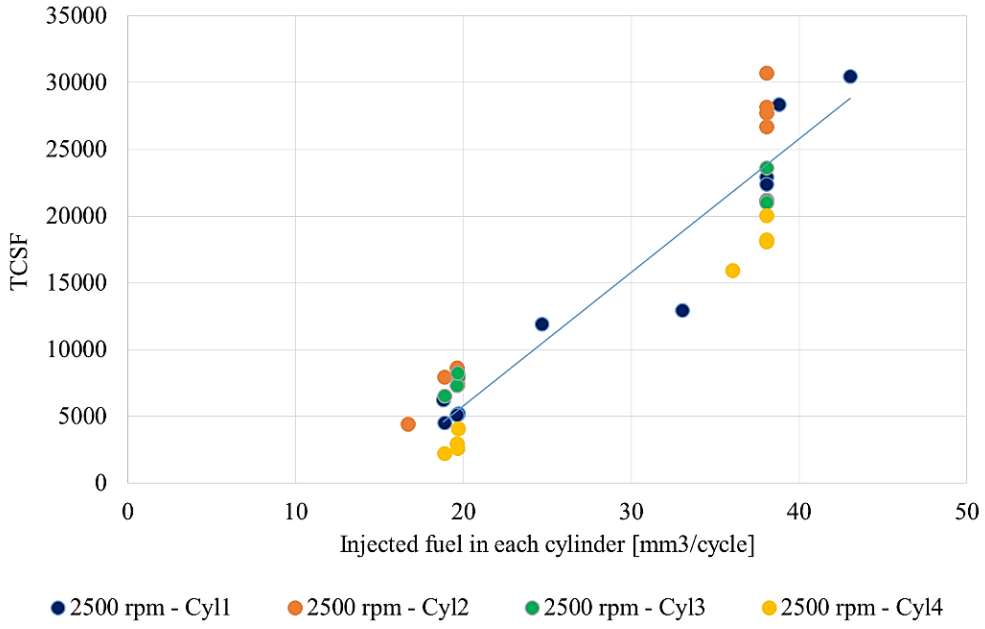

Figure 67. Correlation between TCSF and injected fuel quantity in each cylinder. Engine condition: 3000rpm from load 1 to full load

Moving to high engine speed the dispersion of the TCSF and TCAF increase (Figure 67). In Figure 68, the effects on TCSF of the injection variation compared to standard condition at 2500 and 3000 rpm is reported. By imposing a positive injection variation of injection to the cylinder 1, it is expected to detect only an increase of the TCSF related to the cylinder 1. However, especially at 3000 rpm, variations in terms of TCSF involve also the other cylinders. In this specific case, an unjustified TCSF decrease related to cylinder 2 occurs.

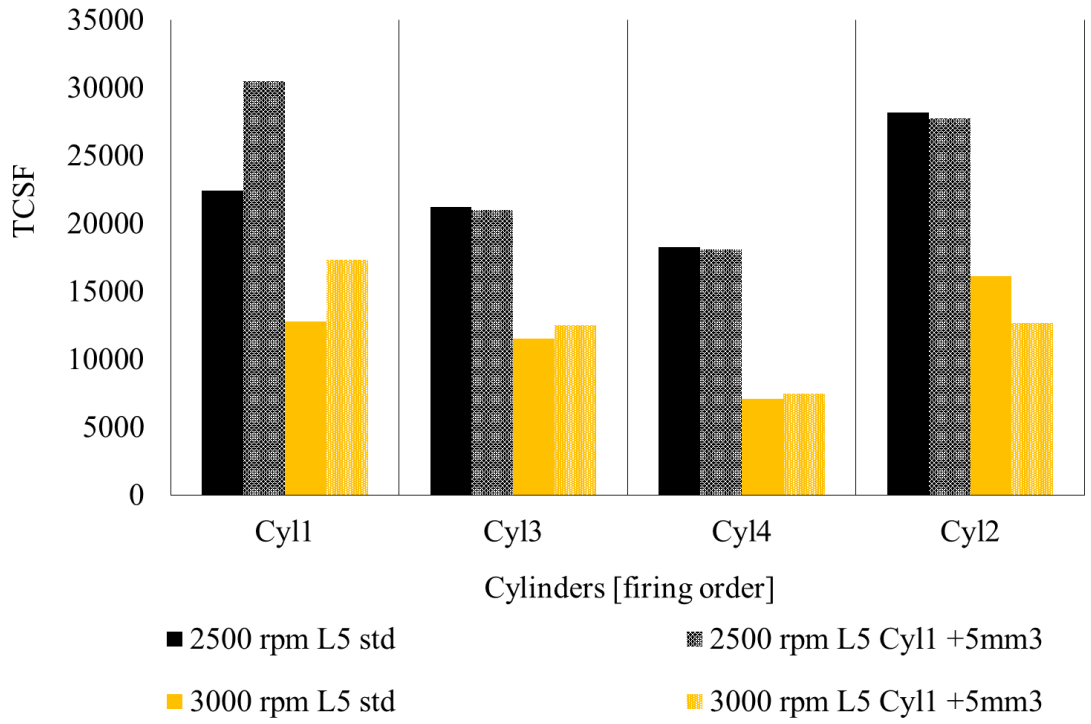

Figure 68. Effects on TCSF of the injection variation compared to standard condition at high engine speed.

In order to overcome the issue related to the high engine speed it is suggested to operate this monitoring methodology at low engine speed, more in detail, once the injection issue is detected by checking the F4 module or TCSFs or TCAFs sum, it will be a good practice to move to medium-low engine speed, where the turbocharger speed dispersion is lower, in order to properly detect and eventually correct the injection quantity in each cylinder.

Experimental tests were carried out to understand the minimum injection quantity variation detectable with the methodologies proposed in this thesis. The tests have been conducted by varying the injection quantity in the cylinder 1 from -1 mm3 per cycle to +1 mm3 per cycle respect to the standard value by step of 0.2 mm3. The engine working point chosen for this tests was at 1500 rpm and full load, with a standard injection quantity of 37 mm^3 per cycle.

4.4 Injection correction test

By taking advantage of the available deteriorated injectors set, the methodologies developed for the monitoring of the injector performance were tested to correct the injection in each cylinder. In the first part of this chapter, the analysis of the results for the deteriorated injectors are showed, then, the application of the methodologies to correct the injection is presented.

4.4.1 Experimental results for the deteriorated set of injectors

The analysis of the experimental tests carried out with the deteriorated set of injectors have led to results in terms of in-cylinder pressure, dynamic exhaust pressure and exhaust temperature that confirm the inhomogeneity of the injector performance consequently, the TC speed is characterized by a non-homogeneous behavior. As can be seen in Figure 69**,** a difference in terms of peaks of dynamic exhaust pressure can be highlighted. More in detail, there is a remarkable difference between cylinder 4 and cylinder 1. In order to understand if these differences are due to another possible influencing factor, such as a difference in the volumetric efficiency, the injectors in cylinder 1 and 4 were switched. The exhaust pressure results, orange line in Figure 69, for the configuration with the injectors inverted confirms that there is a difference in the performance of the four injectors.

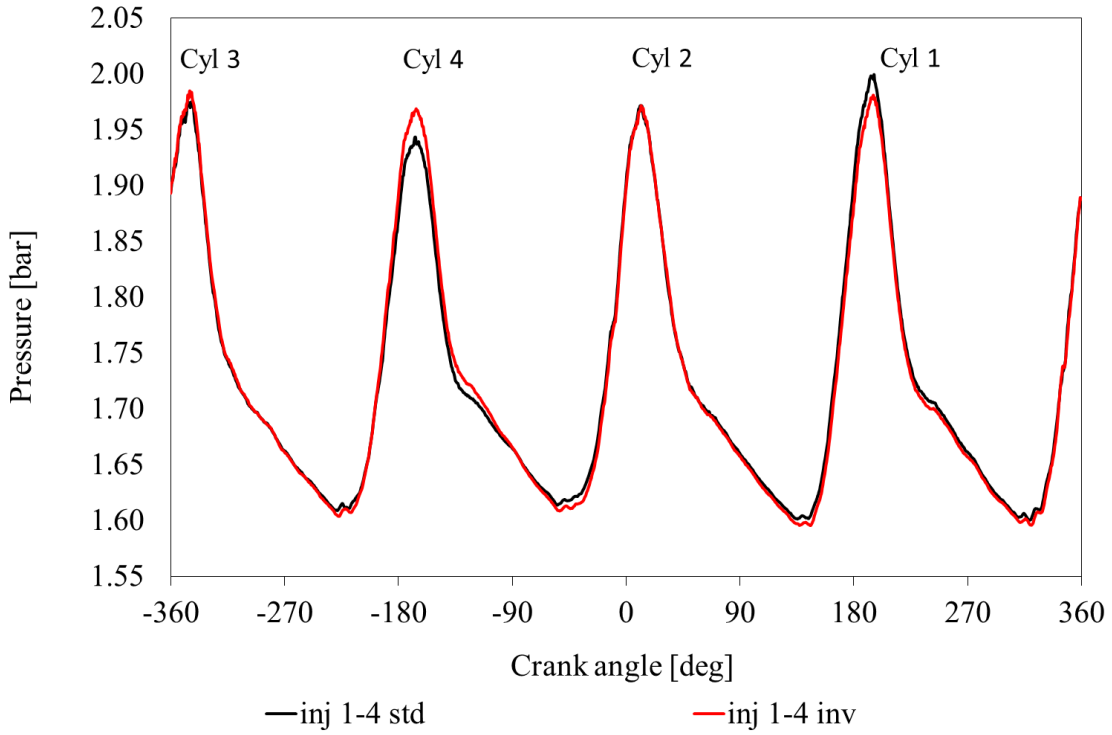

Figure 69. Dynamic exhaust pressure (engine working point: APP_r 40 - ~19 mm3/cycle - 1000 rpm) in case of standard position of the injectors and a configuration with the injectors of cylinder 1 and 4 switched

The irregularity of the injectors' performance is further highlighted by the non-negligible difference in terms of exhaust temperature among the cylinder's exhaust. The temperature at the exhaust of each cylinder is reported in Table 4, in which it a specific condition at 1000 rpm and at load 3 (APP_r 40) is shown.

Table 4. Exhaust temperature (engine working point: APP_r 40 - ~19 mm3/cycle - 1000 rpm)

ExhTemp Cyl 1 C°	ExhTemp Cyl 2 C°	ExhTemp Cyl 3 C°	ExhTemp Cyl 4 C°
251	266	235	223

The inhomogeneity of the injectors influences the TC speed that does not present the periodicity in the 180 degrees characteristic. This condition is represented in Figure 70, where a difference in terms of peaks and valley among cylinders can be noticed.

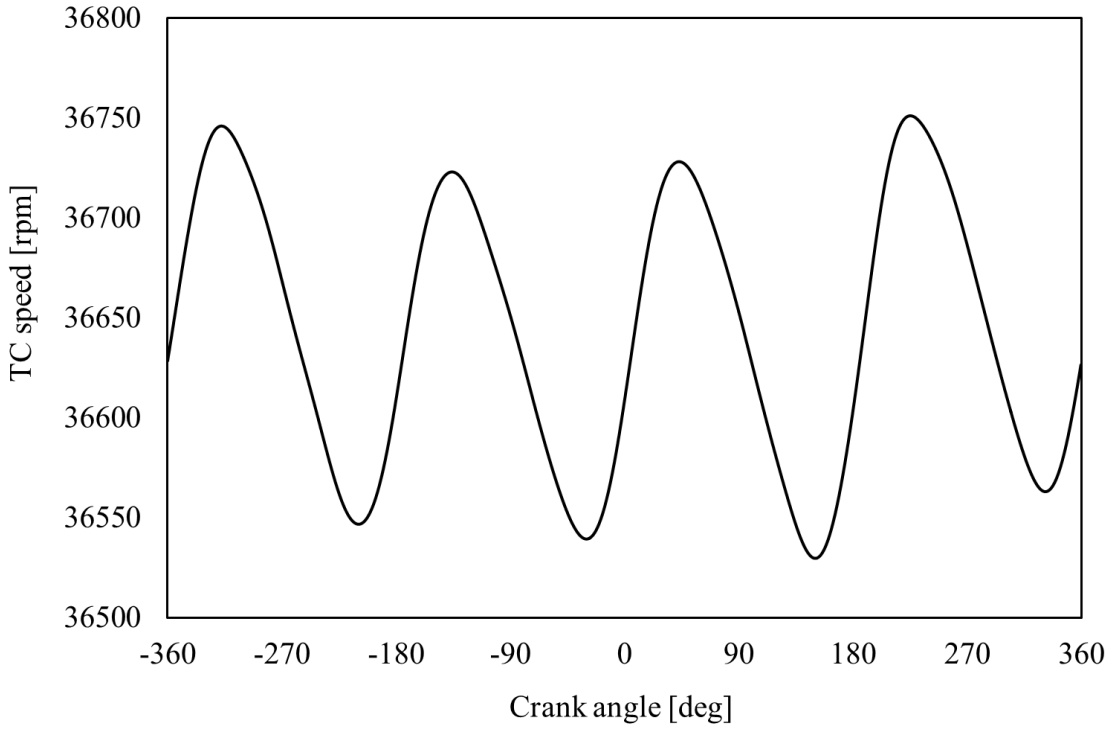

Figure 70. Turbocharger Speed (engine working point: APP_r 40 - ~19 mm3/cycle - 1000 rpm)

The possible causes of this condition could be a difference in terms of volumetric efficiency due to a piston leakage or differences in terms of injectors' performance due to the time degradation.

In order to exclude the influence of piston leakage or volumetric efficiency experimental test was performed with engine motored condition**.** The experimental test results underlined a difference in terms of maximum pressure among cylinders (max 4%), that cannot be associated with blowby effect. In Figure 71 the behavior of the in-cylinder pressure of all the cylinders is reported**.**

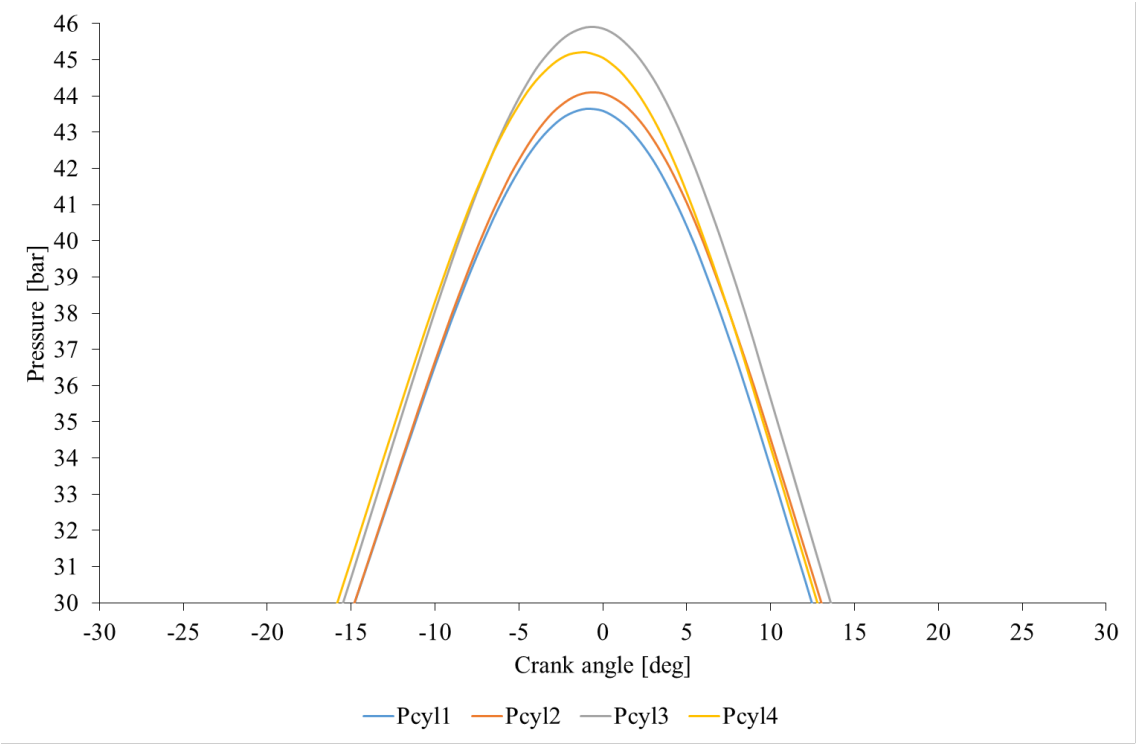

Figure 71. In-cylinder pressure with engine motored

The experimental test carried out with the switched injectors, in two engine working points (configuration 1: APP_r 40 - ~19 mm3/cycle - 1000 rpm; configuration 2: APP_r 100 - ~38.5 mm3/cycle - 1750 rpm), were analyzed deeper. In Figure 72, the exhaust temperature for each cylinder, in case of baseline configuration and with the injectors switched is depicted. A relevant increase in terms of exhaust temperature of the cylinder 4 and a decrease for the cylinder 1 occurs. However, a difference between the two exhaust temperature associated with cylinder 1 and 4 still persist and without the expected inversion of the behaviour due to the inversion of the injectors. This can be mostly explained by the non-reliability of the thermocouple exploited for the test but still underline a great inhomogeneity among cylinders.

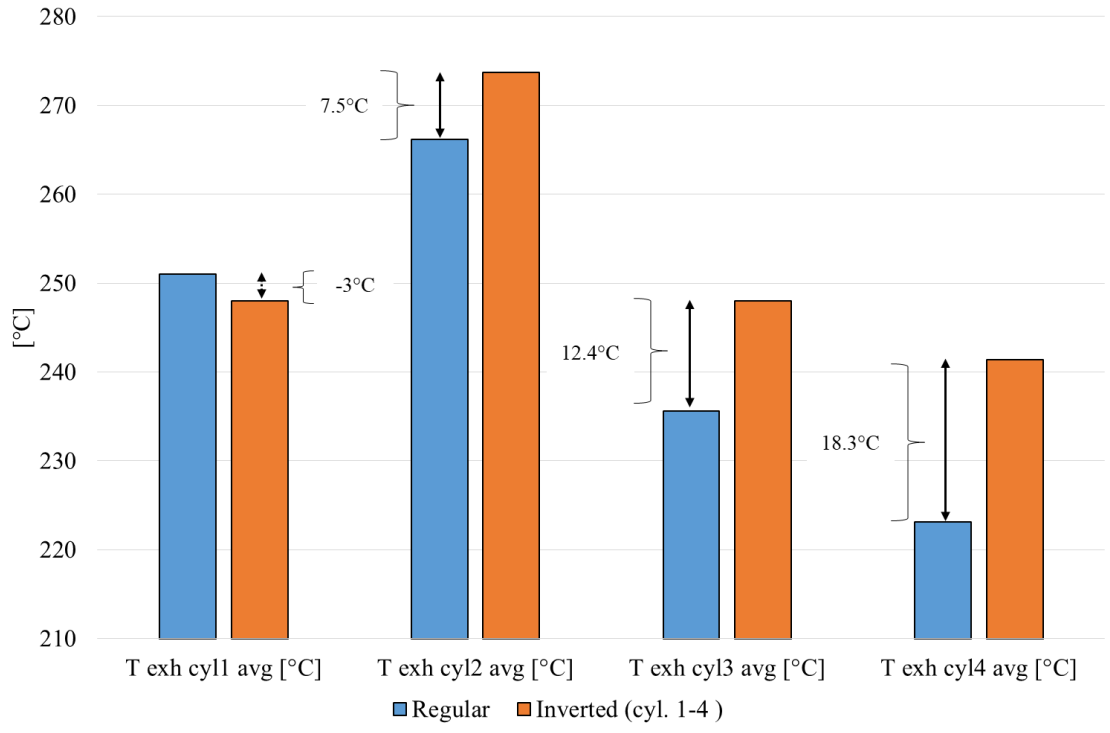

Figure 72. Exhaust temperature in case of injector switching (configuration 1)

More in detail, with the configuration 1 the variation of the exhaust temperature in the cylinder 1 is negligible (-3°C) and very smaller respect to the increase in temperature associated to the cylinder 4 (18.3°C) but for what concern the exhaust pressure peaks (Figure 69), there is a comparable variation between the two cylinders and there is the inversion of the values. In fact, the pressure in cylinder 4 becomes greater than the pressure in cylinder 1 of about the same quantity. Thus, by applying the FFT methodology to the TC speed signal, the first order phase highlights an inversion by inverting the injectors between cylinder 1 and 4. This confirms once more the inhomogeneity of the injection among cylinders (Figure 73).

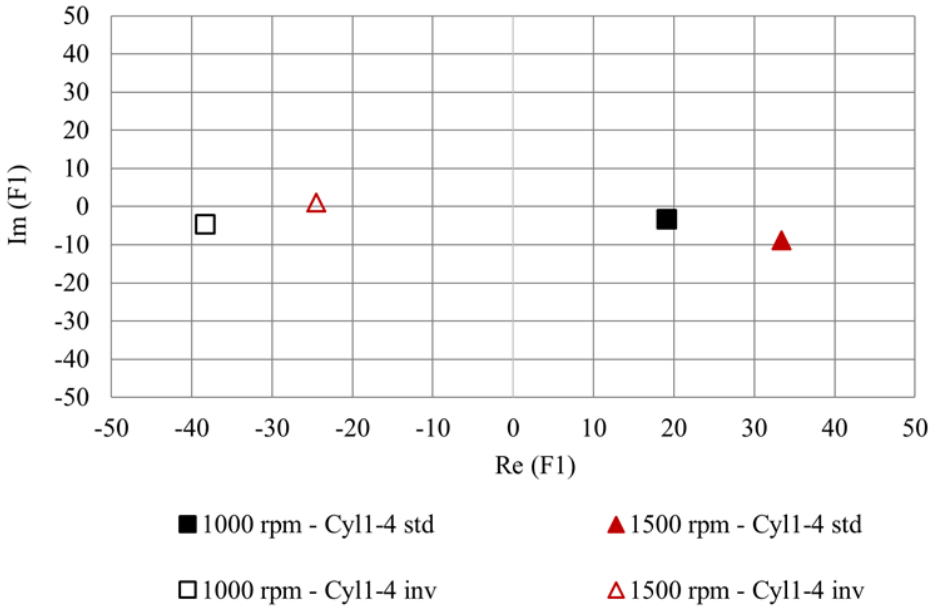

Figure 73. Representation in the complex plan of the order F1 in case of standard (black points) and inverted (red points) position of injector 1 and 4. Engine operating condition: 1500 rpm at full load

After the analysis of the experimental results collected to study the deteriorated injectors, it can be stated that among the injectors exist a relevant performance differences. To understand if the behaviour of the engine provided with the new injectors set and with the old injectors set is the same, the correlations between the F4 module and the total amount of injected fuel for both cases at 1500 rpm by varying engine load were compared.

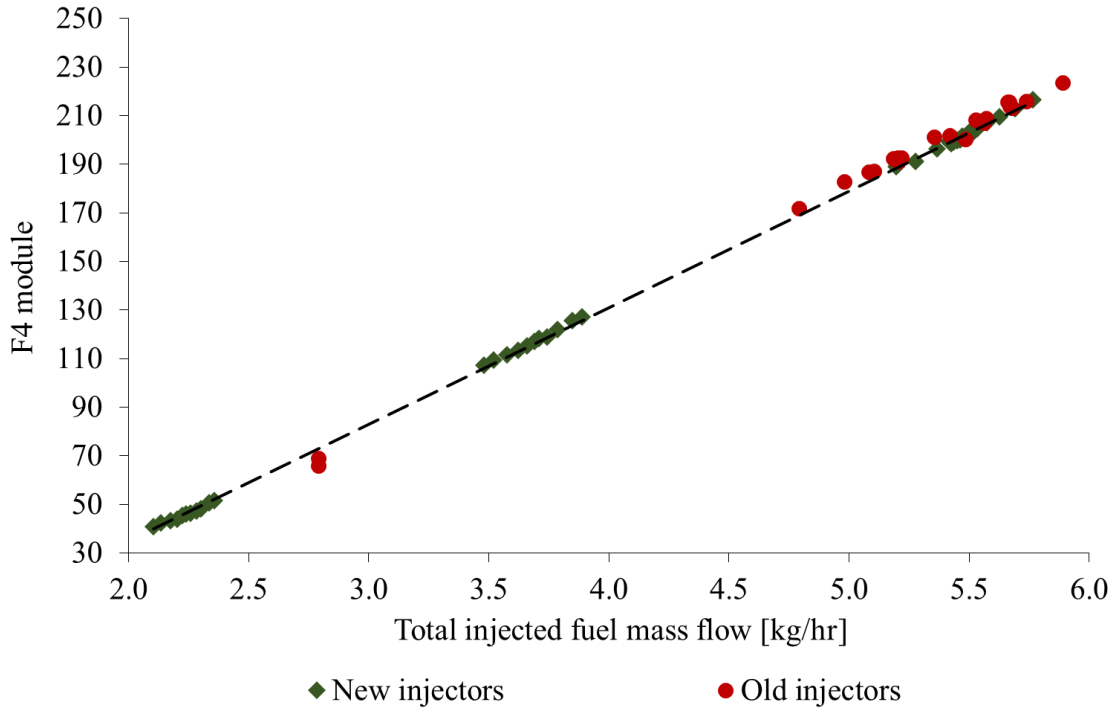

Figure 74. Representation of the F4 module in function of the total injected fuel. Comparison between old injectors (blue points), new injectors (green points).

In Figure 74 are reported all the experimental results for the new and the old injectors in terms of total fuel injected and the fourth order module. The linear correlation obtained with the deteriorated injectors set and the one obtained with the new injectors set correctly installed is constant. Thanks to this result it can be stated that the calibration of the correlation is needed only for each engine typology and not for each singular engine. The results for the TCAF and TCSF methodology are absolutely in line with the FFT and are reported in Figure 75 and Figure 76.

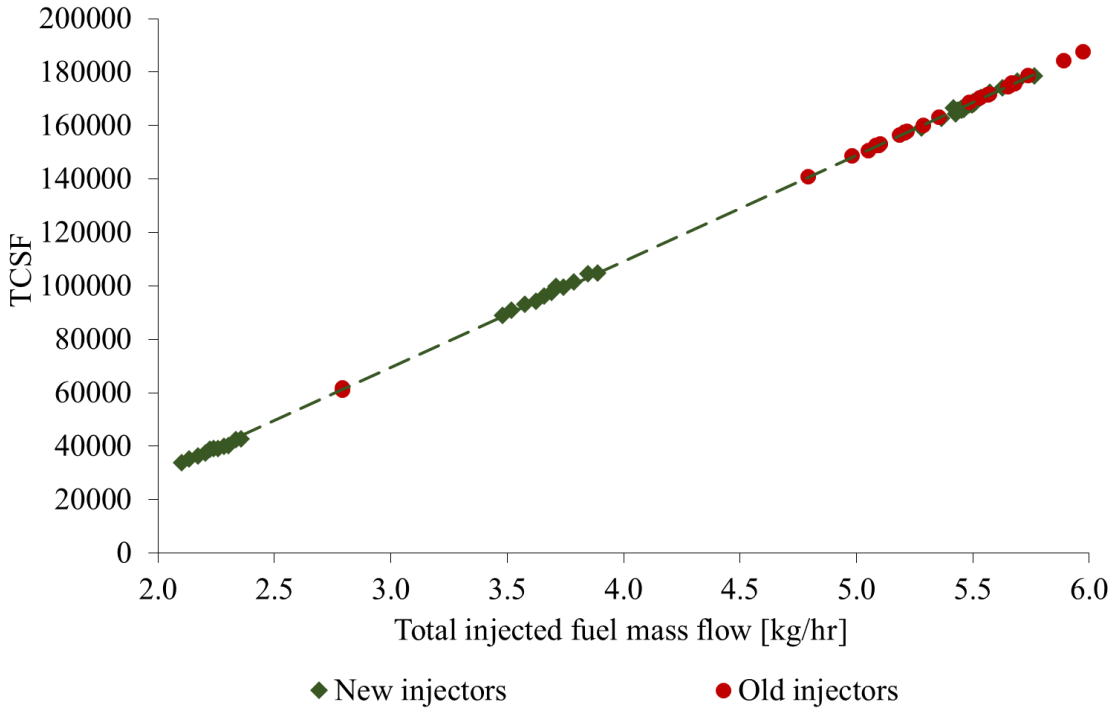

Figure 75. Representation of the TCSF sum in function of the total injected fuel. Comparison between old injectors (blue points), new injectors (green points).

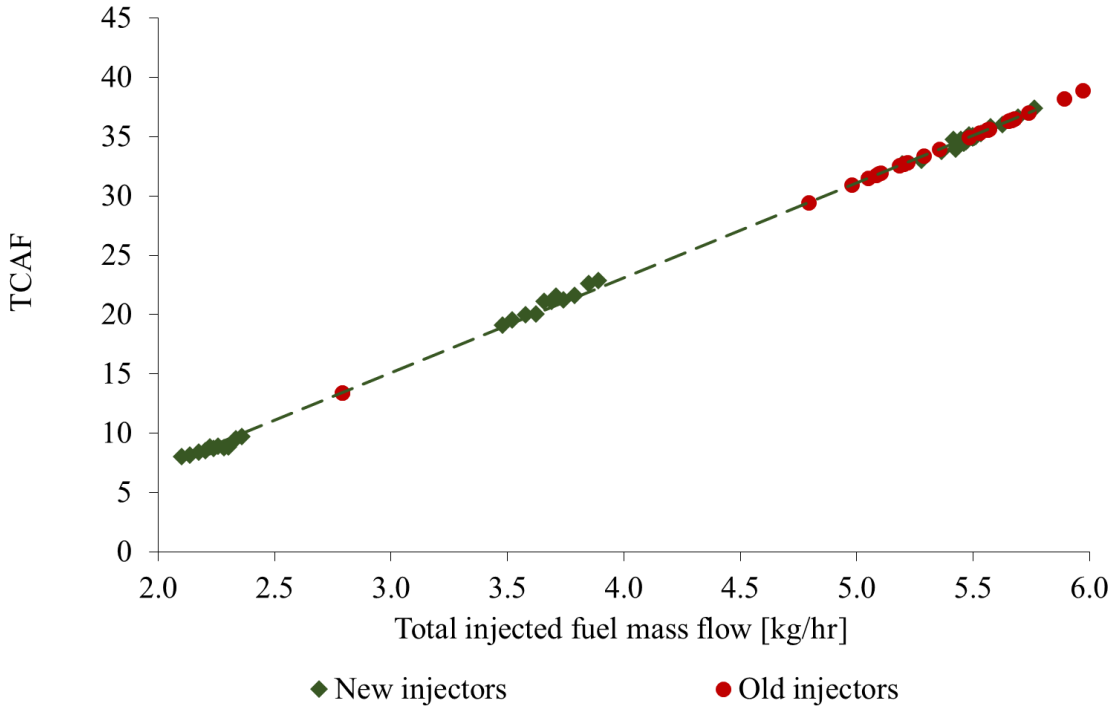

Figure 76. Representation of the TCAF sum in function of the total injected fuel. Comparison between old injectors (blue points), new injectors (green points).

4.4.2 Correction based on the FFT method

In this paragraph, the test of the methodologies developed to correct the injection in case of deteriorated performance of the injectors is reported. Once established that there is an inhomogeneity in terms of mass fuel injection among cylinder, the purpose of the activity was to correct the injection quantity using the methodologies, based on the TC speed.

4.4.3 Injection correction based on FFT method

As explained in the previous chapters when an inhomogeneity in the injectors' performance occurs, the study of the first four orders of the TC speed changes.

By post processing the experimental results of the actual condition of the engine, from the FFT analysis of the TC speed it was observed that both the module (Figure 77) and the phase (Figure 78) of the first order have a value that can be associated to a non-homogeneous injection.

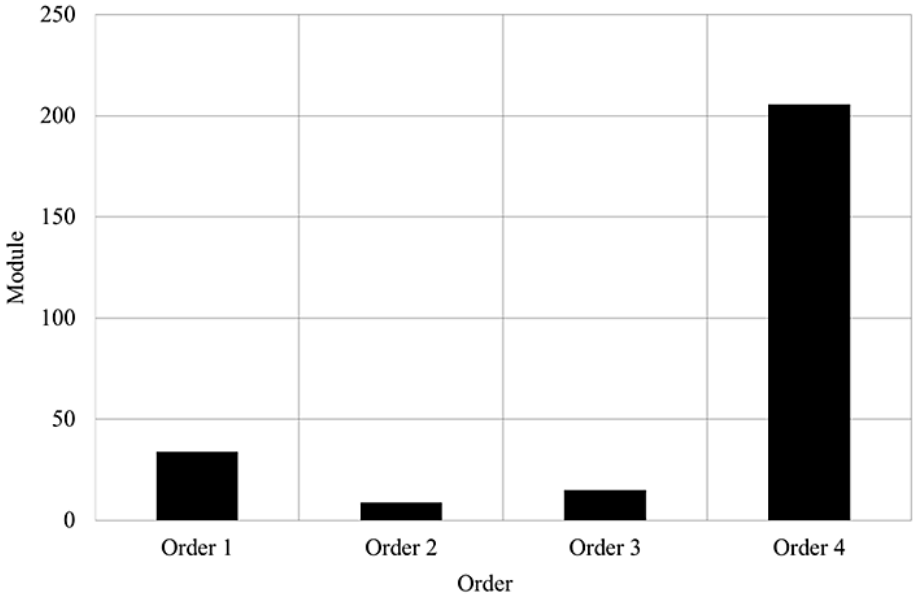

Figure 77. FFT analysis. Engine operating condition: 1500 rpm at full load.

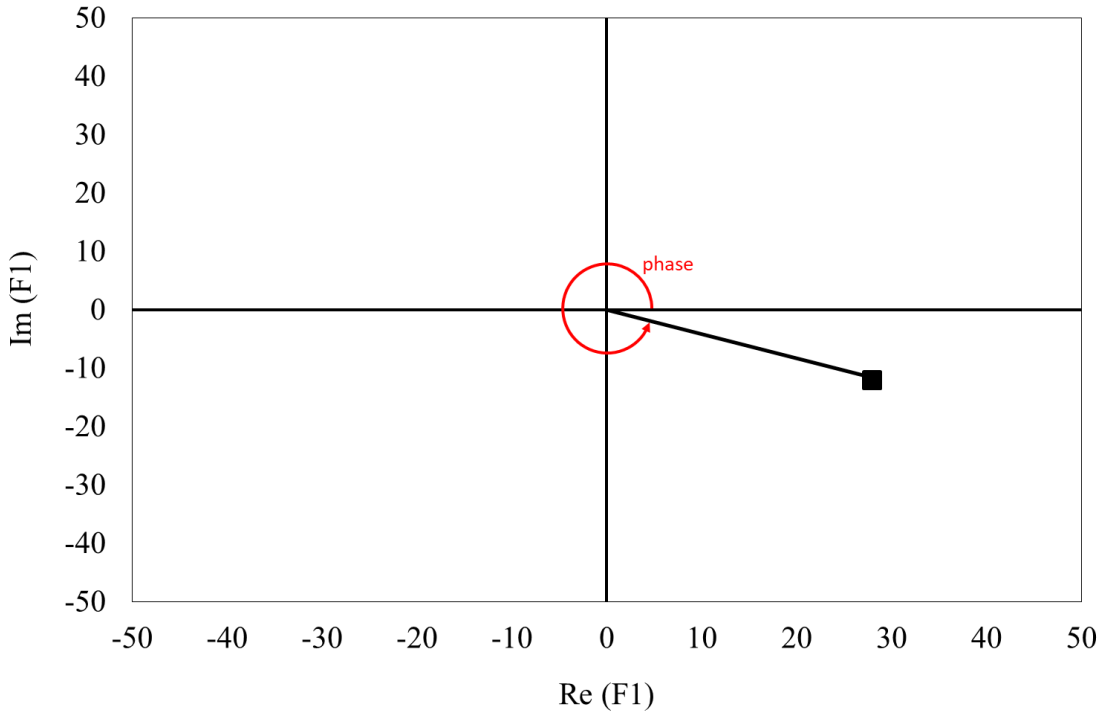

Figure 78. Representation in the complex plan of the phase of the order F1. Engine operating condition: 1500 rpm at full load

Once the injection variation among cylinder is detected, by controlling the ECU a correction in terms of injection can be applied. Hence, the homogeneous engine working condition can be restored.

A preliminary phase to identify the injection variation is to establish the characteristic phase of each cylinder of the engine. With this purpose the calibration of the F1 phase of each cylinder was required. Indeed, without knowing the characteristic phase of the cylinder of the first order, even if a non-homogeneous condition can be detected, it is not possible to detect the cylinders involved in the injection variation.

The calibration of the first order phase of each cylinder requires a set of experimental tests. The tests were performed by strongly increasing and decreasing the injection variation in one cylinder at a time. Imposing a strong variation of injection in one cylinder, a remarkable change in terms of phase occurs, thus, the variation of the phase related to the inhomogeneity preexistent can be neglected. The test was performed at 1500rpm and at full load, by increasing and decreasing the injection of 16% and 26% respect to the standard injection condition.

The results of the calibration for each cylinder are reported in the following figures (From

Figure 79 to Figure 82).

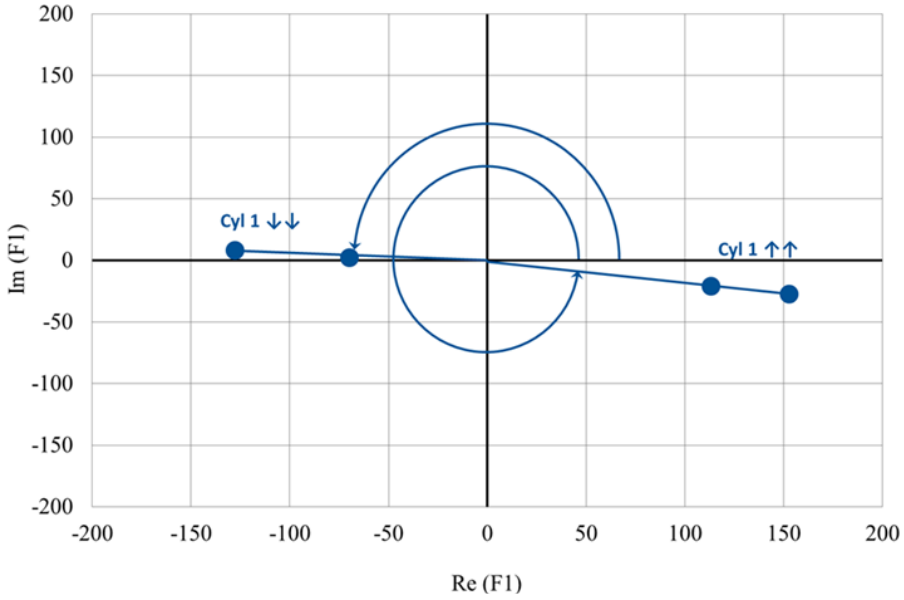

Figure 79. Characteristic phase of cylinder 1 Engine operating condition: 1500 rpm at full load

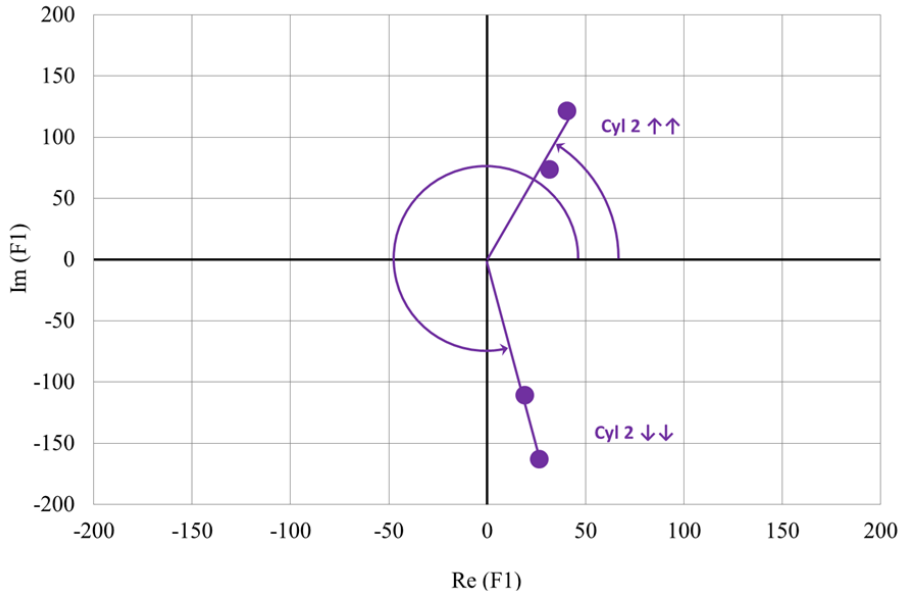

Figure 80. Characteristic phase of cylinder 2. Engine operating condition: 1500 rpm at full load

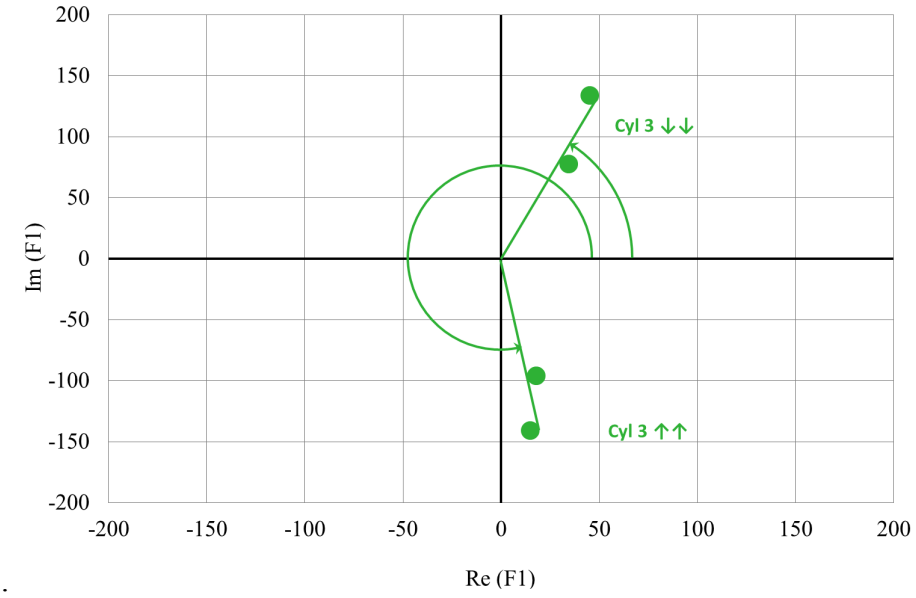

Figure 81. Characteristic phase of cylinder 3. Engine operating condition: 1500 rpm at full load

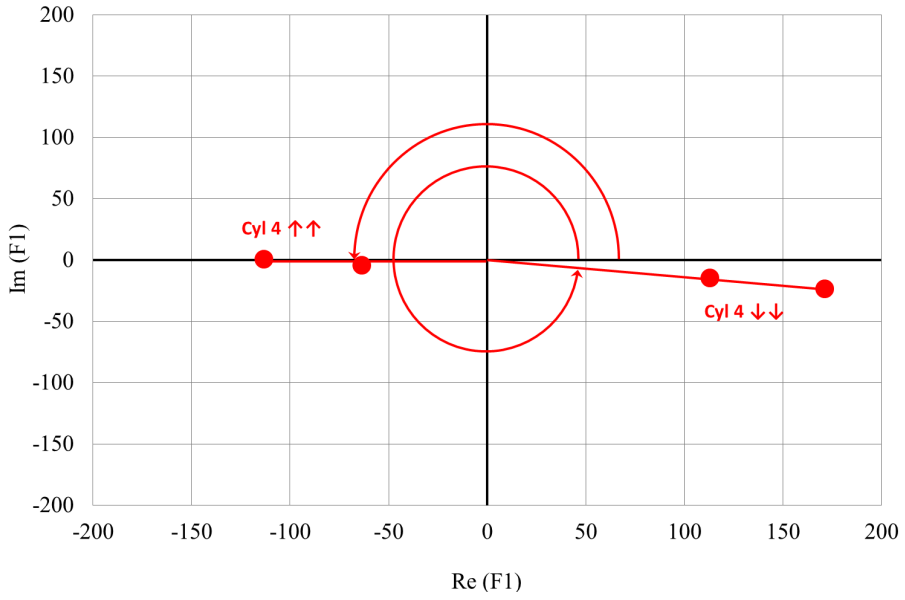

Figure 82. Characteristic phase of cylinder 4. Engine operating condition: 1500 rpm at full load

In case of regular functioning of the engine injectors, by varying the injection in only one cylinder, a difference in phase of 180 deg between the positive variation and the negative variation of the injection occurs. It is worth noting that the phase of the cylinder 2 and 3 are not characterized by a 180 deg difference between the increasing and the decreasing of the injection unlike the cylinder 1 and 4.This suggests that there is an unbalance of the cylinders 1 and 4 already in standard operating conditions. In fact, the characteristic phase obtained by imposing the variation in only cylinder 2 or cylinder 3,

is affected and distorted by a variation in injection in cylinder 1 and 4. In Figure 83, the standard condition point (black point) and the characteristic phases of the cylinders are reported.

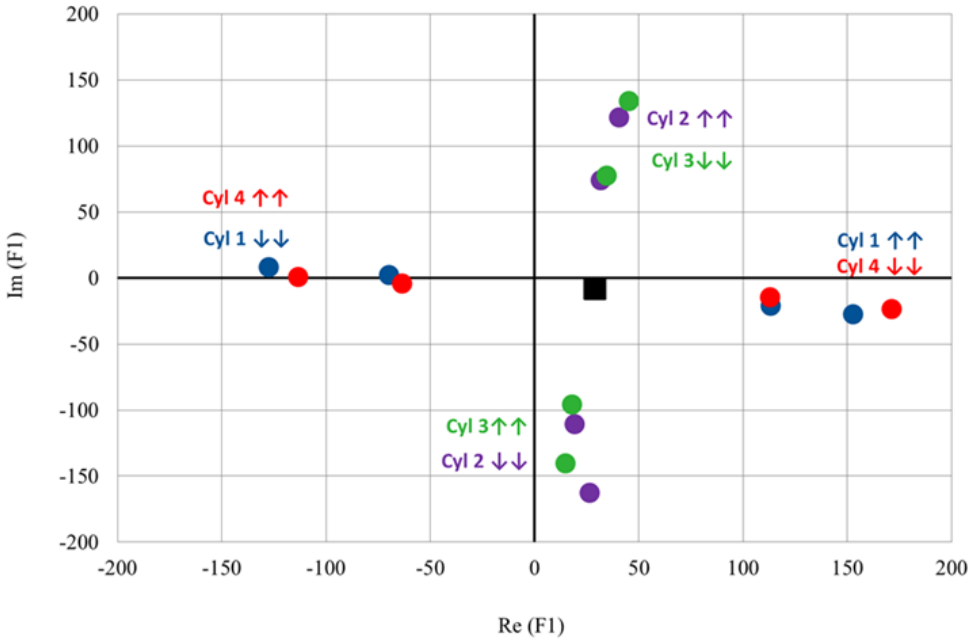

Figure 83. Representation in the complex plan of the order F1 in case of standard injection (black point) and imposed injection variations in one cylinder at a time. Engine operating condition: 1500 rpm at full load.

The position, in the complex plane, of the standard condition point, confirms a higher injected fuel quantity in the cylinder 1 and/or a lower injected fuel quantity in the cylinder 4. In fact, it is positioned along the characteristic phase of the cylinder 1 and 4 with a positive value of the real component. It has to be underlined that by considering as the origin of the axis the baseline point all the phases present a shift of 180 degrees from negative to positive variation, meaning that it is enough to change the origin of the complex plane to eventually reset the injection standard in a different position.

With the aim to balance the behaviour of the TC speed, an injection correction in cylinder 1 and 4 is imposed by considering the information coming from the F1 phase and module.

By applying this strategy for the injection variation, a negative injection correction of 3% to the cylinder 1 and a positive variation of 2% in the cylinder 4 was considered. These corrections were imposed through the ECU of the engine leading to a more

homogeneous behaviour of the cylinders. Indeed, first order module and phase, as can be observed in the complex plan (Figure 84), is very close to the origin of the axes, that corresponds to the increased balance condition respect to the condition without injection correction (black point). In order to evaluate if the correction of the injection imposed leads to a correct injection in all cylinder the TC acceleration has to be considered. Thus, the exhaust pressure presents a very homogeneous behavior in the 720 degrees of the engine cycle.

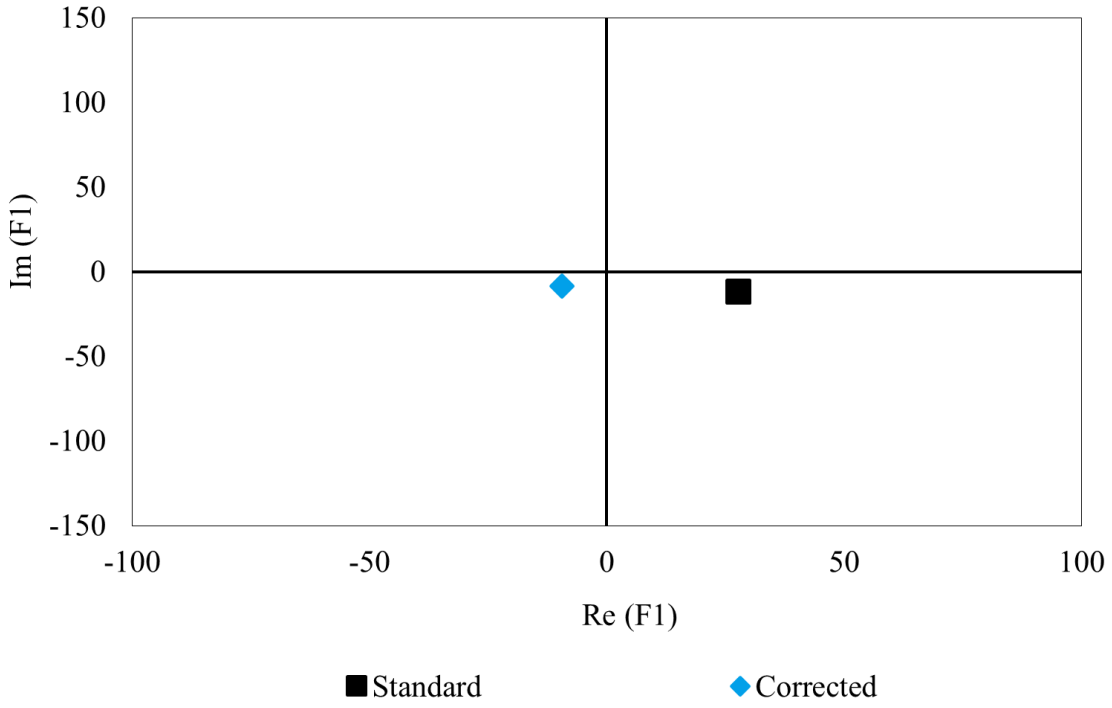

Figure 84. Representation in the complex plan of the order F1. Comparison between the baseline injection conditions and the corrected ones. Engine operating condition: 1500 rpm at full load

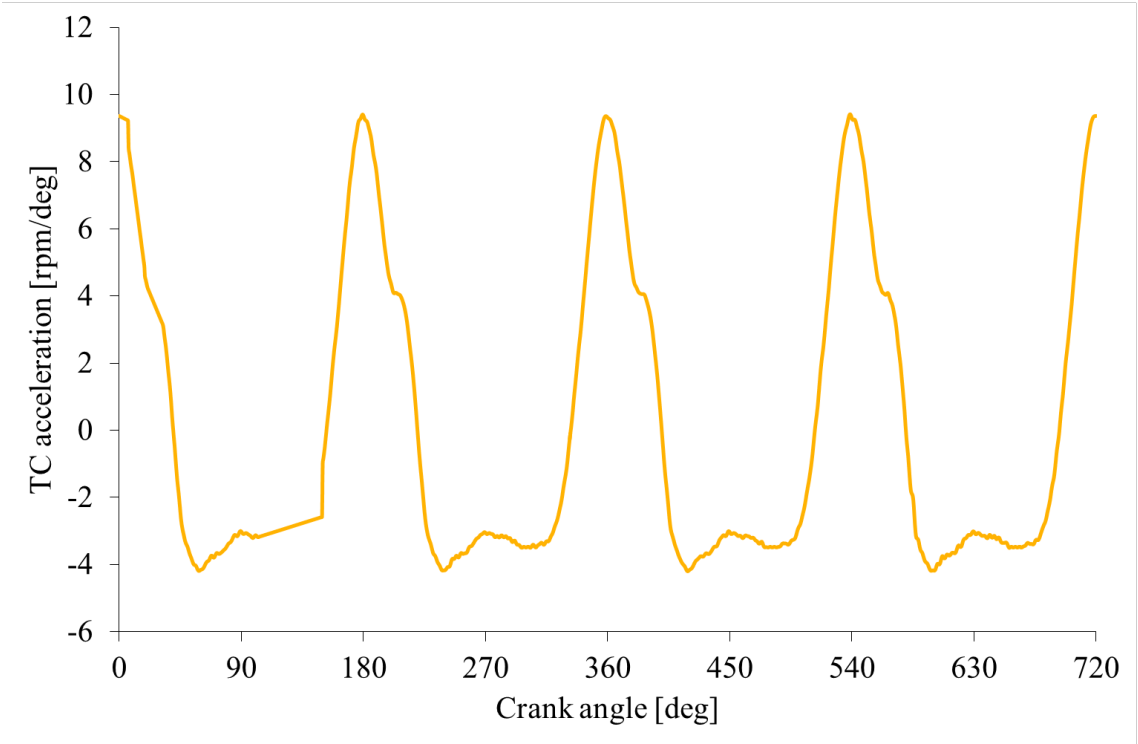

Figure 85. TC acceleration signal with corrected injection of deteriorated injectors

4.4.4 Injection correction based on TCSF method

First, the deteriorated injectors are evaluated with the TCSF to understand the inhomogeneity detected with this methodology. In this regards the experimental results reported in Figure 86 leads to the assumption that the injectors are not performing in the same way.

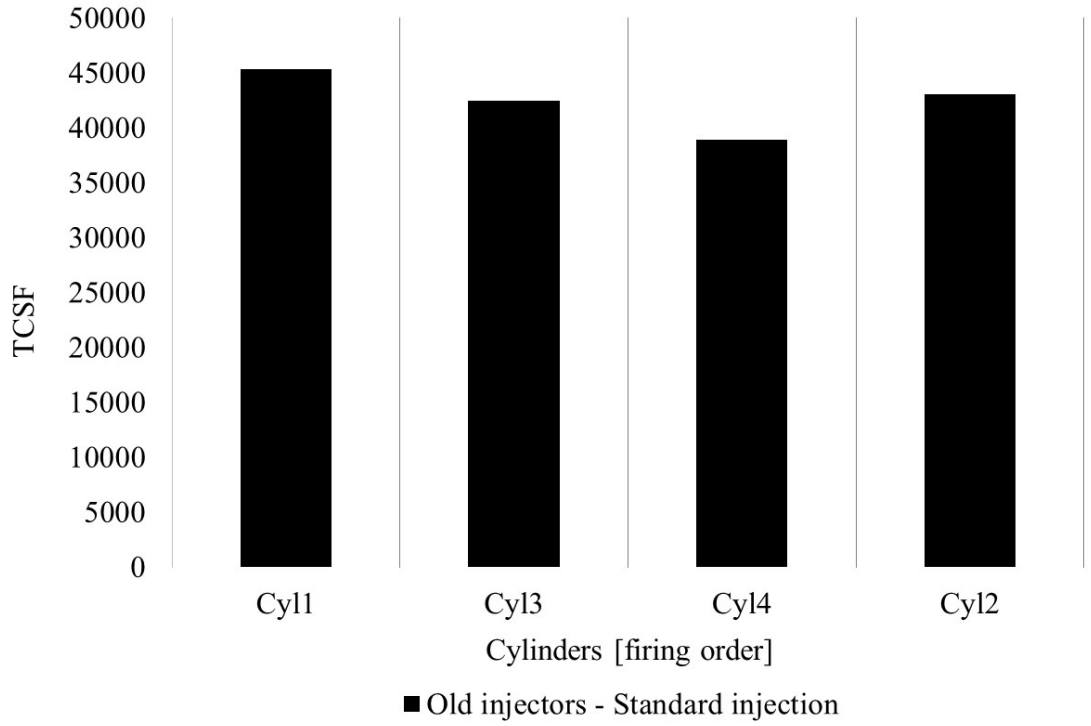

Figure 86. TCSF results for the deteriorated injectors set

The first step of the correction strategy exploited, is to check the cylinder's TCSF values. A correlation between TCSF and injected fuel in the reference cylinder is determined by the values assumed by TCSF in standard condition and exploited for all the injectors. The total amount of injection variation is then evaluated by the sum of all the TCSF collected in all cylinders. Once get the information about the total amount of fuel injected it is possible to correct the injection in each cylinder knowing the relation built between injection and TCSF. By imposing this correlation, since every TCSF values are known, it is possible to define the fuel mass related to each cylinder.

The experimental test for the correction of the injection was performed at the engine speed of 1500 rpm at full load. By following the guidelines aforementioned, and observing the TCSF value among cylinders can be noticed that the cylinder 1 has the highest TCSF. A negligible difference between cylinder 2 and 3 was experienced meaning that the related injectors performance are quite homogeneous. Consequently, the same injection correction can be applied to them. Cylinder 4 is the one characterized by the lowest TCSF value and consequently by the lowest injected quantity. In cylinder 4 the highest injection correction is imposed.

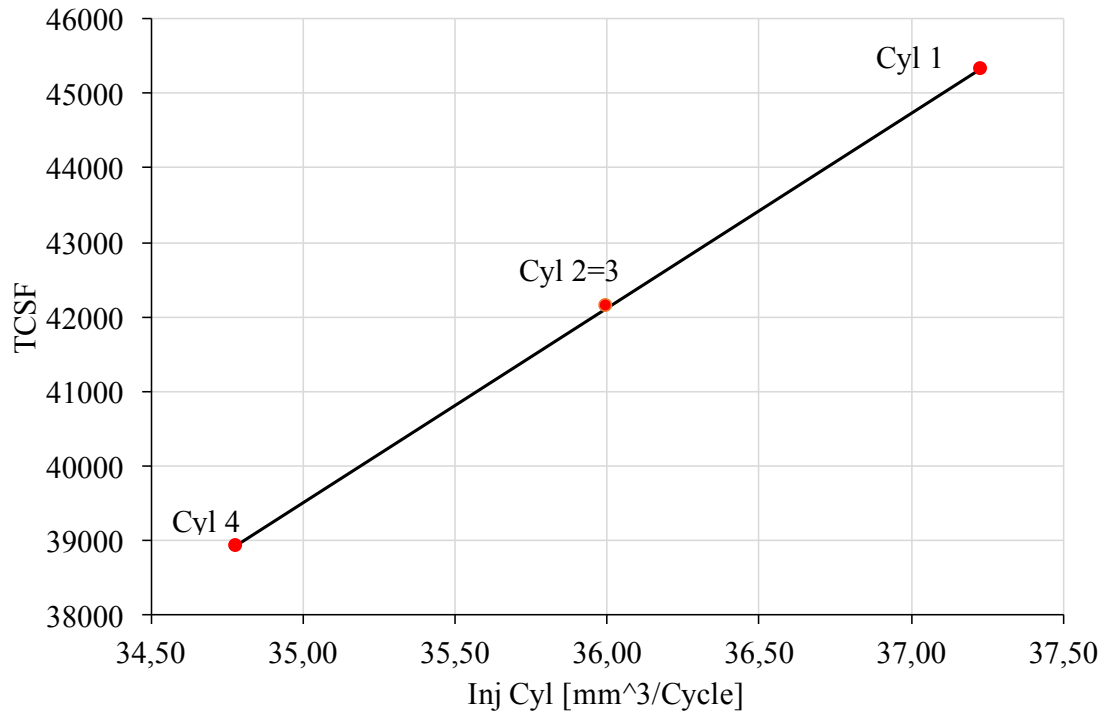

Figure 87. Linear correlation between TCSF and fuel mass flow injected into each cylinder. Engine operating condition: 1500 rpm at full load

Figure 87 highlights the fuel correction quantity that should be imposed in each cylinder to reach a balanced behaviour of the engine. Following the above considerations, considering the fuel injected expected that is equal to 36 mm^3 per cycle, it is possible to calculate the actual mass fuel quantity injected in each cylinder and then the necessary correction that must be applied to cylinders 1 and 4.

In Figure 88, the results of the correction strategy are summarized. An injection correction to cylinder 1 and 4 of about 2.5% have been applied. TCSF values in case of injection correction show a homogeneous behaviour among cylinders (yellow line)

respect to the standard case (red line). More significantly the TC acceleration and the TC speed demonstrate that a homogeneous injection situation was reached (Figure 89).

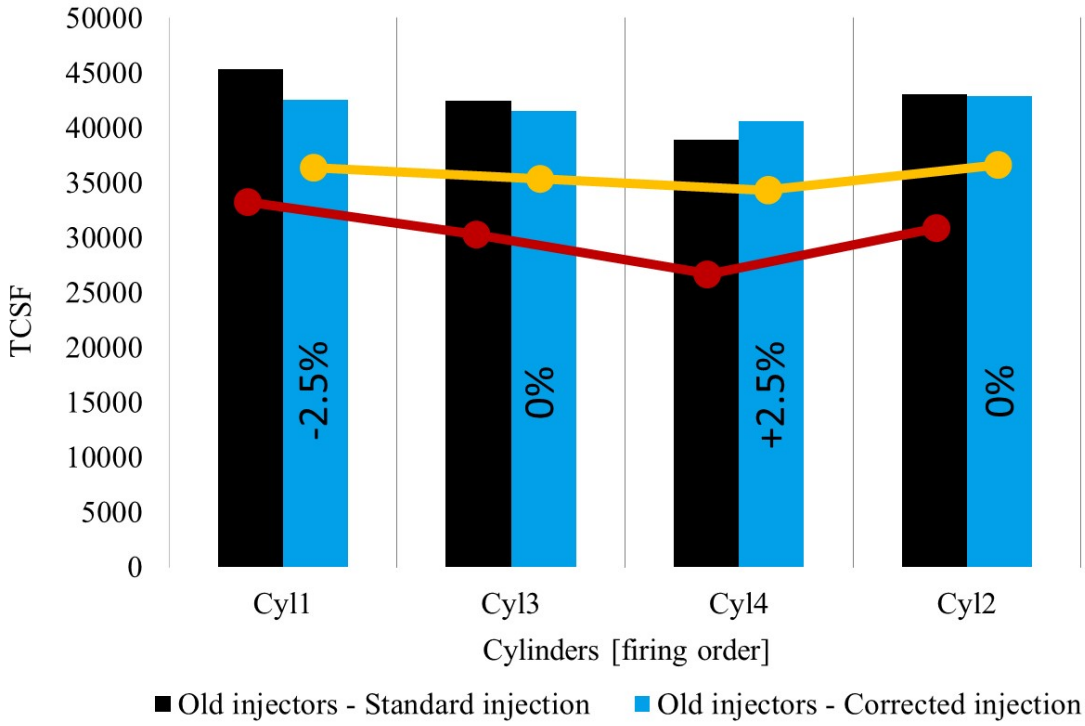

Figure 88. Results of the injection correction based on TCSF data. Engine operating condition: 1500 rpm at full load

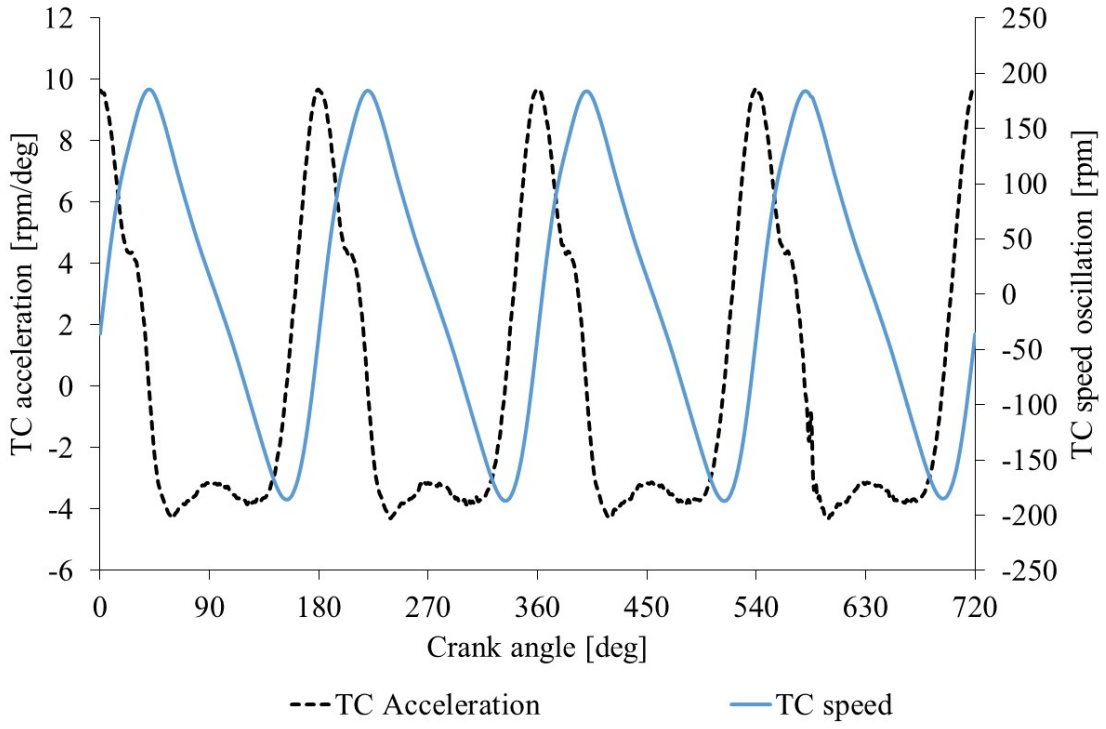

Figure 89. TC acceleration signal with corrected injection of deteriorated injectors

The same procedure can be applied for the TCAF parameter.

4.5 Methodologies Comparison

In this chapter are reported the general performance results of the strategies developed in order to clarify which one the author suggests for further development and use in the commercial application.

The results depicted in the subsequent figures are reported in term of percentage error for the total amount of fuel injected and for the injected fuel in each cylinder respectively for the three methodologies developed and described in the previous chapters (Figure 90, Figure 91 and Figure 92).

It is clear that the FFT methodology is the most promising not only for the result in terms of percentage error but also because the TCAF, that is characterized by a low error too, is affected by the fact that is correlated to one specific point of acceleration in the influence window of each cylinder. Consequently the TCAF need to reckon on a frequency filter to overcome any issue related to the noise of the signal, but once you apply a frequency filter you have all the data related to the FFT methodology that is more reliable and precise as demonstrated by its maximum error in the evaluation of the injected fuel from -4% to +3% compared with TCSF and TCAF that experienced an error from -5% to +5%. In Figure 93 the comparison of the Gaussian distribution of the errors among all the developed methodologies is depicted, the error standard deviation for the FFT, TCAF and TCSF are respectively equal to 1.25, 1.73, 2.05% demonstrating the better reliability of the FFT methodology

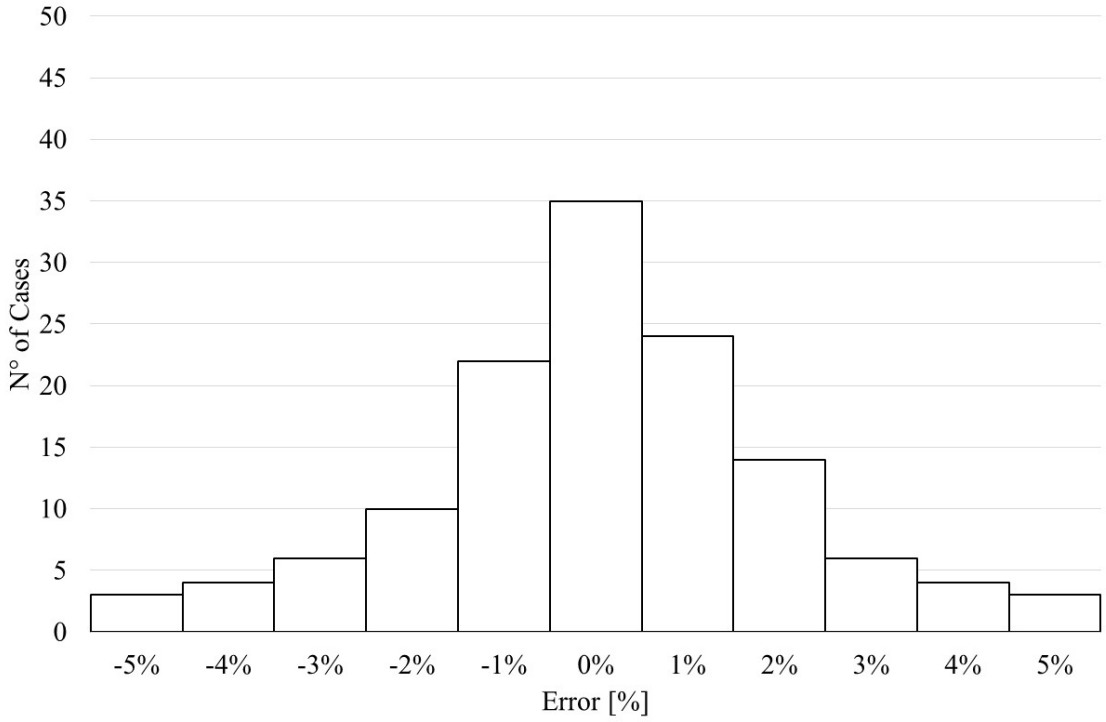

Figure 90. TCSF percentage error in evaluation of the injected fuel

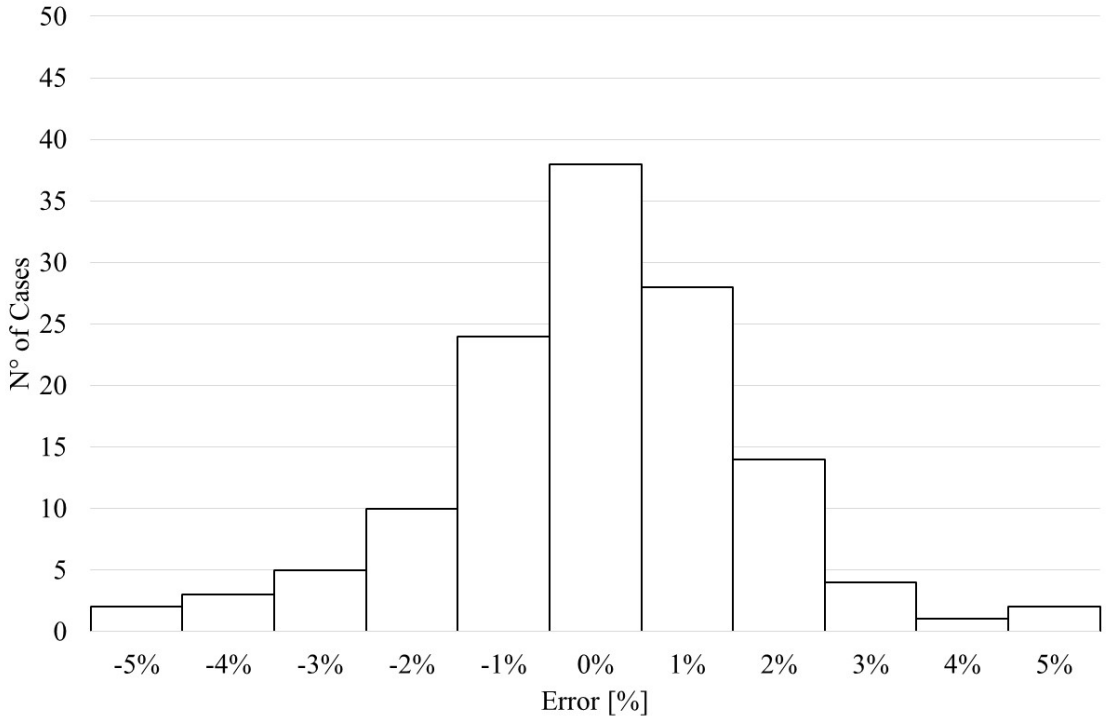

Figure 91. TCAF percentage error in evaluation of the injected fuel

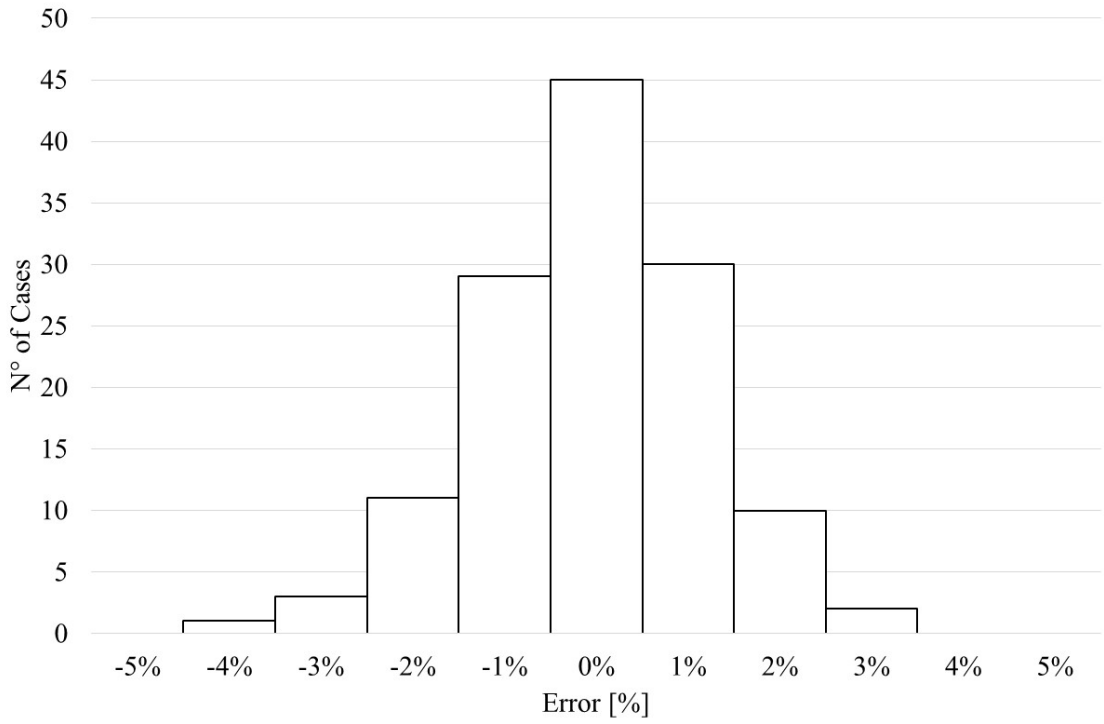

Figure 92. FFT percentage error in evaluation of the injected fuel

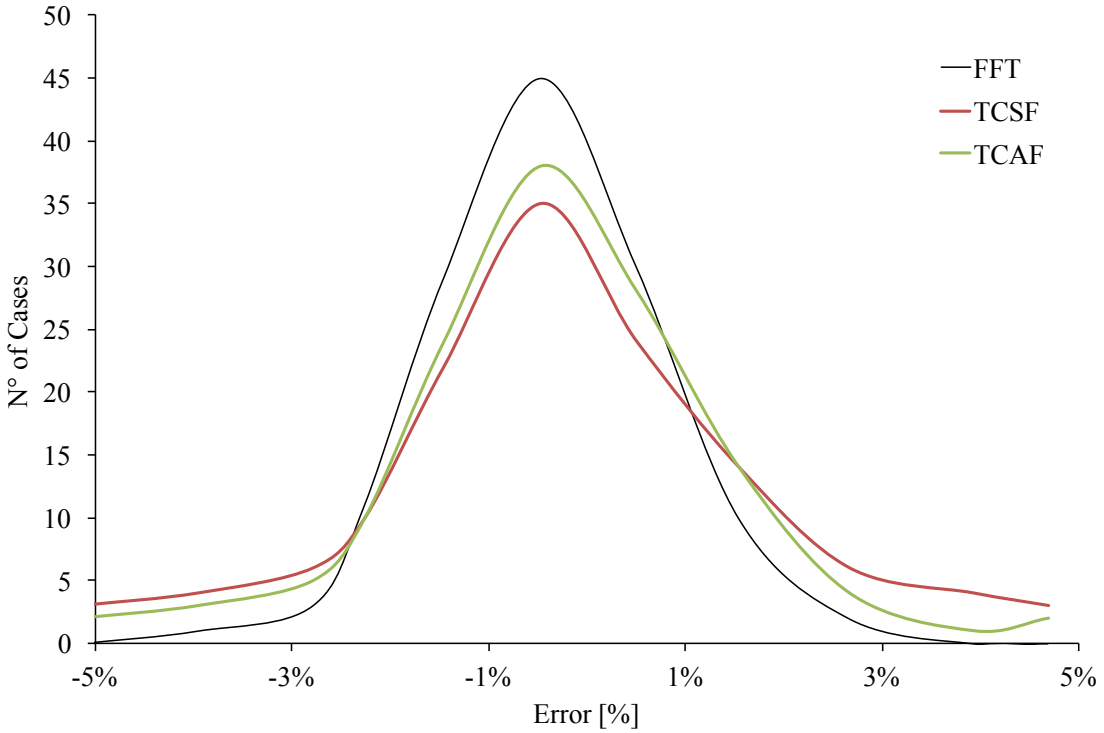

Figure 93. Gaussian Distribution of Errors comparison among TCSF, TCAF and FFT methodologies

4.6 Misfiring detection

Finally, due to the capabilities demonstrated by the methodologies developed it was decided to test the possibility to detect misfiring event that can be associated and replicated as a non-injection event, consequently, a misfiring detection strategy based on the TC speed signal acquisition has been developed and verified.

The misfiring condition was simulated at the test bench by manually switch off, with the ECU, the injection in one or two cylinders for one or maximum two consecutive cycles. Figure 94 shows the case in which misfiring was imposed two times in cylinder 1 for two consecutive cycles. In Figure 94 is reported the TC speed signal for the tested misfiring condition in cylinder 1 at 1000 rpm load 1, it was not physically possible to switch off the injection in one cylinder for less than two cycles for this reason only this particular case it was taken under account.

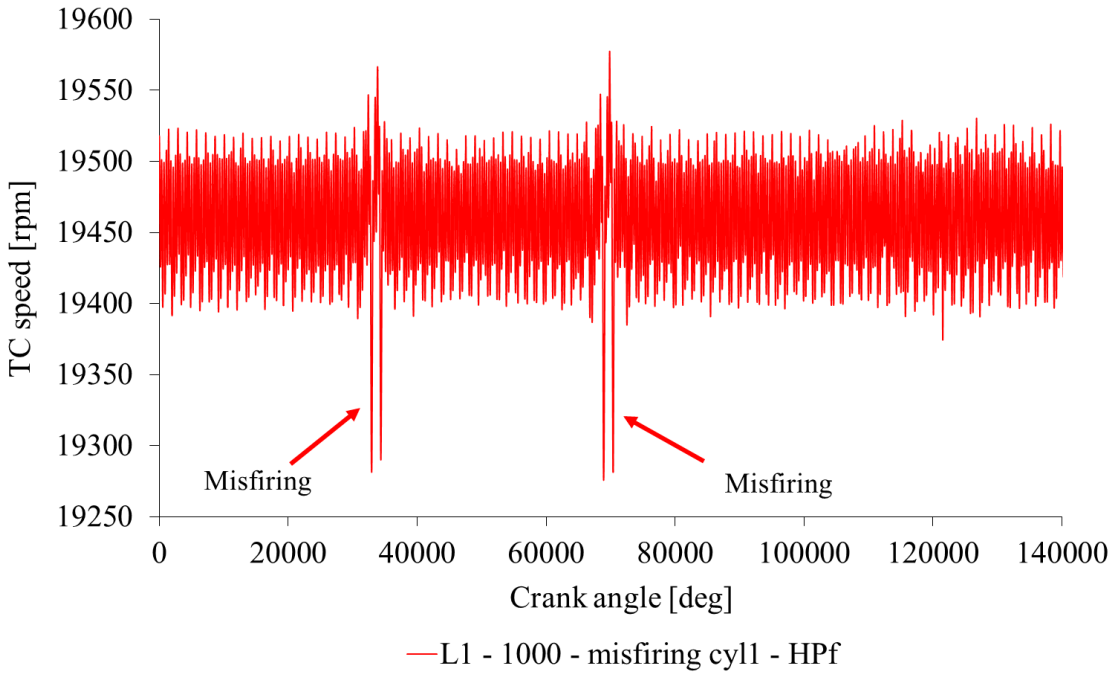

Figure 94. TC speed signal with a misfiring imposed 2 times for 2 consecutive cycles in the cylinder 1. Engine speed 1000 rpm load 1.

By exploiting the FFT methodology for the misfiring detection it has to be highlight that the effect of the misfiring last for at least four consecutive cycles after the event

occurs. For this reason, in order to detect the misfiring, the following parameters could be taken into account by acquiring in continuous mode the TC speed signal:

- The minimum value related to each cylinder of the TC speed
- The minimum value related to each cylinder of the TC acceleration

From the analysis of the exhaust pressure reported in Figure 95, it was noticed, as expected, that a drop in the exhaust pressure it occurs in case of a misfiring. Being the pressure the main driver for the TC speed behaviour, both the TC speed and the TC acceleration (respectively reported in Figure 96 and Figure 97) experience a drop in correspondence of the misfiring cycle and related to the specific cylinder in which the misfiring occurs.

The idea is to define a bottom threshold of TC speed or TC acceleration that can be used as a monitoring parameter for misfiring event by exploiting the TC speed signal. The more reliable and stable value of the TC speed respect to the acceleration combined with a low computational weight, suggest to prefer it for this kind of monitoring.

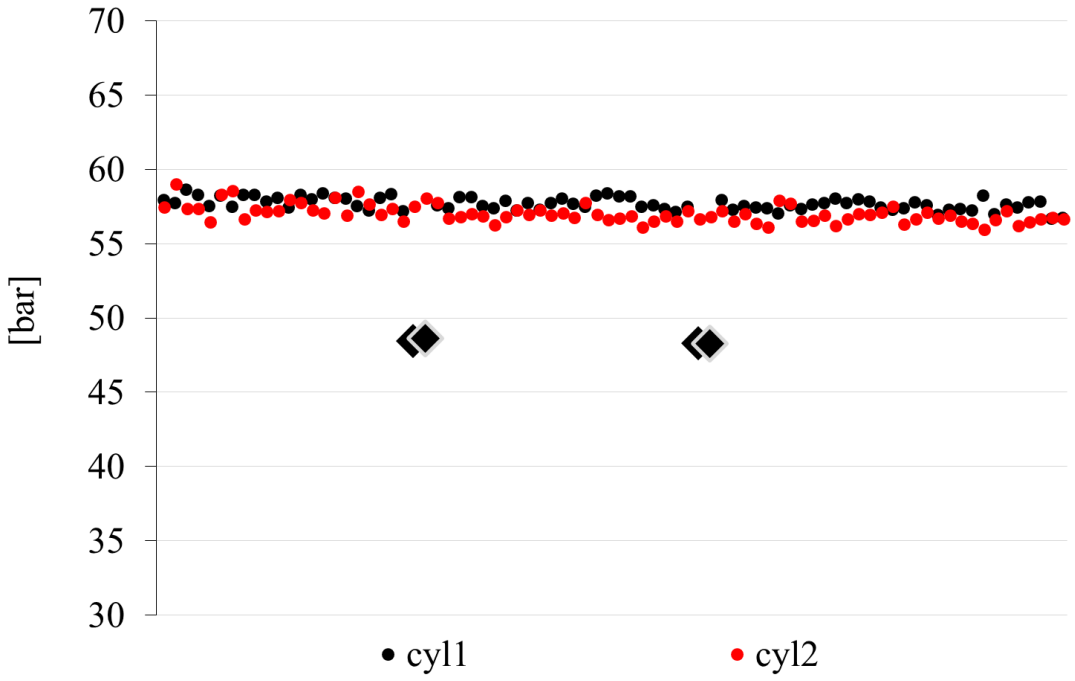

Figure 95. Exhaust pressure minimum value for each cylinder window

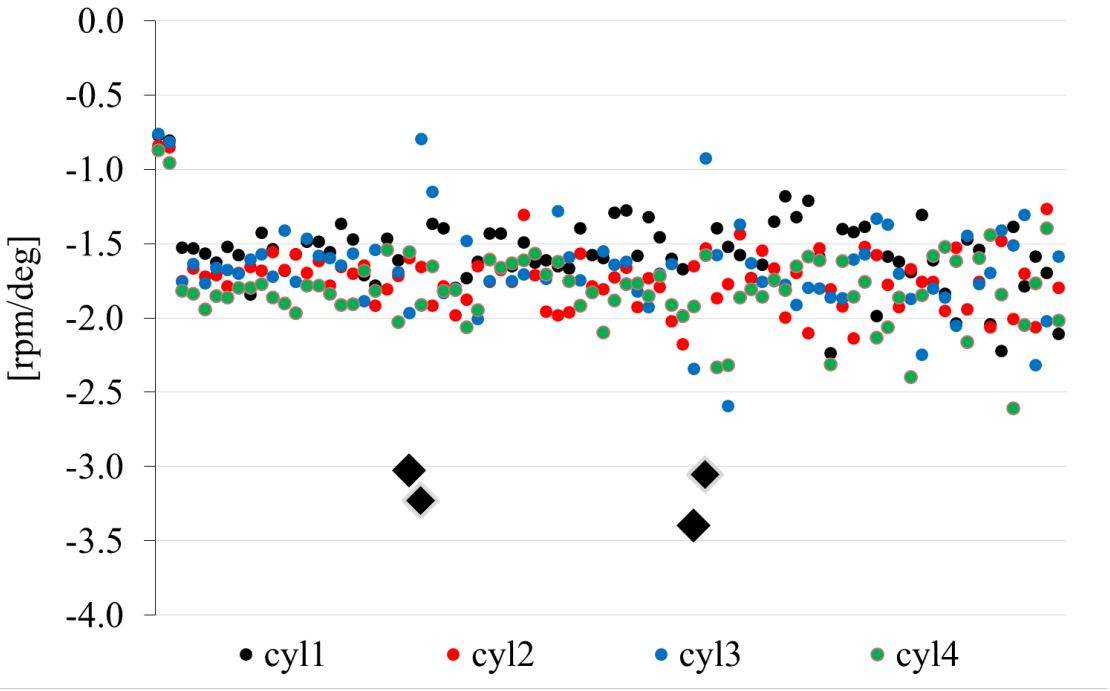

Figure 96. TC Acceleration minimum for each cylinder window

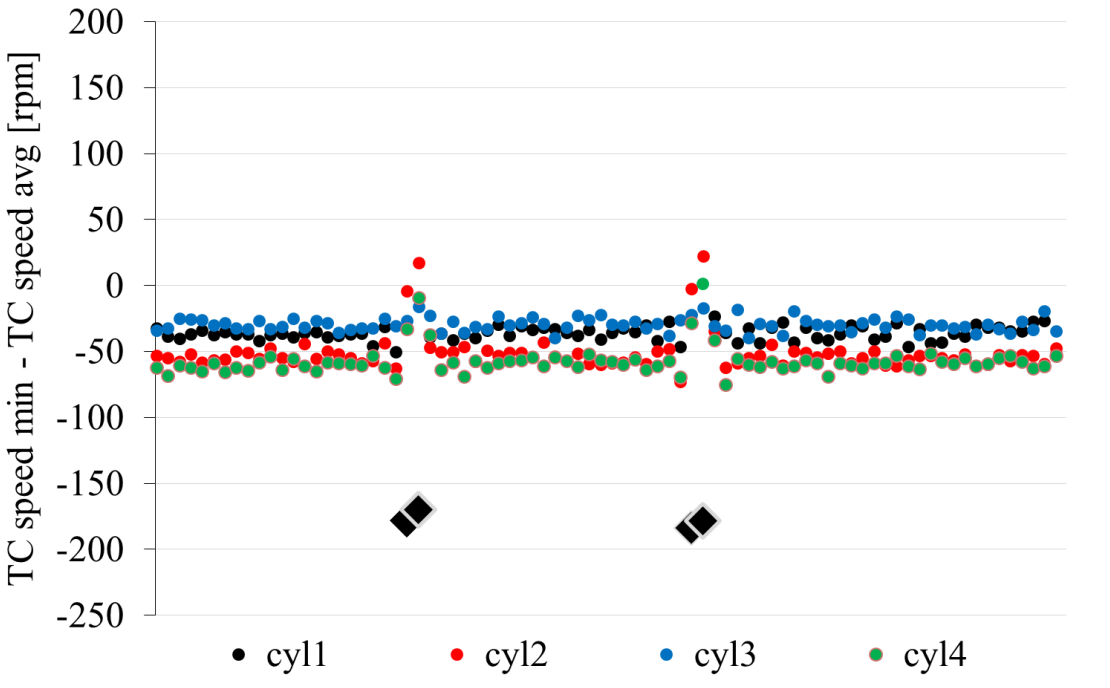

Figure 97. TC speed minimum subtracted of the average one for each cylinder window

5 Fault Detection Strategy

Considering the possibility of multiple faults happening in the same time for a compression ignition engine, in this last chapter, a fault detection strategy based on turbocharger speed, and other parameters such as exhaust temperature and pressure is reported. First, a focus on the development of a fault detection strategy made by taking advantage of the numerical model is explained, then, preliminary experimental tests to verify the strategy are shown. Five different common faults in diesel engine are proposed in agreement with the industrial partner:

- Injected fuel quantity in all cylinders
- Injected fuel quantity in single-cylinder
- Injection timing shift in all cylinders, related to the injector control system
- EGR rate, related to the EGR valve management
- Turbine outlet pressure, related to the condition of the exhaust gas treatment system.

5.1 Fault Condition Investigation

In order to carry out the fault condition investigation, five variations to the engine working parameters, respect to the baseline conditions were imposed, both in experimental and numerical cases. The experimental test reported for the detection fault were conducted by Bosch Japan with the same test configuration described in chapter 2.1. All the tests performed are reported in the following Table 5.

Table 5. Imposed numerical and experimental variations to the engine working parameters.

Type of variation of the engine working parameters	Variation respect to the baseline condition
Injected Fuel Quantity in All Cylinders	± 5 mm3/Hub
Injected Fuel Quantity in One Cylinder	± 5 mm3/Hub
Injection Timing Shifted in All Cylinders	± 3 deg CA
EGR Rate	+10 step EGR valve opening
Turbine Out Pressure at Maximum Power	+270 mbar (without EGR)

These investigated strategies involved, besides the TC average and instantaneous speed, other selected and monitored easy-to-measure parameters. The additional parameters considered were the temperature in the exhaust manifold, the static pressure in the exhaust manifold and the lambda sensor signal.

5.1.1 Uniform Variation of Injected Fuel Quantity

The first analyzed variation of the engine operating parameters was the uniform variation of the injected fuel quantity (± 5 mm3/Hub) in all cylinders with respect to the

baseline conditions studied during the model calibration. As expected, the uniform increase of the injected fuel quantity leads to an increase in the TC speed (Figure 98), except for the range in which the waste-gate valve works limiting the overpressure downstream of the compressor and, as a consequence, the TC speed. As highlighted in the previous chapter the periodicity of the instantaneous TC speed does not change and remains 180° CA.

The trends related to the static pressure in the intake and the exhaust manifold and the exhaust temperature are to grow with the increase of the injection in all cylinder (Figure 100 to Figure 102). To summarize an increase in the injection in all cylinder, that basically corresponds to an increase of the load, all the controlling parameters choose increase and the TC speed periodicity keep constant at 180 deg.

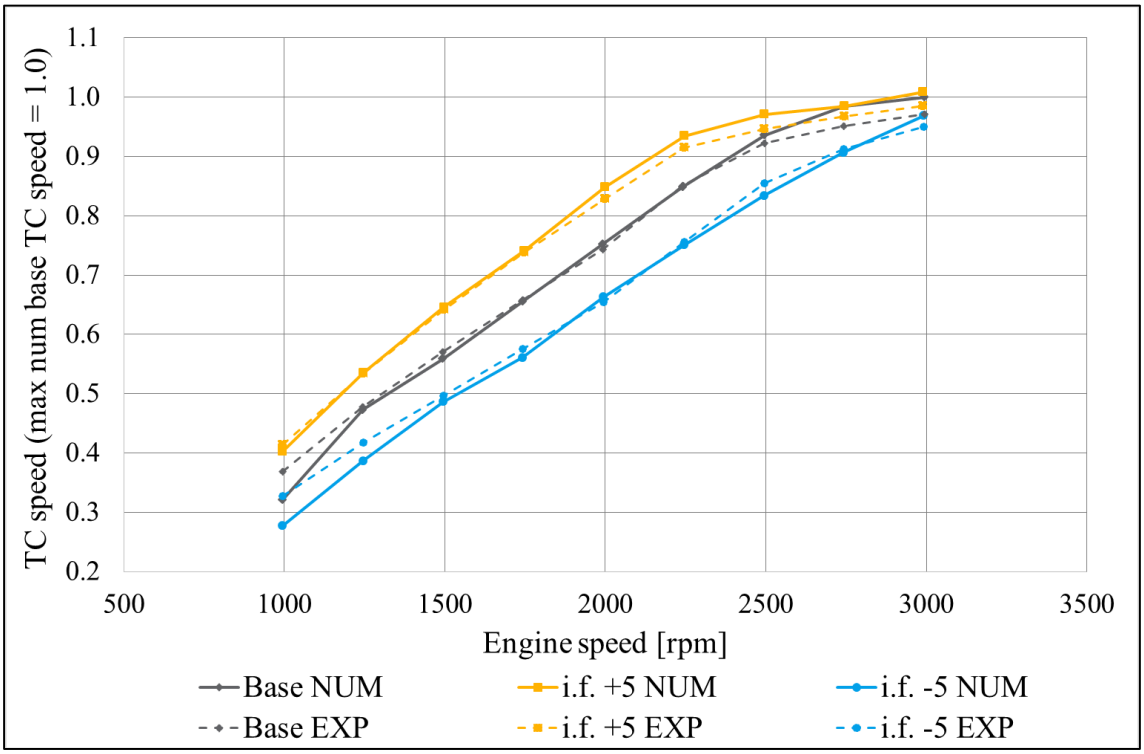

Figure 98. Average TC speed in function of engine speed (numerical and experimental data); uniform variation of injected fuel (i.f. ±5mm3/cycle) in all cylinders starting from the base load 4; data normalized respect to the maximum numerical TC speed of the base configuration.

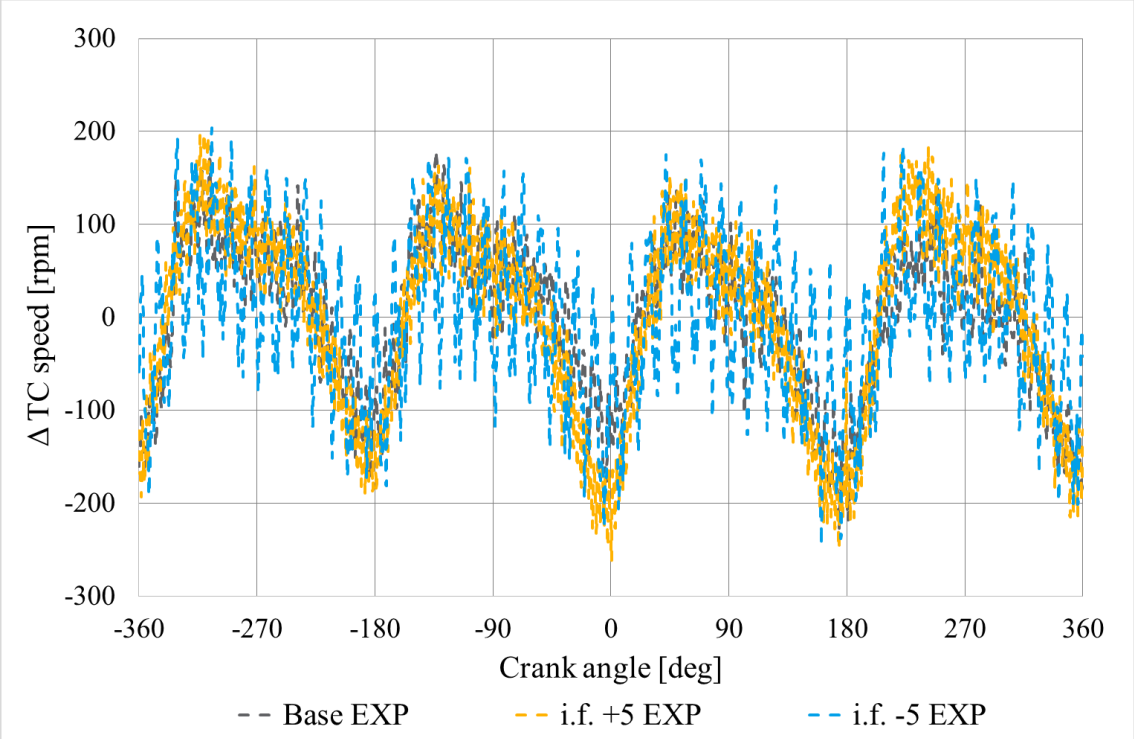

Figure 99. Instantaneous Δ TC speed in function of the crank angle (experimental data); uniform variation of injected fuel (i.f. ±5mm3/hub) in all cylinders starting from the base load 4 at 1750 rpm.

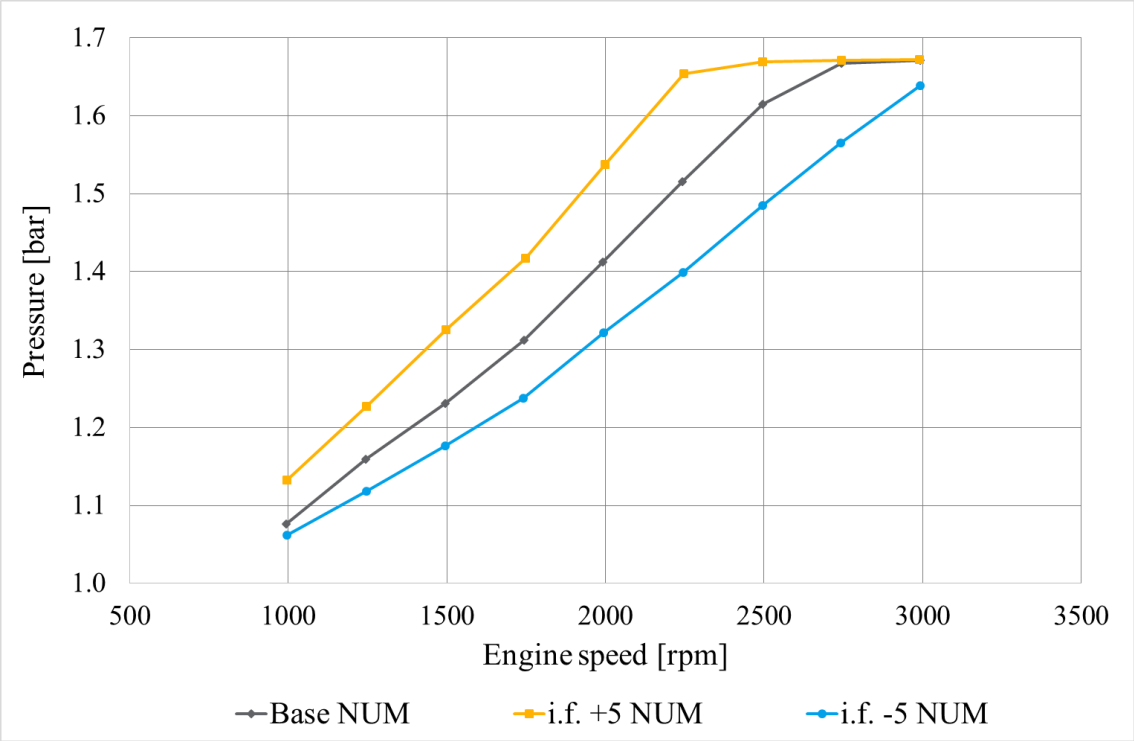

Figure 100. Average pressure in the intake manifold in function of engine speed (numerical data); uniform variation of injected fuel (i.f. ±5mm3/cycle) in all cylinders starting from the base load 4.

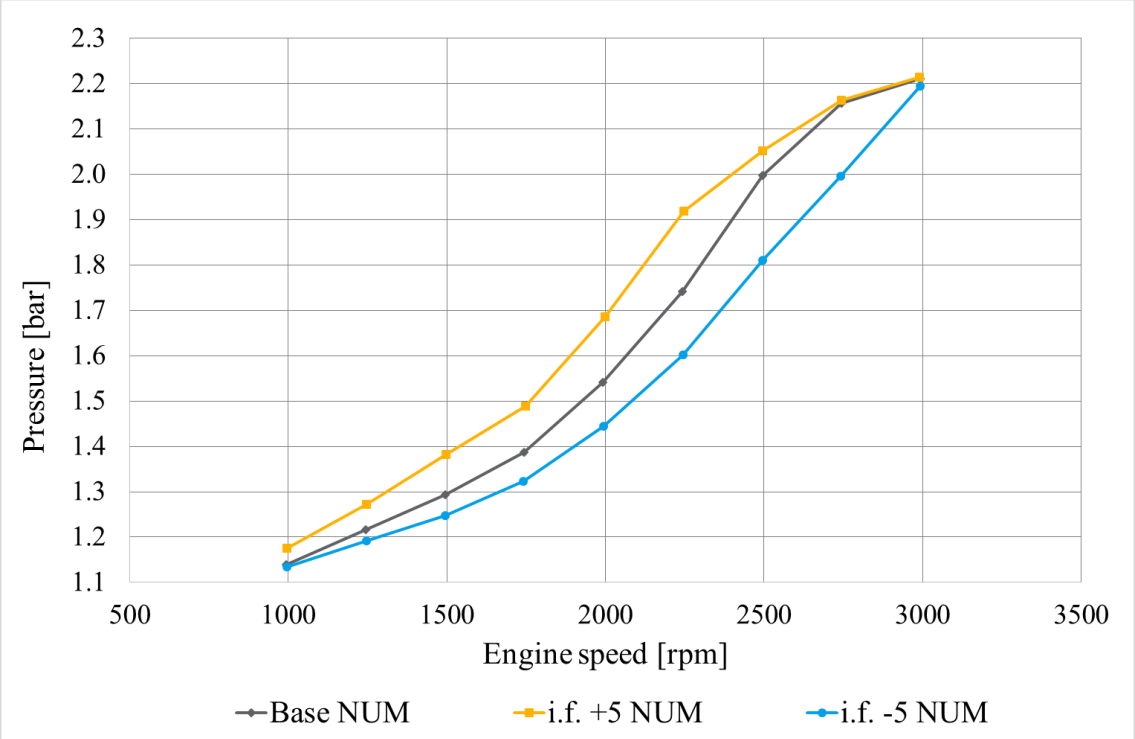

Figure 101. Average pressure in the exhaust manifold in function of engine speed (numerical data); uniform variation of injected fuel (i.f. ±5mm3/cycle) in all cylinders starting from the base load 4.

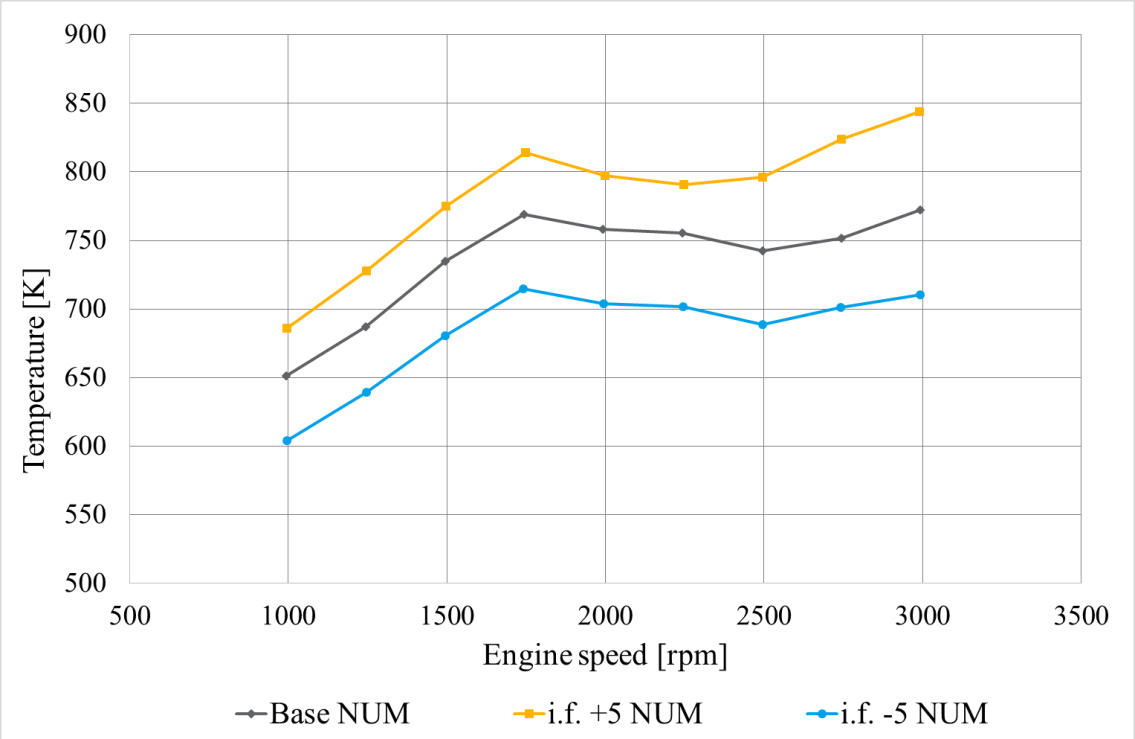

Figure 102. Temperature in the exhaust manifold in function of engine speed (numerical data); uniform variation of injected fuel (i.f. ±5mm3/cycle) in all cylinders starting from the base load 4.

5.1.2 Variation of Injection Timing

The variation of the injection timing can be related to some issues in the opening control system of the injectors. When the injection starts after the reference CA, the combustion process is delayed and slowed because the pressure and temperature inside the cylinder during the injection phase are lower than the reference situation and the injection ends later. The main effects of this modified combustion process are a lower IMEP and a higher value of gas temperature and pressure when the exhaust valve is open, as a consequence the gas temperature and pressure inside the exhaust manifold grow together with the TC speed. The opposite situation can be reached if the injection starts before the reference CA. Moreover, in both cases, an eventual lambda sensor could potentially not give different outputs respect to the reference configuration because the amount of fuel injected is hypothetically the same. So, the lambda sensor output can be used as a parameter to detect this kind of fault. All these affirmations are related to the engine configuration taken into account for this study and they are valid only for reasonable values of the shift of the injection timing.

The shift of the injection timing (±3°) in all cylinders with respect to the baseline condition was numerically and experimentally investigated. From Figure 103 to **Error! Reference source not found.** the aligned agreement between experimental and numerical results is shown. The results for the controlling parameters have the same trend respect to the case with a variation in the injection of all the cylinders(**Error! Reference source not found.** to Figure 107) even for the F4 module, for this reason to distinguish fuel injection variation to injection timing in all cylinders the monitoring of the lambda sensor is necessary.

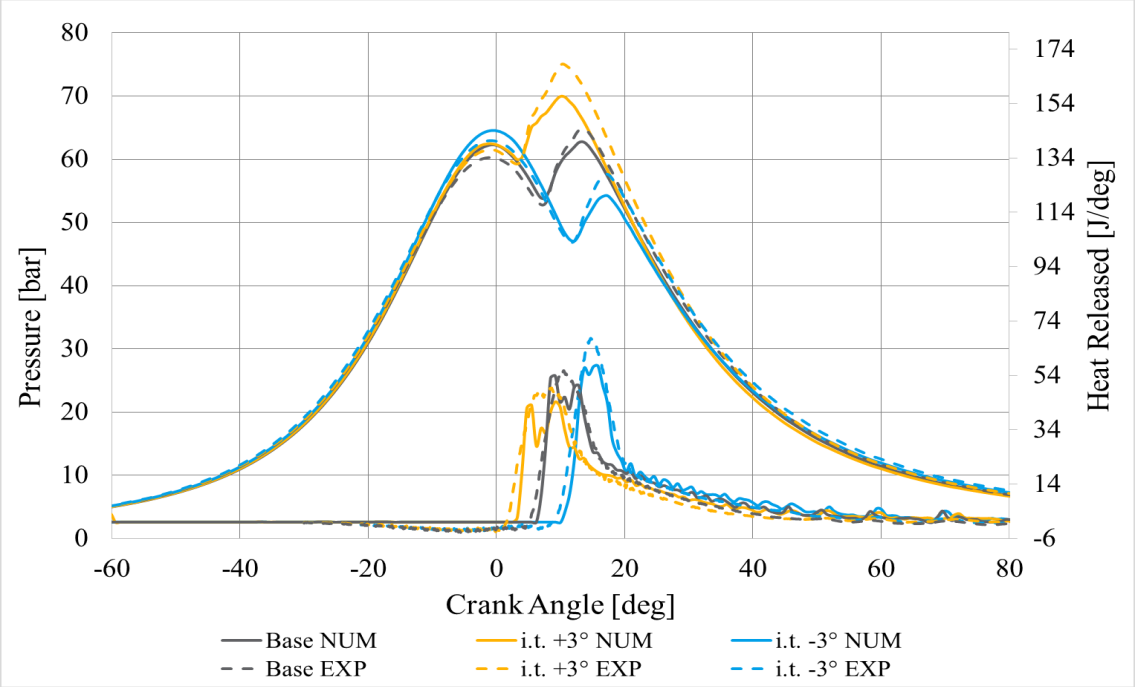

Figure 103. In-cylinder pressure and heat released in function of the crank angle (numerical and experimental data); uniform variation of injection timing (i.t. ±3° CA) in all cylinders starting from the base load 3 at 1750 rpm.

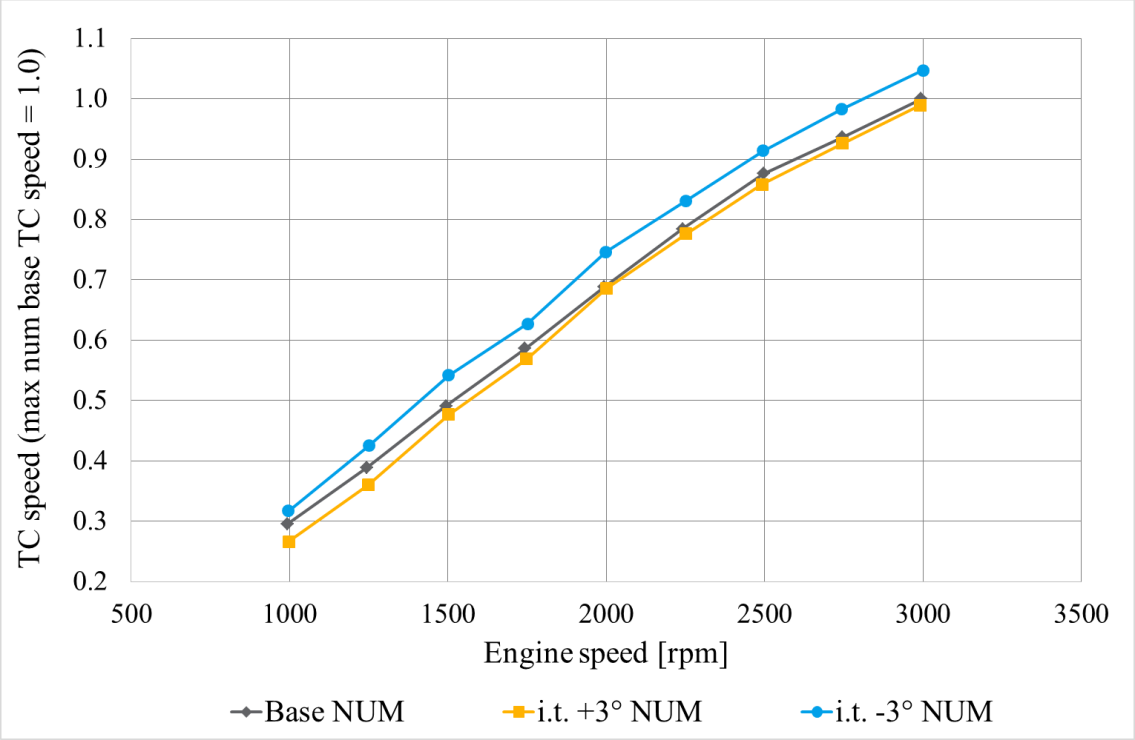

Figure 104. Average TC speed in function of engine speed (numerical data); uniform variation of injection timing (i.t. ±3° CA) in all cylinders starting from the base load 3; data are normalized respect to the maximum numerical TC speed of the base configuration.

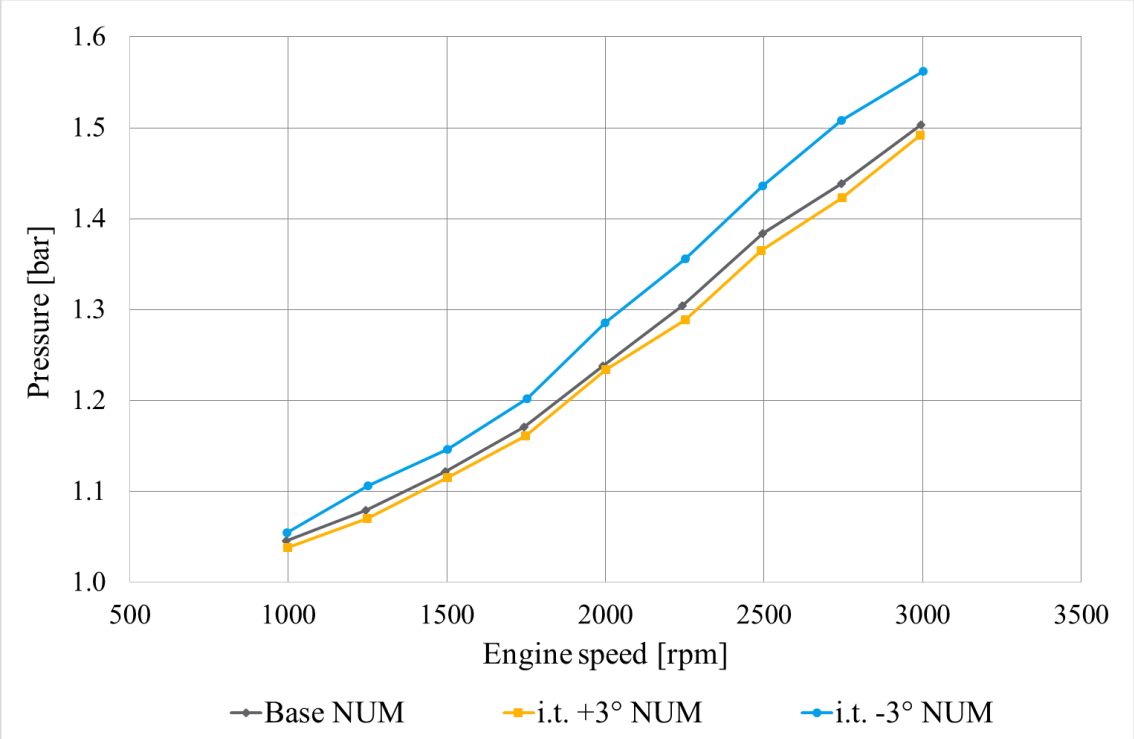

Figure 105. Average pressure in the intake manifold in function of engine speed (numerical data); uniform variation of injection timing (i.t. ±3° CA) in all cylinders starting from the base load 3.

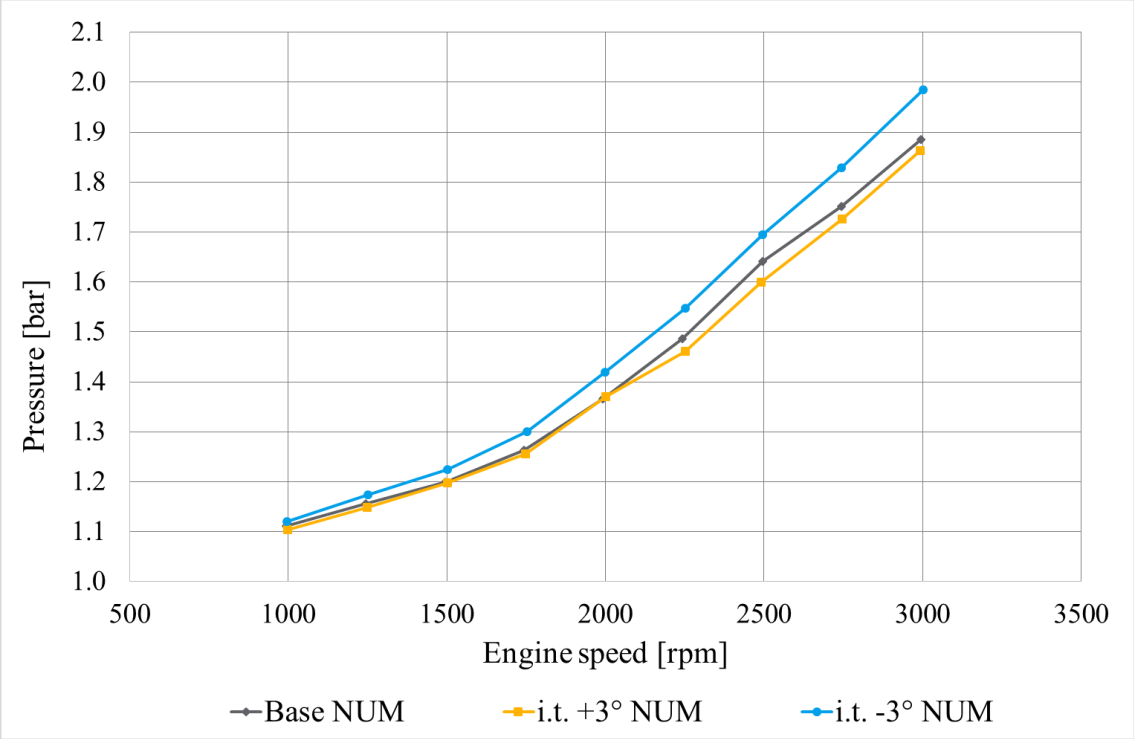

Figure 106. Average pressure in the exhaust manifold in function of engine speed (numerical data); uniform variation of injection timing (i.t. ±3° CA) in all cylinders starting from the base load 3.

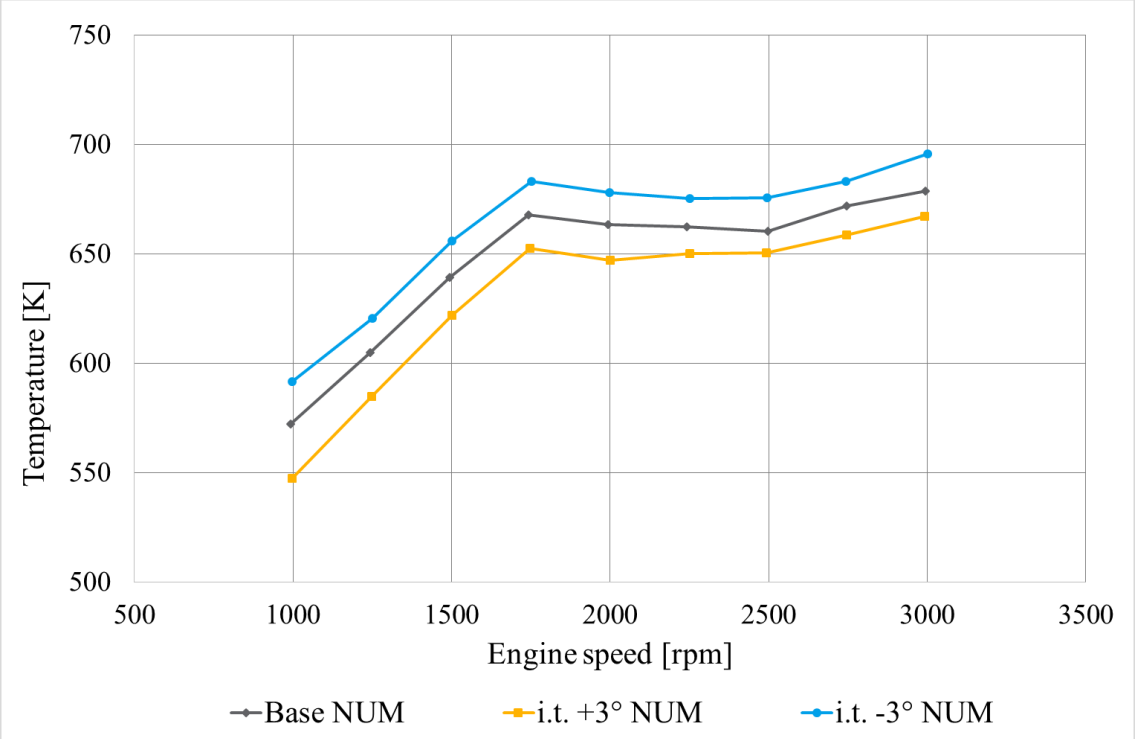

Figure 107. Temperature in the exhaust manifold in function of engine speed (numerical data); uniform variation of injection timing (i.t. ±3° CA) in all cylinders starting from the base load 3.

5.1.3 Variation of the EGR Rate

An EGR rate variation can occur when there are some issues with the EGR valve possibly linked to its control system or the deposits in it. The EGR affects the combustion process, in fact, it is used principally to decrease the maximum temperature of the combustion in order to limit the NO_x emissions. A higher EGR rate with respect to the reference one induces a delay in the combustion process with a consequential increase of the exhaust gas temperature. The EGR rate is also linked to the TC behavior because a variation in EGR rate leads to a variation in terms of inlet turbine mass flow and consequently to a different TC speed.

The EGR rate variation was experimentally tested by varying the opening of the proper valve by 10 steps with respect to the baseline value. This above variation of the valve opening corresponded to an average increase of about 2% of the EGR rate that was also imposed on the numerical model. As shown by **Error! Reference source not found.** and Figure 108, the experimental and numerical results highlight small differences in the average TC speed with respect to the baseline condition. The above variation of the EGR rate (i.e. 2%) does not have a remarkable influence on the engine and TC performances. Therefore, in order to better analyze the sensitivity of the engine parameters, a higher variation of the EGR rate was numerically investigated (+6% with respect to the base configuration). As expected, an increase of the EGR rate produces the reduction of the TC speed (Figure 109).

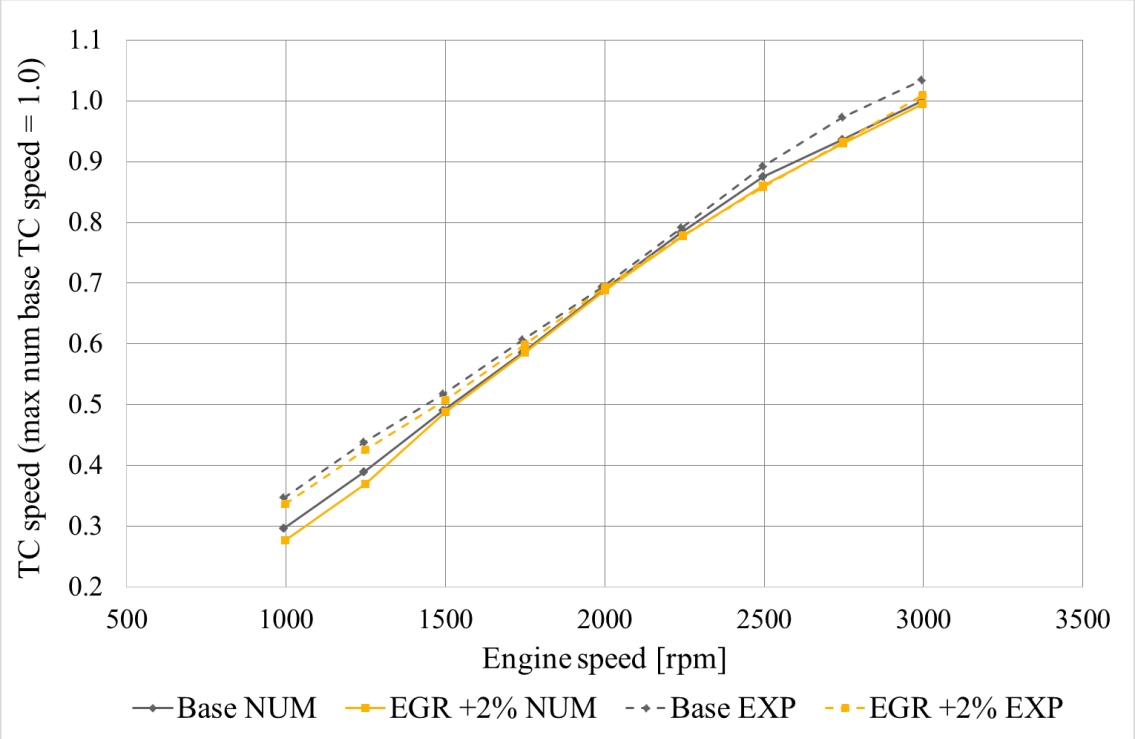

Figure 108. Average TC speed in function of engine speed (numerical and experimental data); variation of the EGR rate (+2%) starting from the base load 3; data are normalized respect to the maximum numerical TC speed of the base configuration.

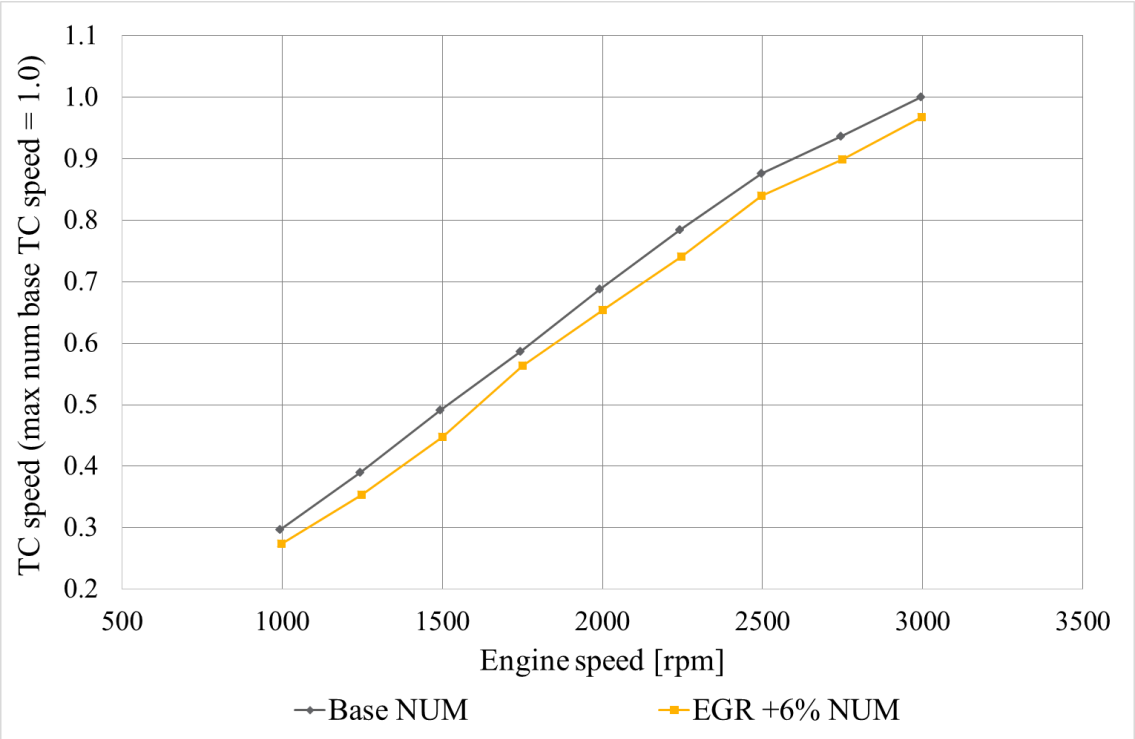

Figure 109. Average TC speed in function of engine speed (numerical data); variation of the EGR rate (+6%) starting from the base load 3; data are normalized respect to the maximum numerical TC speed of the base configuration.

By monitoring only the turbocharger speed, it could be difficult to univocally identify the cause of a variation in the engine behavior with respect to the standard working condition. Indeed, the variation of EGR rate and the uniform variation of injected fuel in all cylinders have the same variation trend in terms of average TC speed.

Below the comparison between the EGR ratio variation (+6%) and the uniform injected fuel variation in all cylinders (-2mm3/cycle) is reported. In Figure 110 the variation trend of both the turbocharger average speed and the exhaust gas temperature for the two cases is shown. It is evident that in the two cases the variation trend of the average TC speed is the same. Conversely, as previously mentioned, the exhaust gas temperature has an opposite variation trend: the uniform decrease of injected fuel quantity in all cylinders produces the decrease of the temperature; otherwise, the increase of EGR rate causes the increase of the temperature. So, it could be possible to recognize variations in the EGR rate also by monitoring the temperature in the exhaust manifold.

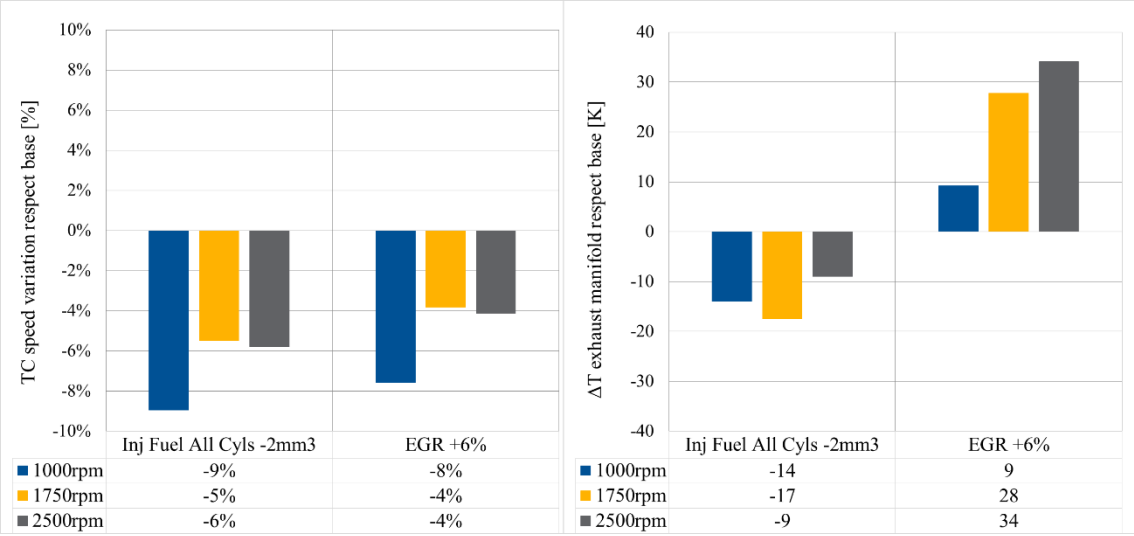

Figure 110. Percentage variation of average TC speed (left) and difference of temperature in the exhaust manifold (right) at three engine speeds (numerical data); uniform variation of injected fuel (i.f. -2mm3/cycle) in all cylinders compared with variation of EGR rate (+6%) starting from the base load 3.

5.1.4 Pressure Loss at the Turbine Outlet

Finally, the effects of a different pressure loss at the turbine outlet were studied. It can be possible to have different amounts of pressure loss at the turbine outlet when the exhaust gas treatment system is partially obstructed by deposits or does not work normally.

Figure 111 compare the numerical and experimental results of TC speed in different turbine outlet pressure cases. The difference of turbine outlet pressure is set to 270 mbar at maximum power by using a valve at tail pipe. The experimental and numerical tests are performed without EGR. The performance difference between the two cases ("Pout Ref" vs "Pout +270mbar") grows with the engine speed because the lumped pressure loss has a greater weight when increasing the flow velocity. Figure 112 highlights that a greater back pressure at the turbine outlet causes the decrease of the TC speed and the increase of the pressure in the exhaust manifold. Conversely, all the other shown cases produce the same variation trend of the TC speed, but a decrease of the exhaust pressure.

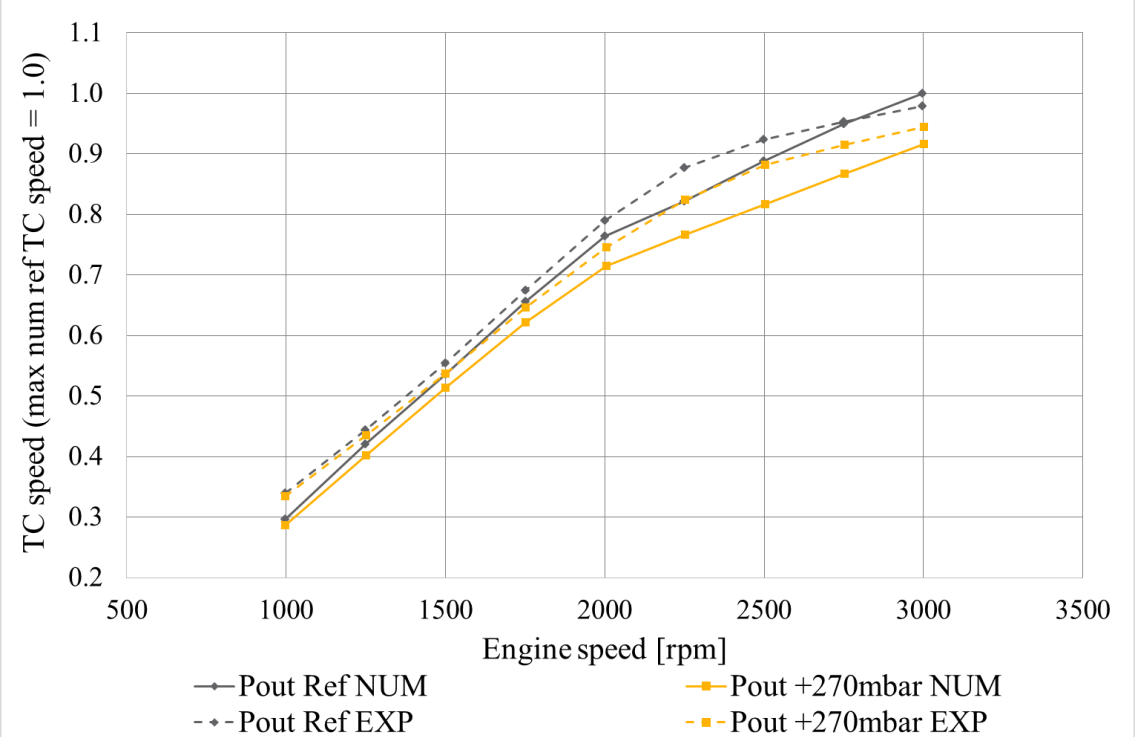

Figure 111. Average TC speed in function of engine speed (numerical and experimental data); variation of the back pressure at the turbine outlet (+270 mbar at the maximum engine power) starting from a reference medium load (base load 3 without EGR); data are normalized respect to the maximum numerical TC speed of the reference configuration.

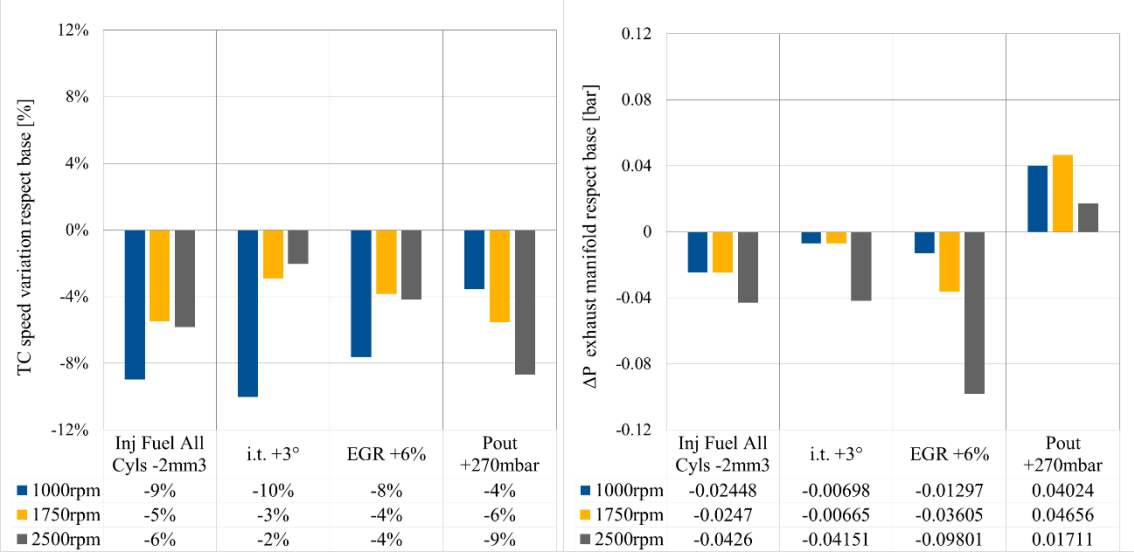

	Inj Fuel All Cyls -2mm3	i.t. +3°	EGR +6%	Pout +270mbar
1000rpm	-9%	-10%	-8%	-4%
1750rpm	-5%	-3%	-4%	-6%
2500rpm	-6%	-2%	-4%	-9%

	Inj Fuel All Cyls -2mm3	i.t. +3°	EGR +6%	Pout +270mbar
1000rpm	-0.02448	-0.00698	-0.01297	0.04024
1750rpm	-0.0247	-0.00665	-0.03605	0.04656
2500rpm	-0.0426	-0.04151	-0.09801	0.01711

Figure 112. Percentage variation of average TC speed (left) and difference of average pressure in the exhaust manifold (right) at three engine speeds (numerical data); uniform variation of injected fuel (i.f. -2mm3/cycle) in all cylinders vs variation of injection timing (+3° CA) vs variation of EGR rate (+6%) vs variation of the back pressure at the turbine outlet (+270 mbar at the maximum engine power) starting from the base load 3.

5.2 Preliminary Detection Strategy

Starting from the results of the analysis performed a preliminary detection strategy was developed and shown in the following Figure. First, the control system verifies the average TC speed comparing it with the reference value of the current engine condition, if there is a difference between the reference value and the current one (in the shown case the current value is lower) the instantaneous TC speed has to be checked. If the instantaneous TC speed is periodic on 720° CA there is an inhomogeneous injection between cylinders. In case of the instantaneous TC speed is periodic on 180° CA the average static pressure in the exhaust manifold is used as a third control parameter. When the pressure in the exhaust manifold has a countertrend with respect to the average TC speed, the problem is related to the turbine back pressure. If the Pressure in the exhaust manifold has the same trend with respect to the average TC speed, the average temperature in the exhaust manifold has to be checked. A countertrend of this temperature with respect to the mentioned pressure means that there is a different value of the EGR rate (higher than the reference value in the showed case). Finally, when the temperature in the exhaust manifold has the same trend of the pressure in the exhaust manifold the problem could be related to the quantity of the fuel injected or to the shift in the injection timing, so by exploiting the data coming from the lambda sensor it is possible to distinguish between these two faults. In fact, in case of the shift in the injection timing, there are no remarkable differences in the lambda sensor output because the amount of injected fuel is supposed constant, with respect to the reference case, and the oxygen concentration in the exhaust gas will be almost the same. Otherwise, a different amount of the injected fuel in all cylinders leads to a different air-fuel ratio and consequently a different oxygen concentration in the exhaust gas.

All the experimental data of the fault investigation were collected by Yanmar Japan, a further experimental investigation was carried out in the experimental test bench in Florence. The results of this investigation are reported in Table 6 and Table 7 in which respectively are reported the data related to the test setup and the results in terms of monitoring parameters. All the consideration and the strategy were confirmed by this activity. The most important result is related to the EGR, for which the previous experimental activity was not useful since the variation applied was too low, and confirm

the trends highlighted thanks to the numerical activity, indeed, by imposing a variation of the EGR opening position of 16 that corresponds to a variation of the EGR of about 10 % while the TC speed and the pressure in the exhaust manifold decrease, the Temperature in the exhaust manifold increase only for this variation.

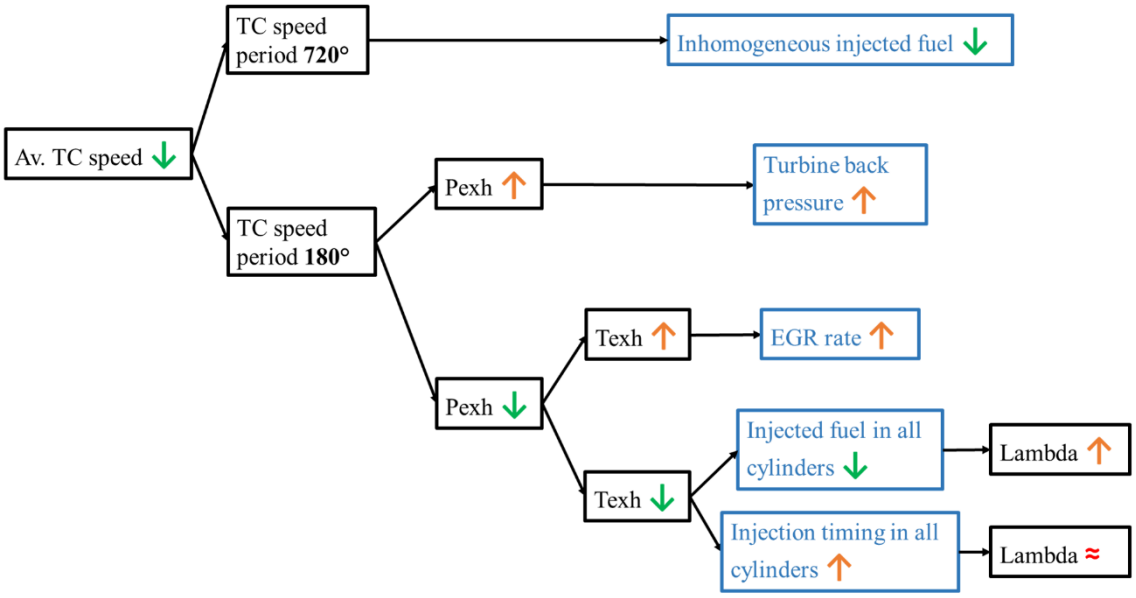

Figure 113 Fault Detection Strategy scheme

Table 6 Experimental configurations to test the fault detection strategy

Imposed cond	*Tot inj cyls*	*Main inj*	*Main inj timing*	*EGR valve pos*	*BMF50 cyl1*	*BMF10 cyl1*	*BMF90 cyl1*	*BMF10-90 cyl1*	*Torque cor*
	mm3/cycle	mm3/cycle	deg		deg	deg	deg	deg	Nm
STD	**149**	**p0p0p0p0**	**3,7**	**16**	**13**	**6**	**29**	**23**	**164**
Inj incr cyl1	153	p4p0p0p0	3,7	16	1	0	4	4	167
Inj decr cyl1	145	n4p0p0p0	3,7	16	-1	0	-3	-3	159
Inj incr cyls	153	p1p1p1p1	3,7	16	0	0	1	1	167
Inj decr cyls	145	n1n1n1n1	3,7	16	0	0	-1	-1	159
EGR incr	149	p0p0p0p0	3,7	40	0	0	4	3	160
EGR incr	149	p0p0p0p0	3,7	55	1	0	5	5	159
Inj Tim incr	149	p0p0p0p0	0,7	16	3	3	3	0	161
Inj Tim decr	149	p0p0p0p0	6,7	16	-3	-3	-3	0	166

Table 7 Experimental results for the monitoring parameter to test the fault detection strategy, in blue is represented positive variation and in red negative one

Imposed cond	*TC speed avg*	*Mod order 4*	*Mod order 1*	*P exh man avg*	*T exh man avg*	*A-F lambda*
	rpm	[none]	[none]	mbar	°C	[none]
STD	**102601**	**207**	**33**	**1439**	**465**	**21.3**
Inj incr cyl1	**1508**	**10**	**9**	**9**	**37**	**-0.3**
Inj decr cyl1	**-1582**	**-9**	**71**	**-9**	**-36**	**0.4**
Inj incr cyls	**1250**	**6**	**-1**	**7**	**8**	**-0.4**
Inj decr cyls	**-1577**	**-8**	**-3**	**-10**	**-7**	**0.4**
EGR incr	**-4400**	**-4**	**-15**	**-49**	**17**	**-2.0**
EGR incr	**-5710**	**-8**	**-15**	**-65**	**25**	**-2.8**
Inj Tim incr	**1964**	**10**	**2**	**10**	**8**	**0.0**
Inj Tim decr	**-1333**	**-7**	**1**	**-10**	**-4**	**-0.1**

Conclusions

The continuous supervision of the engine operating conditions is important to ensure a high level of performance. For Diesel engines, object of interest for this thesis, the injector performance and the monitoring of the fuel injected quantity in each cylinder is crucial since they are affected by many fault events. Taking advantage of the direct connection between the thermo-dynamic and fluid-dynamic conditions of the engine and the turbocharger behavior, this thesis presents a numerical and experimental investigation of the turbocharger speed with the aim to evaluate its capability in detecting injector performance. Further a wider fault detection strategy was preliminary developed exploiting additional sensors. The entire activity was carried out on a compression ignition engine with direct injection for marine application (42 kW @2750 rpm). The numerical model calibration was carried out by exploiting experimental data collected by Yanmar®.

The numerical activity aims to determine the potential of the analysis in the frequency domain and in the time domain of the TC speed signal for the detection of the injector performance. The calibrated numerical model was exploited to develop three different methodologies, one methodology based on the frequency content of the TC speed and two methodologies based on the time domain, more in detail on the integral value of the TC speed signal and on the TC acceleration.

The FFT processing method consists in the analysis of the TC speed signal in a specific frequency spectrum containing the first four orders, all the orders under the firing one, which is representative for the combustion process. Through the FFT method, it is possible to detect the fuel quantity injected into each cylinder by monitoring the module of the fourth firing order and the module and phase of the first and second orders. Thanks

to the fourth order module, it is possible to measure the total injected fuel in the engine, while the phases and modules of the first and second orders allow one to detect if there is an injection inhomogeneity, in which cylinder/s the injected fuel variation is experienced and the percentage distribution of the total injected fuel variation among the cylinders.

The numerical results highlight that the FFT methodology is suitable for the whole engine operating range even if its sensitivity decrease with the engine speed.

The first developed processing method, based on the time domain analysis of the TC speed signal, is based on the integral of the instantaneous TC speed. In order to evaluate the contribution of each cylinder on the TC speed oscillation, the cycle period of the engine was divided by the number of the cylinders. Moreover, the integral area related to each cylinder is limited by the instantaneous TC speed and the rectilinear segment that joins the initial and final values of the cylinder contribution window. The subtracted area represents the contribution of the velocity that varies with constant acceleration in each integration window. The integral parameter obtained is able to quantify the injected fuel in each cylinder.

The second method developed is based on the analysis of the TC acceleration. The TurboCharger Acceleration Factor, defined as the maximum acceleration value reduced by the average one in each cylinder contribution window, is able to detect the quantity injected in each cylinder allowing in addition to detecting misfiring events.

All the three methodologies were tested experimentally exploiting two set of injectors, a new one and a time deteriorated one. The tests carried out to confirm the reliability for the injector performance monitoring of all the methodologies developed, however, the FFT methodology result highlights a lower error in the detection of the injected fuel and a wider application inside the working area of the engine.

Finally, a technique to distinguish among different typical faults of diesel engines was presented. This Fault detection strategy relies on different engine parameters such as the temperature and the pressure of the exhaust manifold and the lambda sensor signal. Exploiting the information coming from these sensors and the TC speed it is possible to detect the fault that is responsible for a change in the engine condition among selected

possibilities: EGR variation, Injection variation in terms of timing and injected fuel mass and turbine backpressure.

Future development will be focused on the onboard control system development that is able to use the information coming from the TC speed sensor by using the methodology proposed here for the monitoring of the injection system. Further, the possibility to use the TC speed for detecting the injection performance in larger engines and in case of spark ignition engines will be studied

References

[1] D. T. Hountalas, G. C. Mavropoulos and G. Kourbetis (2006); Experimental Investigation to Develop a Methodology for Estimating the Compression Condition of DI Diesel Engines; Energy Conversion and Management 47 (2006), 1-18.

[2] D. Watzenig, M. S. Sommer and G. Steiner (2009); Engine State Monitoring and Fault Diagnosis of Large Marine Diesel Engines; Elektrotechnik & Informationstechnik (2009), 126/5: 173-179

[3] William J. Fleming (2008). New Automotive Sensors – A Review. IEEE Sensors Journal, Vol. 8, No. 11, November 2008.

[4] J. D. Gill, R. L. Reuben, M Scaife, E. R. Brown, and J. A. Steel (1998). Detection of Diesel Engine Faults Using Acoustic Emission. Proceedings of the 2nd International Conference on Planned Maintenance Reliability and Quality, 1998, Oxford, England.

[5] L. Barelli , G. Bidini, C. Buratti, R. Mariani; Diagnosis of internal combustion engine through vibration and acoustic pressure non-intrusive measurement; Applied Thermal Engineering 29 (2009) 1707–1713

[6] J. Jiang, F. Gu, R. Gennish, D.J. Moore, G. Harris, A.D. Ball; Monitoring of diesel engine combustions based on the acoustic source characterisation of the exhaust system; Mechanical Systems and Signal Processing 22 (2008) 1465–1480

[7] D. P. Lowe; Characterisation of Combustion Related Acoustic Emission Sources for Diesel Engine Condition Monitoring (2013). PhD Thesis, Queensland University of Technology

[8] N.Cavina, A.Businaro, N.Rojo, M. De Cesare, L. Paiano (2016), "Combustion and Intake/Exhaust Systems Diagnosis Based on Acoustic Emissions of a GDI TC Engine". Energy Procedia 101 (2016) 677 – 684

[9] G. Chiatti, O. Chiavola, F. Palmieri, A. Piolo (2015) "Diagnostic methodology for internal combustion diesel engines via noise radiation" Energy Conversion and Management 89 (2015) 34–42

[10] O. Bondarenko, T. Fukuda (2016),"Potential of Acoustic Emission in Unsupervised Monitoring of Gas-Fuelled Engines". IFAC_PapersOnLine 49-23 (2016) 329-34.

[11] S. Delvecchio, P. Bonfiglio, F. Pompoli (2018) "Vibro-acoustic condition monitoring of Internal Combustion Engines: A critical review of existing techniques" Mechanical Systems and Signal Processing 99 (2018) 661–683

[12] J. Antoni, J. Daniere, and F. Guillet (2002). Effective Vibration analysis of IC Engines Using Cyclostationarity. Part 1 – A Methodology for Condition Monitoring. Journal of Sound and Vibration (2002) 257(5), 815-837.

[13] B. A. Badawi, M. A. Shahin, M. Kolosy, S. A. Shedied and A. Elmaihy (2006). Identification of Diesel Engine Cycle Events using Measured Surface Vibration. SAE Technical Paper 2006-32-0097.

[14] J. Antoni, J. Daniere, F. Guillet and R. B. Randall (2002). Effective Vibration Analysis of IC Engines Using Cyclostationarity. Part II – New Results on the Reconstruction of the Cylinder Pressures. Journal of Sound and Vibration (2002) 257(5), 839-856.

[15] Abhishek Sharma a,⇑, V. Sugumaran b, S. Babu Devasenapati (2014), "Misfire detection in an IC engine using vibration signal and decision tree algorithms" Measurement 50 (2014) 370–380

[16] J Chen. R B Randall, B Peeters, H Van der Auweraer and W Desmet (2012),"Automated misfire diagnosis in engines using torsional vibration and block rotation" Journal of Physics: Conference Series 364 (2012) 012020

[17] X. Zhao, Y. Cheng, S. Ji (2016), "Combustion parameters identification and correction in diesel engine via vibration acceleration signal" Applied Acoustics 116 (2017) 205-215

[18] F.Taglialatela, et al., Determination of combustion parameters using engine crankshaft speed, Mech. Syst. Signal Process. (2013), http://dx.doi.org/10.1016/j.ymssp.2012.12.009

[19] R. Johnsson; Cylinder pressure reconstruction based on complex radial basis function networks from vibration and speed signals; Mechanical Systems and Signal Processing 20 (2006) 1923–1940

[20] J Chen. R B Randall, B Peeters, H Van der Auweraer and W Desmet (2012),"Automated misfire diagnosis in engines using torsional vibration and block rotation" Journal of Physics: Conference Series 364 (2012) 012020

[21] J.Chen, R B Randall (2015) "Improved automated diagnosis of misfire in internal combustion engines based on simulation models".Mechanical Systems and Signal Processing 64-65(2015) 58–8360

[22] Binh Le Khac and Tuma Jiri (2012). Approach to Gasoline Engine Faults Diagnosis Based on Crankshaft Instantaneous Angular Acceleration. 13th International Carpathian Control Conference, 2012 - IEEE Xplore Digital Library.

[23] V Macia´n, J Galindo, J M Luja´n, and C Guardiola, "Detection and correction of injection failures in diesel engines on the basis of turbocharger instantaneous speed frequency analysis", Proceedings of the Institution of Mechanical Engineers, Part D: Journal of Automobile Engineering 2005